

4-8-2011

Characterization of Recombinant Chloroperoxidase, and F103A and C29H/C79H/ C87H Mutants

Zheng Wang

Florida International University, zwang004@fiu.edu

DOI: 10.25148/etd.FI11050313

Follow this and additional works at: <https://digitalcommons.fiu.edu/etd>

Recommended Citation

Wang, Zheng, "Characterization of Recombinant Chloroperoxidase, and F103A and C29H/C79H/C87H Mutants" (2011). *FIU Electronic Theses and Dissertations*. 414.
<https://digitalcommons.fiu.edu/etd/414>

This work is brought to you for free and open access by the University Graduate School at FIU Digital Commons. It has been accepted for inclusion in FIU Electronic Theses and Dissertations by an authorized administrator of FIU Digital Commons. For more information, please contact dcc@fiu.edu.

FLORIDA INTERNATIONAL UNIVERSITY

Miami, Florida

CHARACTERIZATION OF RECOMBINANT CHLOROPEROXIDASE, AND F103A
AND C29H/C79H/C87H MUTANTS

A dissertation submitted in partial fulfillment of the

requirements for the degree of

DOCTOR OF PHILOSOPHY

in

CHEMISTRY

by

Zheng Wang

2011

To: Dean Kenneth Furton
College of Arts and Sciences

This dissertation, written by Zheng Wang, and entitled Characterization of Recombinant Chloroperoxidase, and F103A and C29H/C79H/C87H Mutants, having been approved in respect to style and intellectual content, is referred to you for judgment.

We have read this dissertation and recommend that it be approved.

Noriega Fernando

Watson Lees

Bruce McCord

Kathleen Rein

Xiaotang Wang, Major Professor

Date of Defense: April 8, 2011

The dissertation of Zheng Wang is approved.

Dean Kenneth Furton
College of Arts and Sciences

Interim Dean Kevin O'Shea
University Graduate School

Florida International University, 2011

© Copyright 2011 by Zheng Wang

All rights reserved.

DEDICATION

I dedicate this dissertation to my son Alec F. Lin, my brother Feng Wang, my mother Yulan Zhao and my father Yanhua Wang. Without their understanding, encouragement, support, and most of all love, the completion of this work would not have been possible.

ACKNOWLEDGMENTS

In the past six years, my graduate study at FIU has been a remarkable and rewarding journey of my life. I am so grateful that many people help me to achieve my goals in academics and personal life. First of all, I wish to thank my major professor, Dr. Xiaotang Wang, for giving me incredible guidance, support and encouragement over these years. I would never achieve so much without his patience and faith in me. Beyond academics, Dr. Wang is a wonderful person who is thoughtful, kind and always willing to help others. I would like to extend my thanks to my committee members, Dr. Noriega Fernando, Dr. Watson Lees, Dr. Bruce McCord and Dr. Kathleen Rein, for their insightful advices and guidance of my research, and helpful comments and suggestion to my dissertation.

I would like to thank Hui Tian for her help on acquiring NMR data, and Tanyi Chen for her help on HPLC. I also like to thank all members in Dr. Wang's research group: Jiang Lin, Zhonghua Wang, Rui Zhang. Special thanks to Xi Chen, Yisi Cao, Hua Ling and all my friends and colleagues at FIU.

I would like to acknowledge National Science Foundation, Department of Chemistry & Biochemistry at Florida International University for the financial support. Finally, I wish to express my appreciation to those who has helped me in any respect during my six years study at FIU.

ABSTRACT OF THE DISSERTATION
CHARACTERIZATION OF RECOMBINANT CHLOROPEROXIDASE, AND F103A
AND C29H/C79H/C87H MUTANTS

by

Zheng Wang

Florida International University, 2011

Miami, Florida

Professor Xiaotang Wang, Major Professor

Mechanistically and structurally chloroperoxidase (CPO) occupies a unique niche among heme containing enzymes. Chloroperoxidase catalyzes a broad range of reactions, such as oxidation of organic substrates, dismutation of hydrogen peroxide, and mono-oxygenation of organic molecules. To expand the synthetic utility of CPO and to appreciate the important interactions that lead to CPO's exceptional properties, a site-directed mutagenesis study was undertaken.

Recombinant CPO and CPO mutants were heterologously expressed in *Aspergillus niger*. The overall protein structure was almost the same as that of wild type CPO, as determined by UV-vis, NMR and CD spectroscopies. Phenylalanine103, which was proposed to regulate substrate access to the active site by restricting the size of substrates and to control CPO's enantioselectivity, was mutated to Ala. The ligand binding affinity and most importantly the catalytic activity of F103A was dramatically different from wild type CPO. The mutation essentially eliminated the chlorination and dismutation activities but enhanced, 4-10 fold, the epoxidation, peroxidation, and *N*-demethylation activities. As expected, the F103A mutant displayed dramatically improved epoxidation activity for

larger, more branched styrene derivatives. Furthermore, F103A showed a distinctive enantioselectivity profile: losing enantioselectivity to styrene and *cis*- β -methylstyrene; having a different configuration preference on α -methylstyrene; showing higher enantioselectivities and conversion rates on larger, more branched substrates. Our results show that F103 acts as a switch box that controls the catalytic activity, substrate specificity, and product enantioselectivity of CPO. Given that no other mutant of CPO has displayed distinct properties, the results with F103A are dramatic.

The diverse catalytic activity of CPO has long been attributed to the presence of the proximal thiolate ligand. Surprisingly, a recent report on a C29H mutant suggested otherwise. A new CPO triple mutant C29H/C79H/C87H was prepared, in which all the cysteines were replaced by histidine to eliminate the possibility of cysteine coordinating to the heme. No active form protein was isolated, although, successful transformation and transcription was confirmed. The result suggests that Cys79 and Cys87 are critical to maintaining the structural scaffold of CPO.

In *vitro* biodegradation of nanotubes by CPO were examined by scanning electron microscope method, but little oxidation was observed.

TABLE OF CONTENTS

CHAPTER	PAGE
I Introduction	1
1.1 Background	1
1.2 Chloroperoxidase structure and reaction mechanism	4
1.2.1 Chloroperoxidase reaction mechanism	4
1.2.2 Structure of CPO	8
1.3 Heterologous CPO expression	15
1.3.1 <i>Aspergillus niger</i> expression system	16
1.3.2 Factors that affect CPO expression in <i>Aspergillus niger</i>	20
1.4 Objectives of this work	25
II Optimization of <i>Aspergillus niger</i> expression system and NMR study of recombinant CPO	26
2.1 Material and methods.....	26
2.1.1 Strains and reagents.....	26
2.1.2 Genomic DNA extraction and sequencing	26
2.1.3 Expression of rCPO.....	27
2.1.4 Purification of rCPO.....	27
2.1.5 Western blotting procedure.....	28
2.1.6 Circular Dichroism spectrum study.....	28
2.1.7 UV-visible absorption spectrum study	28
2.1.8 Enzyme activity Assays.....	29
2.1.9 NMR spectroscopy	29
2.2 Results and discussion	30
2.2.1 Optimization of rCPO production and purification procedure for rCPO. 30	30
2.2.2 Validation of rCPO	35
2.2.3 UV-vis & CD spectroscopic study of rCPO	37
2.2.4 NMR spectroscopic study of rCPO	38
2.3. Conclusion	48
III F103A CPO mutant preparation and properties	50
3.1 Material and methods.....	50
3.1.1 Strains and reagents.....	50
3.1.2 CPO mutant gene construction.....	50
3.1.3 Plasmid transformation into <i>Aspergillus niger</i> protoplast.....	51
3.1.4 Genomic DNA extraction and sequencing	52
3.1.5 Expression of F103A mutant.....	52
3.1.7 Western blotting procedure.....	53
3.1.8 Circular Dichroism spectrum study	53
3.1.9 UV-Visible absorption spectrum study.....	53
3.1.10 Determination of extinction coefficients of CPO mutant.....	53
3.1.11 Activity assays	54

3.1.12 Optimum pH for the chlorination activity.....	56
3.1.13 Ligand binding study.....	56
3.2. Results and discussion.....	57
3.2.1 Preparation and purification of F103A mutant.....	57
3.2.2 Structure and function study of F103A mutant.....	61
3.2.3 F103A mutant as a possible industrial catalyst.....	76
3.3 Conclusion.....	82
IV C29H/C79H/C87H CPO mutant purification and characterization.....	85
4.1 Material and methods.....	85
4.1.1 Strains and reagents.....	85
4.1.2 CPO mutant gene construction of expression plasmid.....	85
4.1.3 Plasmid transformation into <i>Aspergillus niger</i> protoplast.....	85
4.1.4 Genomic DNA extraction and sequencing.....	85
4.1.5 Expression of C29H/C79H/C87H CPO mutant.....	86
4.1.6 Total mRNA extraction and reverse transcription PCR.....	86
4.1.7 Western blotting procedures.....	86
4.2 Results and discussion.....	86
4.3 Conclusion.....	89
V In <i>vitro</i> biodegradation of carbon nanotube by CPO.....	91
5.1 Material and methods.....	91
5.1.1 Reagents.....	91
5.1.2 Nanotube biodegradation by CPO and H ₂ O ₂	91
5.1.3 Measurement of H ₂ O ₂ concentration.....	92
5.1.4 Scanning electron microscope (SEM).....	92
5.2 Results and discussion.....	92
5.3 Conclusion.....	93
VI Perspectives.....	96
REFERENCES.....	96
APPENDICES.....	105
VITA.....	112

LIST OF TABLES

TABLE	PAGE
2.1 Optimized condition for production of rCPO after 72 h culture	31
2.2 Purification result of rCPO from <i>A. niger</i> culture	35
2.3 Spin lattice relaxation times (T1) of paramagnetic shifted resonances for rCPO and Wt CPO in 0.1 M phosphate buffer, pD 5.5 and 25 °C	47
2.4 Distance between the selected protons and the heme iron in rCPO based upon spin-lattice relaxation values and from the X-ray structure of Wt CPO	48
3.1 F103A purification result	59
3.2 Spectral properties of heme thiolate proteins (P450cam, Wt CPO and F103A) and their ligand complexes	64
3.3 Optical absorption data, dissociation constants, and spin states of ferric Wt CPO & ferric F103A ligand complexes	73
3.4 Apparent K_d for cyanide binding of Wt CPO and F103A at various pH	74
3.5 Enantioselectivity study of F103A catalyzed of epoxidation reactions	81

LIST OF FIGURES

FIGURE	PAGE
1.1 Typical non-halogenating oxidation reactions catalyzed by CPO from <i>C. fumago</i> ...	3
1.2 Cpd I formation from ferric hydrogen peroxide (Fe-HOOH) via Cpd 0.....	5
1.3 Structures of a variety of intermediates formed during CPO catalyzed reactions	8
1.4 Chloroperoxidase crystal structure (complex with Mn ²⁺).....	9
1.5 <i>cis</i> - β -methylstyrene docked in the substrate pocket of CPO.....	12
1.6 The active center of CPO	14
1.7 The chromosomal integration of vector DNA into <i>Aspergillus</i>	18
1.8 The expression vector for co-transformation of <i>A. niger</i>	21
1.9 The secretion pathway in filamentous fungi	23
2.1 rCPO production yields versus days after inoculation	33
2.2 Chromatogram of ion exchange chromatography of rCPO.....	34
2.3 Chromatogram of gel filtration chromatography of rCPO.....	35
2.4 12% SDS-PAGE result of rCPO purification	36
2.5 Western blotting results of Wt CPO and rCPO	36
2.6 UV-vis spectra of rCPO and Wt CPO in 50 mM phosphate buffer, pH 5.0	37
2.7 The CD spectra of rCPO (0.4 μ M in 10 mM phosphate buffer, pH=6) and Wt CPO (0.35 μ M in 10 mM phosphate buffer, pH=6)	38
2.8 NMR spectrum of rCPO at 25 °C in 0.1 M potassium phosphate buffer.....	41
2.9 Selected signals from the NMR spectra of rCPO at various relaxation times at 25°C and pD 5.5.....	42
2.10 Determination of the spin-lattice relation times from peak intensities versus delay times.....	43

2.11 Curie plots for selected signals of rCPO	44
2.12 rCPO COSY plot and crosspeak assignments based on analogy with Wt CPO	45
2.13 rCPO NOESY plot and crosspeak assignments based on analogy with Wt CPO	46
3.1 Chromatogram of ion exchange chromatography of F103A.....	58
3.2 Chromatogram of gel filtration chromatography of F103A.....	58
3.3 Visible spectra of the free ferrous heme-pyridine complex of F103A and Wt CPO	59
3.4 15% SDS-PAGE result of F103A purification	60
3.5 Western blotting analysis results of F103A, Wt CPO and rCPO	60
3.6 UV-vis spectra of Wt CPO, and F103A in 0.05 M potassium phosphate buffer, pH 5.0, and P450 camphor in 0.05 M potassium phosphate buffer, pH 7.4.....	63
3.7 UV-vis spectra of the ferric, ferrous, and ferrous-CO complexes of the F103A in 0.05 M potassium phosphate buffer, pH 5.0.....	63
3.8 The CD spectra of F103A (0.375 μ M in 10 mM phosphate buffer, pH=6) and Wt CPO (0.3 μ M in 10 mM phosphate buffer, pH=6).....	65
3.9 Relative activities of Wt CPO, C29H, F103A and E183H mutants	65
3.10 Catalase activity assays of Wt CPO and F103A.....	66
3.11 <i>N</i> -demethylation activity comparison between Wt CPO and F103A.....	66
3.12 UV-vis spectra of F103A mutant in 0.1 M potassium phosphate buffer at pH 3	69
3.13 UV-vis spectra of the cyanide complexes of ferric Wt CPO and F103A	70
3.14 UV-vis spectra of the azide complexes of ferric Wt CPO and F103A	70
3.15 UV-vis spectra of the imidazole complexes of ferric Wt CPO and F103A.....	71
3.16 UV-vis spectra of the thiocyanate complexes of ferric Wt CPO and F103A	71
3.17 UV-vis spectra of the formate complexes of ferric Wt CPO and F103A	72

3.18 UV-vis spectra of the acetate complexes of ferric Wt CPO and F103A	72
3.19 pH profiles for chlorination activity of Wt CPO and F103A	75
3.20 UV absorbance decrease at 242 nm profiles for F103A (39 nM) catalysis of the epoxidation of α -methylstyrene, α -ethylstyrene, and α -propylstyrene (300 μ M) in 100 mM citrate buffer, pH = 5.5.....	77
3.21 UV absorbance decrease at 243 nm profiles for F103A (39 nM) catalysis of the epoxidation of 2-methyl-phenyl-1-propene and 1,2-dimethyl-propenyl-benzene (300 μ M) in 100 mM citrate buffer, pH = 5.5	78
3.22 UV absorbance decrease at 250 nm profiles for F103A (39 nM) catalysis of the epoxidation of trans- β -methylstyrene, trans-1-phenyl-1-butene, and trans-1-phenyl-1-pentene (300 μ M) in 100 mM citrate buffer, pH = 5.5.....	78
3.23 Chiral HPLC trace of the products obtained from the epoxidation of styrene catalyzed by Wt CPO	80
3.24 Chiral HPLC trace of the products obtained from the epoxidation of styrene catalyzed by F103A.....	81
4.1 Confirmation of positive transformation and transcription of C29H/C79H/C87H mutant	88
4.2 Western blotting analysis on extracted both cellular and extracellular protein samples from <i>A. niger</i> strain (ATCC 62590) transformed with CPO expression vector pCPO#3C to detect CPO mutant expression	89
5.1 SEM images of SWNTs treated with CPO for 8 weeks	93

LIST OF ABBREVIATIONS

ABBREVIATION	FULL NAME
Aa	Amino acid
ABTS	2,2'-azino-bis-3-ethyl-benzthiazoline-6-sulfonic acid
ALA	δ -Aminolevulinic Acid
<i>A.niger</i>	<i>Aspergillus niger</i>
ATCC	American type culture collection
BSA	Bovine serum albumin
BHT	Butylated hydroxytoluene
<i>C. fumago</i>	<i>Caldariomyces fumago</i>
CD	Circular Dichroism
COSY	Correlation spectroscopy
CPD	Cyclopentanedione
Cpd 0	Compound 0
Cpd I	Compound I
Cpd II	Compound II
Cpd X	Compound X
CPO	Chloroperoxidase
DNA	Deoxyribonucleic acid
DMF	<i>N,N</i> -dimethylformamide
ee%	Enantiomeric excess
ER	Endoplasmic reticulum

ϵ	Extinction coefficient
<i>E. coli</i>	<i>Escherichia coli</i>
F103A	CPO with F103 to A mutation
GLA	Glucoamylase
HPLC	High-performance liquid chromatography
HRP	Horseradish peroxidase
MCD	Monochlorodimedone
Mnp	Manganese peroxidase
rMnp	Recombinant manganese peroxidase
NMR	Nuclear magnetic resonance spectroscopy
NOESY	Nuclear overhauser enhancement spectroscopy
P450	Cytochrome P450
P450cam	P450 camphor
PCR	Polymerase chain reaction
rCPO	Recombinant CPO
RNA	Ribonucleic acid
RT PCR	Reverse transcription PCR
Rz value	Reinheitzahl value
ROS	Reactive oxygen species
SWNTs	Single-walled nanotubes
SDS-PAGE	Sodium dodecyl sulfate polyacrylamide gel electrophoresis
SEM	Scanning electron microscope

T1	Spin-lattice relation time
TBST buffer	Tris buffered saline with tween buffer
UV-vis	Ultraviolet-visible
Wt CPO	Wild type CPO

Chapter I

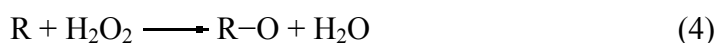
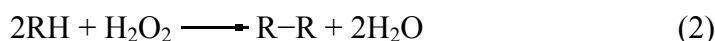
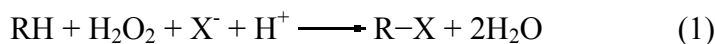
Introduction

1.1 Background

Chloroperoxidase (CPO, EC 1.11.1.10) was originally isolated by Morris and Hager from the marine filamentous fungus, *Caldariomyces fumago* (*C. fumago*) in 1966 (Hager, Morris et al. 1966; Morris and Hager 1966; Brown and Hager 1967), as the enzyme responsible for the halogenations of caldariomycin, an antibiotic secreted by *C. fumago*. Chloroperoxidase is a heavily glycosylated monomeric heme protein with carbohydrates accounting for 19% ~25% of the total molecular weight and one ferriprotoporphyrin IX prosthetic group per enzyme molecule (Hallenberg and Hager 1978). Chloroperoxidase derives its catalytic activity from its heme prosthetic group, and has a Soret band with an absorbance maximum at 398 nm and an extinction coefficient of $9.10 \times 10^4 \text{ M}^{-1} \text{ cm}^{-1}$ (Hallenberg and Hager 1978). Initially, two isoforms with molecular weights of approximately 42 and 46 kDa were reported, but later work found additional isoforms that also differed in their carbohydrate content (Kenigsberg, Fang et al. 1987). The pH optimum for chlorination and the isoelectric point (pI) were determined to be 2.7 and 4 respectively (Makino, Chiang et al. 1976).

Chloroperoxidase occupies a key position amongst heme containing proteins, and it is the most versatile and efficient enzyme within the heme-peroxidase family. In addition to peroxide dependent halogenations (Thomas and Hager 1968; Thomas, Morris et al. 1970), CPO is also able to catalyze a broad spectrum of reactions (Thomas, Morris et al. 1970; Hofrichter and Ullrich 2006), including the typical peroxidase reactions, catalase reactions (Thomas, Morris et al. 1970), some P450-like oxidation reactions (Hollenberg

and Hager 1973), as outlined in scheme 1.1. Site directed mutagenesis of CPO offers the possibility of determining residues important for the catalase, cytochrome P450 mono-oxygenase, and peroxidase activities of CPO, and the potential of elucidating the relationship between these diverse activities.



Scheme 1.1 Halogenase, peroxidase, catalase, and mono-oxygenase types of reactions catalyzed by CPO are given in Equations 1→4, respectively. E represents the resting form of enzyme CPO; both RH and R represent substrates; X⁻ is the halide ions.

In addition, CPO has the potential to catalyze the synthesis of a wide range of chiral or prochiral products. Chloroperoxidase can catalyze many reactions that are important in synthesis such as sulfoxidation (Silverstein and Hager 1974; Doerge 1986), hydroxylation (Miller, Tschirret-Guth et al. 1995) and epoxidation (Geigert, Lee et al. 1986), enantioselectively and in high yield (Casella, Poli et al. 1994; Lakner and Hager 1996), such as the epoxidation of olefins (Ortiz de Montellano, Choe et al. 1987), where traditional peroxidases have failed. Other reactions such as *N*-demethylation (Kedderis, Koop et al. 1980) and dehalogenation (Osborne, Raner et al. 2006) are also possible. Some selected non-halogenating oxidation reactions catalyzed by CPO are listed in fig. 1.1. Unlike P450, CPO can catalyze these reactions without cofactors like NAD(P)H, which are difficult to recover and recycle in industry; other peroxidases and catalases catalyze these reactions very slowly, if at all.

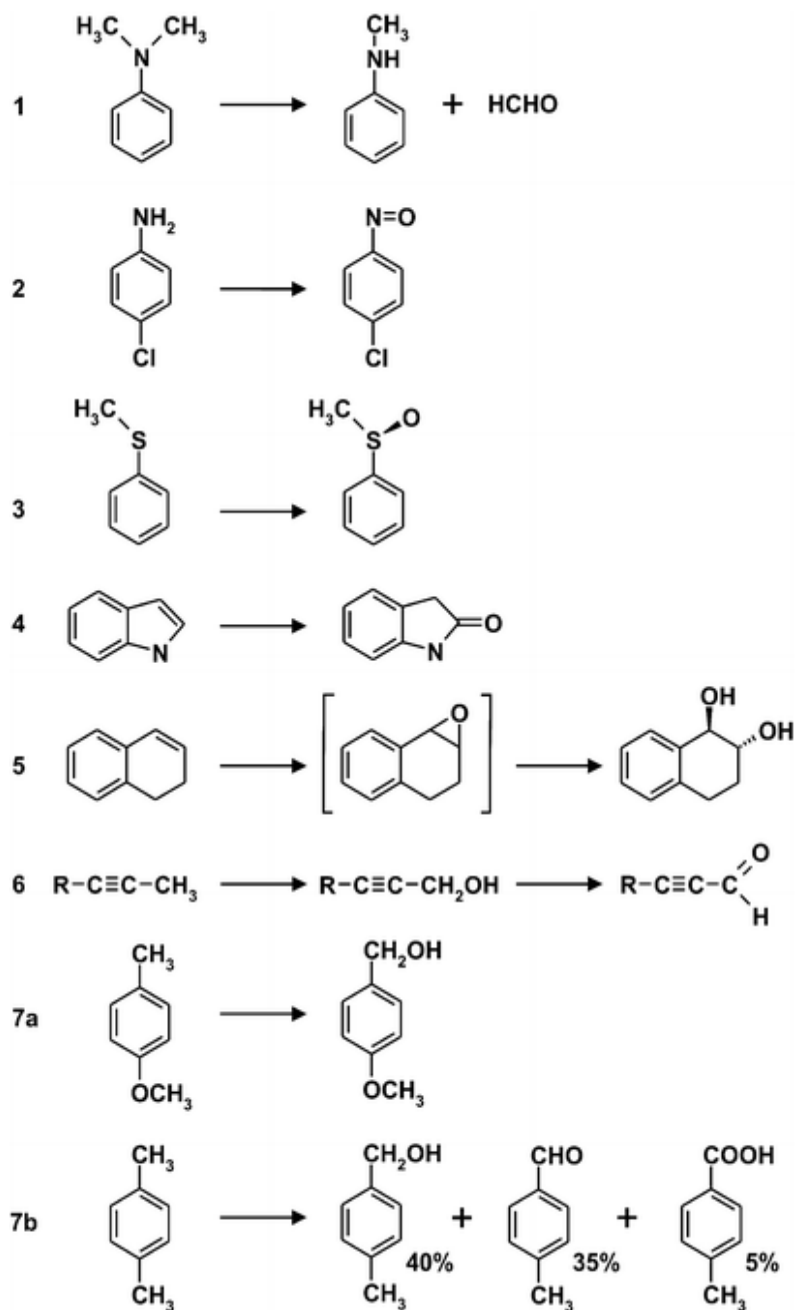


Figure 1.1 Typical non-halogenating oxidation reactions catalyzed by CPO from *C. fumago*. The figure was copied from Ullrich et al (Hofrichter and Ullrich 2006). 1. *N*-dealkylation, e.g. *N,N*-dimethylaniline to *N*-methylaniline; 2. oxidation of an amine to the corresponding *N*-oxide, e.g. *p*-chloroaniline; 3. enantioselective sulfoxidation of thioethers, e.g. thioanisole to (*R*)-methylphenylsulfoxide; 4. oxidation of indole to oxindole; 5. epoxidation / hydroxylation of 1,2-dihydronaphthalene; 6. hydroxylation of a propargyl group; 7a. hydroxylation of *p*-methylanisole; and 7b. sequential oxidation of one methyl group in *p*-xylene to the carboxylic acid.

Chloroperoxidase, however, suffers from two drawbacks as a choice of catalyst for industrial uses: CPO is able to accept only a few substrates and has limited stability under catalytic conditions. Generally, substrates with at most nine carbon atoms, or equivalent are accepted (Hofrichter and Ullrich 2006). The limited stability is because of a self-destructive reaction with hydrogen peroxide, which is problematic for slow reactions, including hydroxylations (Miller, Tschirret-Guth et al. 1995) and epoxidations (Hager, Lakner et al. 1998). It is possible that site-directed mutagenesis and protein engineering will help to overcome these shortcomings.

1.2 Chloroperoxidase structure and reaction mechanism

1.2.1 Chloroperoxidase reaction mechanism

Reactions catalyzed by CPO can be classified into four categories. The first is halogenation reactions, which utilize three substrates: hydrogen peroxide or other hydroperoxides, halide ions except fluoride, and a wide range of suitable substrates (Corbett, Chipko et al. 1980). The second is the classic peroxidase reactions with a substrate and hydrogen peroxide, but without a halide ion. In the absence of a halide ion and organic substrate, CPO can catalyze reactions as a catalase: the disproportionation of hydrogen peroxide into dioxygen and water. Lastly, CPO shares some catalytic activities with cytochrome P450, such as mono-oxygenase reactions (Geigert, Neidleman et al. 1983).

In the resting state, CPO has a ferric protoporphyrin IX in its active site. The ferric center then reacts with peroxide to form a short-lived intermediate, termed as “compound 0” (Cpd 0). Heterolytic cleavage of the O-O bond in the loosely bound hydrogen peroxide molecule of Cpd 0 results in the formation of Compound I (Cpd I) and one

molecule of water (Penner-Hahn, McMurry et al. 1983; Frew and Jones 1984; Penner-Hahn, Smith Eble et al. 1986; Kim, Perera et al. 2006; Denisov, Dawson et al. 2007), as showed in Fig 1.2.

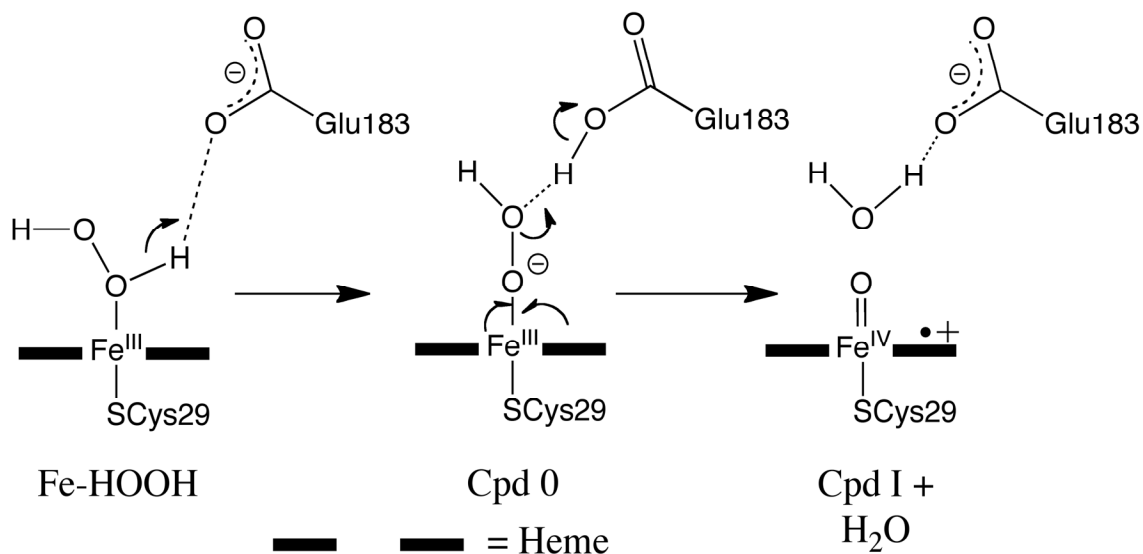
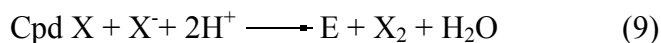
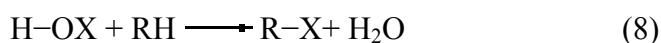
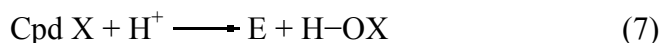
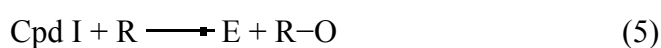
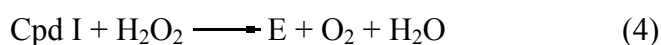
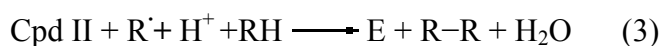
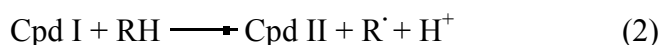
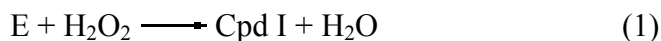


Figure 1.2 Cpd I formation from ferric hydrogen peroxide (Fe-HOOH) via Cpd 0.

Compound I is a typical intermediate of many heme peroxidases, and its structure is an oxo-ferryl porphyrin cation-radical complex [heme ($\text{Fe}^{4+}=\text{O})^{\cdot+}$] (Kobayashi, Nakano et al. 1987). It is widely accepted that the formation of Cpd I is the first step for all the reactions that CPO catalyzes (Libby and Rotberg 1990; Green, Dawson et al. 2004). Although Cpd I of CPO is short-lived (Araiso, Rutter et al. 1981), it is the only Cpd I of a thiolate-ligated heme enzymes that is well characterized by many spectroscopic methods including UV-vis absorption, EPR, Mossbauer, and resonance Raman (Palcic, Rutter et al. 1980; Sono, Eble et al. 1985; Hosten, Sullivan et al. 1994). Since CPO and P450 share the same proximal thiolate ligand, they also have many spectroscopic similarities. Therefore, the information from Cpd I of CPO may be relevant to the putative and elusive

P450 Cpd I species. The basic pathways of CPO-catalyzed reactions are summarized in Scheme 1.2.



Scheme 1.2 Pathways of basic reactions catalyzed by CPO are listed in Equations 1 to 7. Cpd I, Cpd II, and Cpd X are the enzymatic cation radical intermediate compound I, reduced intermediate compound II, and electrophilic halogenation intermediate compound X, respectively. Eqn. 1 CPO reacts rapidly with H_2O_2 to form Cpd I, this is the initial step in all CPO catalyzed reactions. Eqn. 2 & 3 completes the classic peroxidase reaction. Eqn. 4 is the catalase reaction. Eqn. 5 is the mono-oxygenase reaction. Eqn. 6 is the initiation step of the halide dependent reactions. Eqn. 7 & 8 completes the normal halogenation pathway. Finally, Eqn. 9 is the pathway for formation of molecular halogen. It should be noted that a variety of organic hydroperoxides (ROOH's) or peroxy acids can replace H_2O_2 in reactions.

In the peroxidase mode, Cpd I abstracts a hydrogen atom from an organic substrate (RH) to produce an organic radical (R^\cdot), and in the process Cpd I is converted to Cpd II, which is assumed to be a $Fe^{IV}=O$ (Green, Dawson et al. 2004; Stone, Behan et al. 2006). The reaction involves a one-electron transfer. The intermediate Cpd II then oxidizes another substrate molecule to return to the ferric resting state (Nakajima, Yamazaki et al.

1985; Terner, Palaniappan et al. 2006; Gebicka and Didik 2007). Again a one-electron transfer reaction. CPO catalyzes the dehalogenation reaction using a similar mechanism (Zhang, Nagraj et al. 2006).

In the catalase mode, Cpd I reacts with a second molecule of hydrogen peroxide, in a two electron process, to produce dioxygen and the resting ferric state of the heme iron (Araiso, Rutter et al. 1981; Sun, Kadima et al. 1994).

In halogenase mode, Cpd I reacts with a halogen ion to form compound X (Cpd X), then Cpd X reacts with the substrate or water, either generating a chlorinated product (Champion, Munck et al. 1973; Suh and Hager 1991) or HOX, respectively (Libby, Shedd et al. 1992). The HOX can also oxidize organic molecules. The dual mechanism of halogenations is proposed to explain the general lack of enantioselectivity during halogenation reactions catalyzed by CPO. Compound X can react with a variety of substrates to perform halogen dependent peroxidatic, catalatic, and peroxygenase reactions (Dunford, Lambeir et al. 1987; Kobayashi, Nakano et al. 1987; Aaronson, Hager et al. 1988; Libby, Rotberg et al. 1989). Cpd X can also react with a halogen ion to form molecular halogen.

In the mono-oxygenase mode, Cpd I reacts directly with the substrate in a two-electron process, this is the underlying mechanism for a variety of reactions that CPO catalyzes, such as mono-oxygenation (Geigert, Lee et al. 1986; Ortiz de Montellano, Choe et al. 1987; Horner, Mouesca et al. 2007), hydroxylation (Miller, Tschirret-Guth et al. 1995), sulfoxidation (Casella, Gullotti et al. 1992) and demethylation (Kedderis, Koop et al. 1980; Kedderis and Hollenberg 1984).

The structures of the above reaction intermediates, together with how they convert to other intermediates in the catalytic cycles are summarized in Fig. 1.3; as indicated, halide ions, organic substrates, and H₂O₂ compete with each other for reaction with Cpd I (Sun, Kadima et al. 1994), thus the actual reaction depends on several factors including pH, substrate, and solvent (Araiso, Rutter et al. 1981).

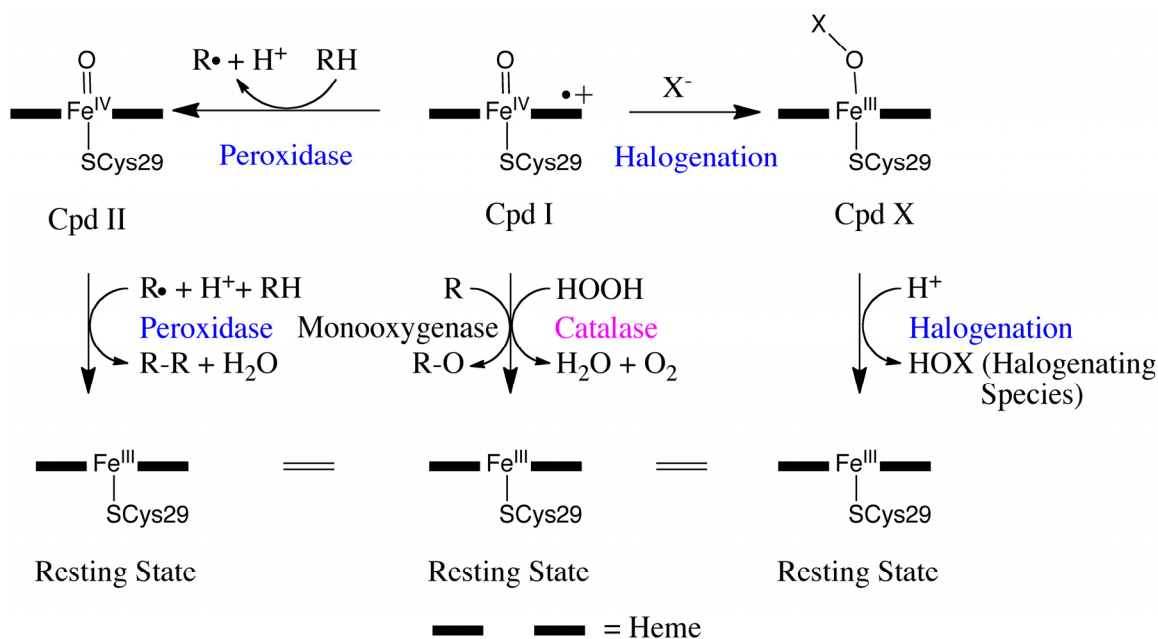


Figure 1.3 Structures of a variety of intermediates formed during CPO catalyzed reactions. For classic peroxidase reaction: Cpd I \Rightarrow Cpd II \Rightarrow Resting state (without oxygen transfer to the substrate); for halogenations reactions: Cpd I \Rightarrow Cpd X, Cpd X could release hypohalous acid (HOX) as one of the halogenating species; for epoxidation, and sulfoxiation reactions: Cpd I \Rightarrow Resting state (oxygen transfer to the substrate).

1.2.2 Structure of CPO

Although mature CPO contains 299 aa, it is initially produced as a 372-aa precursor which is subsequently processed by proteolytic cleavage: A 21 aa N-terminal signal peptide, and a 52 aa C-terminal propeptide are removed, (Fang, Kenigsberg et al. 1986).

The 3-dimensional structure of mature CPO was solved by crystallographic refinement in 1995 (Sundaramoorthy, Turner et al. 1995) (Fig 1.4). Structural studies offer insights into the mechanism, versatility, and enantioselectivity of CPO.

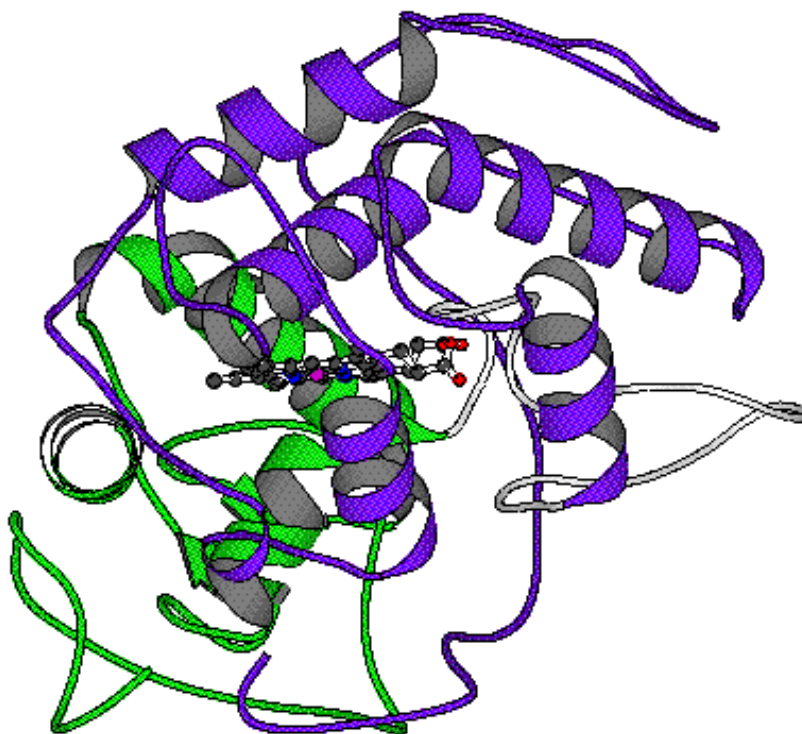


Figure 1.4 Chloroperoxidase crystal structure (complex with Mn^{2+}). The figure was copied from Sundaramnoorthy et al (Sundaramoorthy, Turner et al. 1995).

As shown in Fig. 1.4, the scaffold of CPO consists of eight α -helices (Rubin, VanMiddlesworth et al. 1982; Sundaramoorthy, Turner et al. 1995). Unlike most peroxidases and cytochrome P450s, where the α -helix on the proximal side is near the C-terminal, and lies parallel to the heme; in CPO, it is near the N-terminal, and lies perpendicular to the heme. The exact role of this structural feature, however, is still unknown (Sundaramoorthy, Turner et al. 1998). The crystal structure also shows that CPO is extensively glycosylated with both N- and O-linked oligosaccharide chains. There

are three N-linked oligosaccharide chains and eleven O-linked oligosaccharide chains. The O-glycosylation sites are in the C-terminal domain, which contains numerous serine and threonine residues. (Sundaramoorthy, Turner et al. 1995).

The catalytic center of CPO contains a single high spin protoporphyrin IX (heme) that is sandwiched between an N-terminal and a C-terminal helix. In CPO, the iron atom is penta-coordinated, with four pyrrole nitrogens of the porphyrin and a sulfur of cysteine, a feature that had only been observed previously in P450s (Boddupalli, Hasemann et al. 1992; Hasemann, Kurumbail et al. 1995). For other peroxidases, it is histidine ligated to the heme center.

Even though CPO's uniquely folded tertiary structure does not resemble that of peroxidase or P450, CPO shares some structural similarities with both types of enzymes. Both P450 and CPO have cysteine as the proximal ligand, while peroxidases have histidine. The hydrogen-bonding networks close to the proximal cysteine are also similar. P450 and CPO allow organic substrates to approach the heme iron, but peroxidases only allow organic substrates to approach the side of the heme. The distal heme surface that surrounds the peroxide binding site is polar in both peroxidases and CPO, but not P450.

An important difference between peroxidase and P450 is the accessibility of the heme center. In peroxidase, substrate-protein interactions are limited to the heme edge as access to the ferryl center is blocked. Therefore, radicals are produced from aromatic organic substrates as only electrons are transferred. (Hewson and Hager 1979; Schulz, Devaney et al. 1979). P450s, however, allow organic substrates access to the ferryl center, as they have an active-site pocket directly adjacent. Thus, P450s can lock the substrate in place and transfer oxygen atoms for stereoselective and regioselective hydroxylations. In

a similar fashion as P450, CPO allows organic substrates access to the ferryl center. On the distal side of the heme center in CPO, there is a shallow hydrophobic pocket, where hydrophobic substrates likely bind (Hasemann, Kurumbail et al. 1995). The channel to access the ferryl center is relatively polar and wide at the top but mostly hydrophobic near the heme (Sundaramoorthy, Turner et al. 1998). Three hydrophobic amino acids Phe103, Val182, and Phe186 are positioned at the bottom of the opening to the ferryl center (Sundaramoorthy, Turner et al. 1995) and are proposed to interact with the substrates, as well as to control the size of substrate that enters the active center. Compared to other peroxidases, such a structure can enable CPO to hold substrates in a specific conformation, and accounts for its highly enantioselective and regioselective reactions.

Chloroperoxidase, in general, chlorinates substrate with low regioselectivity and non stereospecificity; however, glycols and steroids are exceptions. Therefore, there must be an interaction between glycols and steroids, and CPO (Libby, Thomas et al. 1982; Geigert, Neidleman et al. 1983). Stereospecific epoxidation and sulfoxidation of organic substrates also suggests binding at the active site of CPO (Casella, Gullotti et al. 1992; Casella, Poli et al. 1994). The binding of CPO to *cis*- β -methylstyrene has been modeled using information from the crystal structure as shown in Fig. 1.5, since CPO catalyze the expoxidation of substrates with an enantiomeric excess (ee %) up to 96%. Both Phe103 and Phe186 are proposed to interact with the substrate and account for the high enantioselectivity

Except for the absence of a sixth ligand, the distal region has little similarity to other peroxidases. On the distal side of CPO, there is a water molecule 3.4 Å away from the

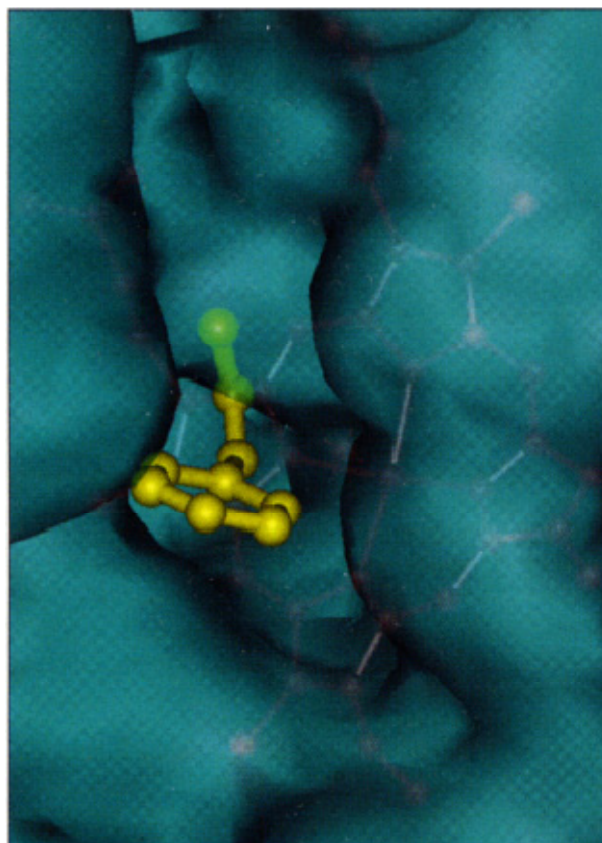


Figure 1.5 *cis*- β -methylstyrene docked in the substrate pocket of CPO. The figure was copied from Sundaramoorthy et.al. (Sundaramoorthy, Turner et al. 1998). A semi-transparent molecular surface diagram with the docked *cis*- β -methylstyrene (in yellow) located just above the heme outlined (in red).

heme iron (Sundaramoorthy, Turner et al. 1995; Wang, Tachikawa et al. 2003). This water molecule is displaced by the incoming H_2O_2 during reactions. Instead of a distal histidine or arginine found in other peroxidase, Glu183 is the residue closest to the heme iron, and is proposed to be responsible for breaking the peroxide bond during the formation of Cpd I. The required high redox potential to oxidize substrate like chloride may explain why CPO has an acidic pH optimum, since the acidic amino acid Glu183 needs to perform a similar role as the basic amino acid in other peroxidase and Cpd I usually exhibits higher redox potential at acidic pH value (Sundaramoorthy, Turner et al. 1998).

Glutamic acid 183 is thought to act as a shuttle that transfers a proton from the proximal O atom of the Fe-HOOH complex to the distal O atom. Initially, deprotonated Glu183 removes a proton from the incoming HOOH (Kuhnel, Blankenfeldt et al. 2006). The resulting HOO⁻ anion then binds at the heme producing a ferric-hydroperoxo species, also called compound 0 (Cpd 0) (Denisov, Dawson et al. 2007). Subsequently, the distal oxygen of Cpd 0 is protonated by neutral Glu183, the O–O bond is broken, and water is released to form Cpd I. The mechanism is similar to the Poulos-Kraut mechanism for peroxidases except that Glu is used instead of His. Glutamic acid 183 is proposed to be held in position by a hydrogen bond to His105, which may also provide charge-charge stabilization. Furthermore, the cleavage of H₂O₂ could be facilitated by Glu183, His105, and Asp106 acting as a proton relay shuttle (Fig. 1.6) (Pelletier, Altenbuchner et al. 1995; Wang, Tachikawa et al. 2003).

Among CPO-substrate complexes, only the binding of CPD and acetate caused minor conformational changes at the active site. In both cases, to make room for the substrate, there was a 0.5 Å shift of the side chain of Phe103 away from the active site. In all structures determined so far, the position of the catalytically important Glu183 has been fixed. The side chain carboxylate group of Glu183 is “locked”, because it is hydrogen bonded to His105 and a water molecule that is hydrogen bonded with the propionate group of the heme. In addition, the carboxylate group of Glu183 is held in position by pi-pi interactions with the heme. Not surprisingly, the “locked” Glu183 side chain has similar B-factors as the nearby main-chain atoms. Asn74 was also involved in stabilizing several substrate by forming hydrogen bond with their carboxyl group (Kuhnel, Blankenfeldt et al. 2006).

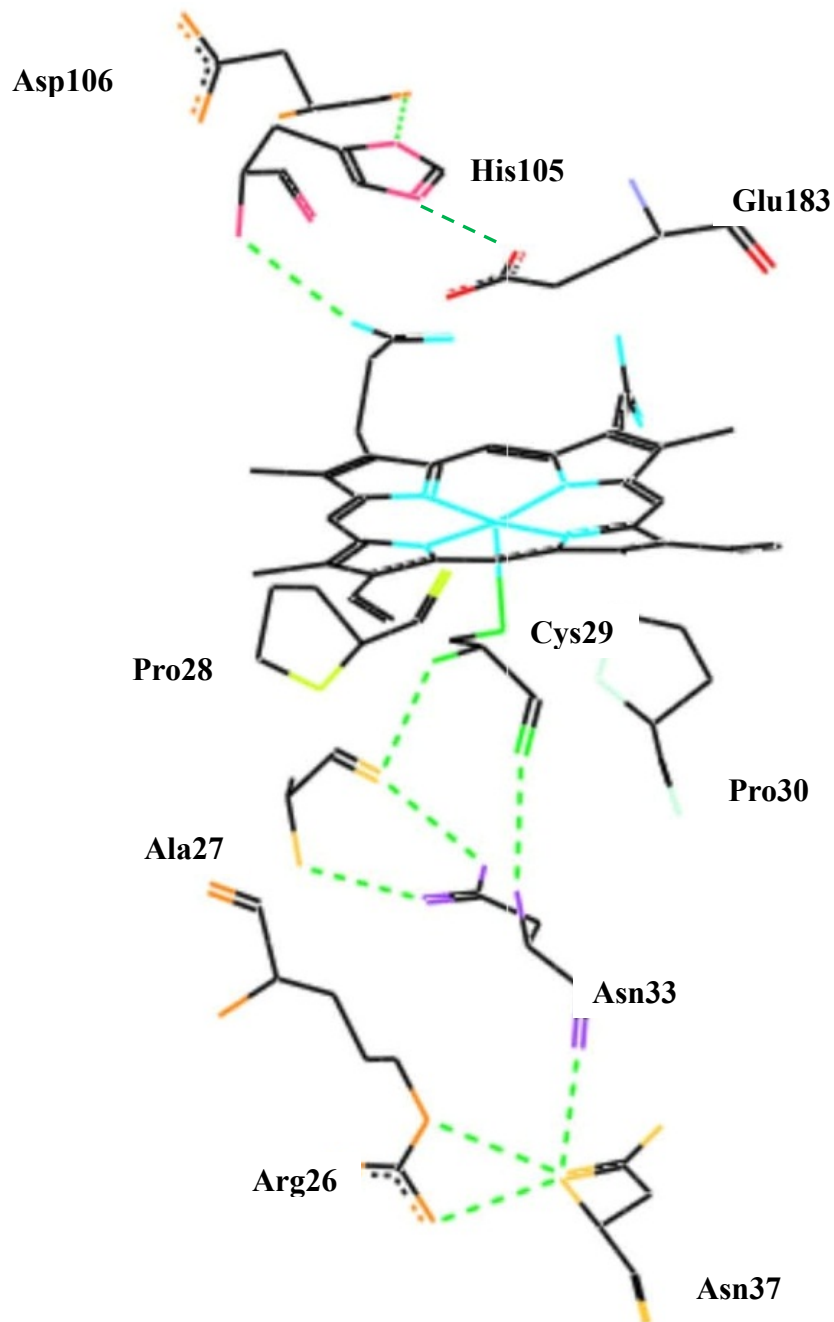


Figure 1.6 The active center of CPO. Residues His105, Asp 106, and Glu183 on the distal side and residues from Arg26 to Pro30, Asn33, and Asn37 on proximal side of the heme are indicated. Coordination of the proximal ligand to the heme is represented by a solid line. Hydrogen bonds are indicated by dashed lines.

1.3 Heterologous CPO expression

Due to advances in biotechnology, cloned genes can be heterologously expressed in a controlled manner and the resulting protein purified, however, the system needs to be carefully selected. Site directed mutagenesis studies are usually undertaken only after the successful expression of the native protein, (Frandsen, Dupont et al. 1994; Inoue, Hayashi et al. 1996; Sriprang, Asano et al. 2006). Because the expression of native CPO involves glycosylation, incorporation of a heme prosthetic group, formation of disulfide bonds, and the cleavage of N- and C-terminal peptides, production of CPO in prokaryotes, which perform these activities poorly, if at all, will be challenging. Not surprisingly, the expression of CPO in *Escherichia coli* (*E. coli*) has had only limited success, the results showed that the non-glycosylated enzyme was obtained in its apoform without the heme being incorporated into the enzyme. Only under high pressure, can the protein be refolded with heme to generate a somewhat active enzyme in very low yield (Zong, Osmulski et al. 1995).

Therefore, the expression of CPO in several eukaryotic systems was investigated. When the CPO gene was expressed in *Baculovirus* only an inactive form of the protein was obtained (Wang, Yao et al. 2003), and the active protein could not be reconstituted. Expression of the CPO gene in yeast, *Saccharomyces cerevisiae* and *Pichia pastoris* also did not lead to the production of active protein (Zong 1997). Expression of a mutant of CPO in the parental host itself, *C. fumago* has also been reported (Yi, Mroczko et al. 1999). However, the presence of residual wild type CPO (Wt CPO), complicated the selection of recombinant CPO producing strains and did not provide sufficient recombinant protein (rCPO) for subsequent investigations.

Recombinant CPO with catalytic properties almost identical to Wt CPO was reported in 2001 by Conesa et al. (Conesa, van De Velde et al. 2001). The rCPO was produced in the filamentous fungus *Aspergillus niger* (*A. niger*). Two years later, the same group reported the successful expression and characterization of the E183H mutant of CPO (Yi, Conesa et al. 2003).

1.3.1 *Aspergillus niger* expression system

The industrial production of heterologous proteins in filamentous fungal species is wide spread for three main reasons: First, filamentous fungi can secrete large quantities of protein into the surrounding media (Lubertozzi and Keasling 2009); Second, their use in the commercial production of small molecules via fermentation has led to familiarity (Lubertozzi and Keasling 2009); Third, the availability of a complete genetic map for some species, the successful development of procedures for performing molecular biology, and a good genetic system (Visser, Bussink et al. 1995; Gouka, Punt et al. 1996). One of the most common fungal species of the genus *Aspergillus* is *A. niger*. It is characterized by its black spore, by which it is named after (Daboussi, Djeballi et al. 1989). *Aspergillus niger* is used for the commercial production of both small molecules and proteins. Citric acid and gluconic acid are obtained from *A. niger* fermentations. Glucoamylase, used in the production of high fructose corn syrup, comes from *A. niger* (Kriechbaum, Heilmann et al. 1989). Isotopically labeled macromolecules for NMR analysis can be obtained from *A. niger* fermentations (Roth and Dersch 2010).

In the past decade, *A. niger* and other filamentous fungi have emerged as powerful host systems for expressing recombinant proteins (Punt, van Biezen et al. 2002). *Aspergillus niger* is a eukaryotic host, able to perform post-translational modifications,

and is extraordinary in its capability of secreting large amounts of proteins, metabolites, and organic acids into the growth medium (Visser, Bussink et al. 1995; Withers, Swift et al. 1998). For decades, the food and beverage industry has used these advantageous properties to successfully obtain compounds from the secretion of filamentous fungi. Recombinant proteins of fungal origin can be produced in *A. niger*, at the grams per liter level (Spencer, Morozov-Roche et al. 1999; Conesa, van den Hondel et al. 2000). In addition, a full genetic map is available and annotation is nearly complete (Swart, Debets et al. 2001).

Methods for the genetic manipulation of *Saccharomyces* and *E. coli* were greatly simplified by the discovery of plasmids, natural extrachromosomally replicating DNA elements. Unfortunately, *Aspergillus* lacks such elements, as is the case for most fungi. Transformations in *Aspergillus* occur via genomic integration of the transforming DNA. The transforming DNA can be incorporated at homologous and non-homologous (ectopic) sites, and even multiple times. The situation is half way between that of yeast and mammalian cells. In yeast, transforming DNA is usually incorporated at the homologous site with low frequency while in mammalian cells, transforming DNA is incorporated at non-homologous sites with high frequency and any homologous recombination is difficult to detect (Fig. 1.7) (Chakraborty, Patterson et al. 1991). Although 50 or more copies of the transforming DNA can be incorporated into *Aspergillus*, single digit frequencies are more common (Turnbull, Smith et al. 1990). *Aspergillus* cells containing multiple copies are, in general, mitotically stable (Liu, Liu et al. 2003). For several reasons, it would, however, be desirable to have a single event at the homologous site (Verdoes, van Diepeningen et al. 1994). Firstly, the number of copies in the genome does

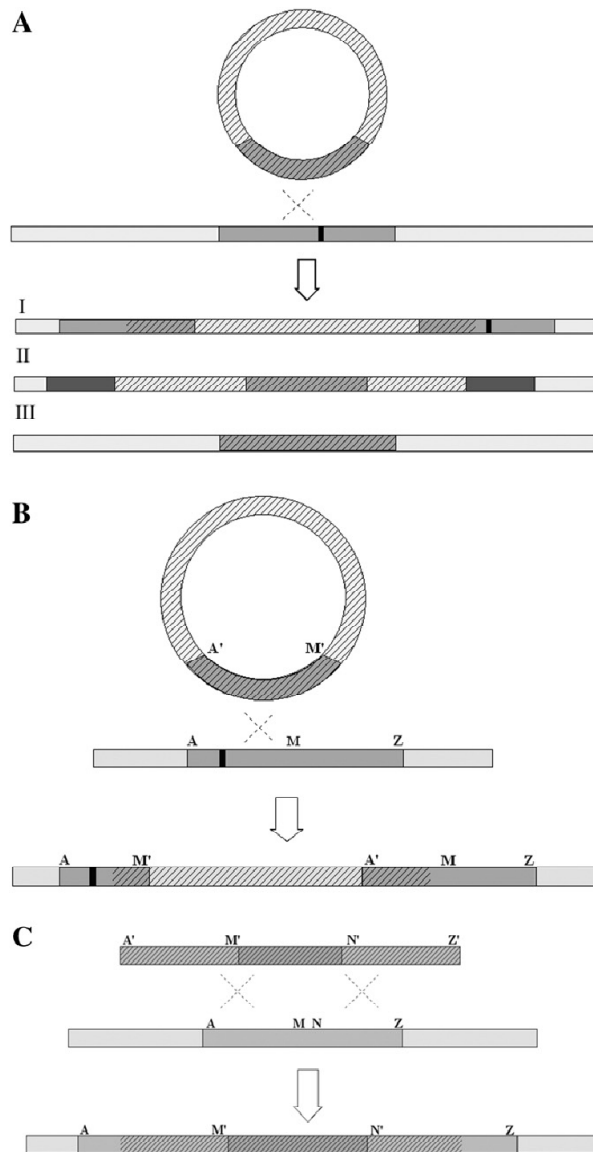


Figure 1.7 The chromosomal integration of vector DNA into *Aspergillus*. The figure was copied from (Lubertozzi and Keasling 2009). (A) Integration of circular plasmid by single crossover. Plasmid (shaded) bearing wild type marker (gray) recombines with auxotrophic mutant host chromosome (gray with black bar indicating mutation). (I) Type I or homologous integration. (II) Type II or ectopic integration; the dark gray bars represent an interrupted gene sequence. (III) Type III gene replacement; here the chromosomal marker is replaced by the plasmid copy, restoring it to wild-type. (B) Integration of a plasmid bearing a truncated wild-type marker; only recombination at the homologous locus reconstitutes the functional marker gene. Sequence A' to M' on the plasmid is homologous to A to M in the target; the black bar indicates location of amutation in auxotrophic host. (C) Insertion of linear DNA; here A' to M' and N' to Z' flanking the marker (darker gray) are homologous sequences corresponding to those at A to M and N to Z, respectively, in the chromosomal target (lighter gray).

not correspond with protein expression levels. Secondly, the location of the DNA within the genome can alter its expression level significantly. When the position of native genes within the genome are changed, their expression levels vary dramatically (Conesa, van den Hondel et al. 2000). Thirdly, incorporation of DNA randomly into the genome will cause mutations and, correspondingly, unpredictable side effects (Ruiz-Diez 2002). Cells with at least one homologous integration event can be selected for by using a truncated or mutated form of a wild-type selection marker (Hanegraaf, Punt et al. 1991). Although several systems have been developed based on the method outlined above, and *Aspergillus* is used to produce small molecules and proteins commercially, the expression of proteins in *Aspergillus* is still not straight forward and remains quite challenging (Mooibroek, Kuipers et al. 1990; Turnbull, Smith et al. 1990; Verdoes, Punt et al. 1993).

Since versatile DNA transfer and gene expression systems are developed for these organisms, the necessary tools are available for the production of recombinant proteins (Juge, Svensson et al. 1998). Furthermore, *A. niger* has no detectable extracellular and intracellular peroxidase, and therefore, in contrast to the *C. fumago* system, no interference of endogenous oxidizing activities when screening for CPO producing transformants (Conesa, van den Hondel et al. 2000). In the past ten years, several reports on the expression of metalloproteins in filamentous fungi have been published (Juge, Svensson et al. 1998; Conesa, Jeenes et al. 2002). However, although production of active recombinant enzymes was found in most cases, yield levels were still far away from those obtained for less complex fungal proteins, making the secretion of metalloproteins an intriguing subject of study (Gordon, Khalaj et al. 2000; Ngiam, Jeenes et al. 2000).

The host of choice for CPO expression, *A. niger* MGG029, is frequently used for the heterologous expression of proteins because it has many favorable attributes. The strain is protease deficient as result of a regulatory mutation, which reduces the number of endogenously expressed proteases. In addition, the strain is missing the *glaA* gene, which is responsible for the production of glucoamylase (GLA). Therefore, the secretion of GLA can be used to indicate the successful expression of a GLA fusion construct. Furthermore, *A. niger* MGG029 carries a nonfunctional *pyrG*, thus, *pyrG* can be used as a selection marker (Conesa, van De Velde et al. 2001).

The transforming vector pCPO3.I contains the full length CPO coding sequence placed under control of the *A. niger* glucoamylase promoter and *A. nidulans trpC* terminator. *Aspergillus nidulans AmdS* selection marker was introduced in pCPO3.I at a unique *NotI* site to obtain the CPO expression vector pCPO3.I-AmdS (Fig. 1.8) (Conesa, van De Velde et al. 2001). The vector also contains the pU19 vector sequence to enable its multiplication in *E. coli* and so that it can be shuttled between *E. coli* and *A. niger*.

1.3.2 Factors that affect CPO expression in *Aspergillus niger*

As described earlier, one advantage of the *A. niger* expression system is its ability to secrete peroxidase into the extracellular medium in high quantity (Conesa, Punt et al. 2002). This property of extracellular secretion is very important for the expression of sufficient recombinant protein for structure and mechanism studies in the laboratory, since CPO is more stable in the acidified culture media, and can also help to simplify the purification procedures. In order to improve the in general low production yields, the process of overproduction of heme-containing proteins, has been subjected to numerous studies in the past, (Gouka, Punt et al. 1997; Conesa, van den Hondel et al. 2000).

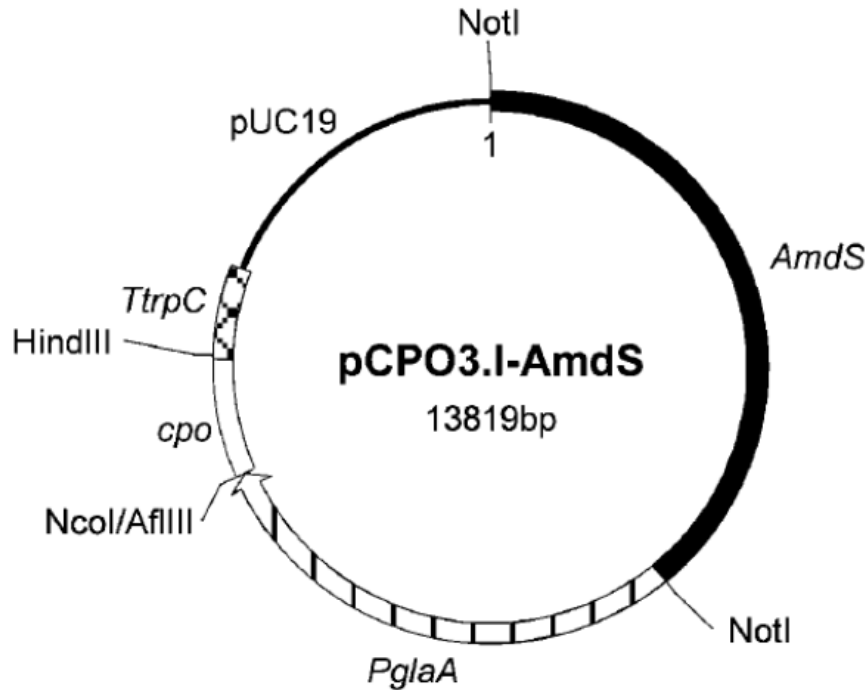


Figure 1.8 The expression vector for co-transformation of *A. niger*. The figure was copied from Conesa et.al (Conesa, van De Velde et al. 2001)

For heme-containing proteins, limited heme availability has been indicated as a limiting factor. The production of rCPO could be increased by heme addition to the culture medium (Conesa, van De Velde et al. 2001). Similar results have been obtained in previous studies by our group and other groups on the expression of fungal peroxidase in *Aspergillus* species (Yi, Conesa et al. 2003). However, experiments show that despite heme supplementation, rCPO was only partially (40%) incorporated with heme (Yi, Conesa et al. 2003). It is in contrast to observations on the production of *Phanerochaete chrysosporium* manganese peroxidase in *A. niger*, where the recombinant enzyme could be produced with the same heme content as the native protein (Conesa, Punt et al. 2002). A possible reason for this different behavior may be the different nature of heme

attachment in the manganese peroxidase (axial ligand: histidine) and CPO (axial ligand: cysteine).

The addition of δ -aminolevulinic acid (ALA) as heme precursor to the culture medium increased the secretion level of the E183H mutant of CPO by 4-fold (Yi, Conesa et al. 2003). δ -aminolevulinic acid synthase is thought to be a crucial enzyme in the regulation of heme synthesis. There are a few reports regarding an increase in heme protein production by ALA inducement. Another alternate way to overcome heme limitation is addition of hemoglobin to culture media. During the production of manganese peroxidase (MnP), heme supplementation in the form of hemoglobin or hemin was shown to significantly increase protein production as measured by extracellular MnP activity, although, the specific activity of MnP did not increase. Therefore, the apoform of rMnP is probably being degraded inside or outside of the cell, while only the haloform is stable enough to be secreted and preserved in the extracellular medium. Interestingly, iron supplementation alone did not increase the production of MnP, suggesting that the increased activity was not a consequence of the additional iron within the hemoglobin or hemin. Higher production yields were achieved with hemoglobin supplementation rather than hemin supplementation, indicating that adding heme to the culture media was important but that adding protein to the culture media might also be favorable. The addition of bovine serum albumin (BSA) or apohemoglobin had a positive effect on production levels, strongly suggesting that addition protein in the media protects rMnP from degradation caused by proteases or other pathways (Conesa, van den Hondel et al. 2000).

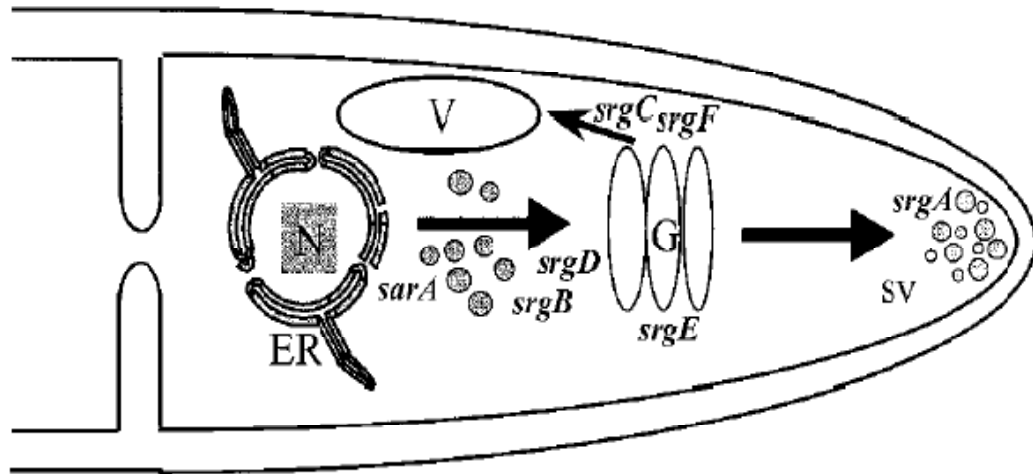


Figure 1.9 The secretion pathway in filamentous fungi. The figure was copied from Conesa et al. (Conesa, Punt et al. 2001). Cloned secretion related GTPases (*srg A–F*), involved in vesicular trafficking, are indicated: N, nucleus; V, vacuole; ER, endoplasmic reticulum; G, Golgi apparatus; SV, secretion vesicles.

Overproduction of heme-peroxidases places a heavy load on the protein secretory machine. Overall, the protein secretory machine in filamentous fungi does not differ greatly from those in yeast and higher eukaryotes, for which a more complete picture is available. However, there must be important differences in the details. The level of protein secretions in filamentous fungi can reach 30 g/L (*Aspergillus* and *Trichoderma* strains) (Punt, Veldhuisen et al. 1994), while in yeast a level of more than a gram per liter is found for only a few species, such as *Pichia* (Visser, Bussink et al. 1995).

The fungal secretory pathway is illustrated in Fig. 1.9. For secretory proteins, the first step is to enter the endoplasmic reticulum (ER). In the ER, the proteins are folded and undergo some distinct posttranslational modifications, including disulfide bridge formation, glycosylation, phosphorylation, and subunit assembly (Conesa, Punt et al. 2001). The proteins then leave the ER inside vesicles, which are directed to the Golgi

apparatus. In the Golgi apparatus, additional posttranslational modifications may take place including additional glycosylation and peptide processing. The proteins then leave the Golgi apparatus packed inside secretory vesicles. In most cases, the secretory vesicles are then sent to the plasma membrane and the proteins inside are secreted into the extracellular media. In some cases, instead of being directed to the plasma membrane, the vesicles and the proteins inside are sent to other intracellular compartments, such as vacuoles. Inside the vacuole, the protein will most likely be degraded via proteolysis catalyzed by proteases. Protein secretion is proposed to occur from the apical or subapical hyphal portions of the fungus (Conesa, Punt et al. 2001).

One key factor that regulates the production of recombinant proteins is presence of molecular chaperones. Molecular chaperones promote protein folding by binding transiently and noncovalently to protein folding intermediates. Once bound to the chaperone the folding intermediates are less likely to have unfavorable protein-protein interactions that might lead to protein aggregation or misfolding. Therefore, molecular chaperones are not regarded as “true” catalysts but as proteins that assist folding. Chaperones and foldases are conserved between organisms and are present throughout the cell including in the cytosol, chloroplasts, the ER, and mitochondria (Gouka, Punt et al. 1996). For CPO, the CPO C-terminal pro-peptide may behave as a molecular chaperone, so that it can assist CPO to fold into its correct conformation, because the CPO sequence corresponding to the mature protein produced no active CPO when cloned into *A. niger*. The mechanism of this function, however, is still unknown (Conesa, Weelink et al. 2001).

1.4 Objectives of this work

For my dissertation, I first attempted to optimize the growth and expression condition for the *A. niger* strain to increase the purity and yield of recombinant proteins, so that I could rely on such a system for future studies. Also verification and a structural study using NMR spectroscopy were done on rCPO. Next, I produced site-directed mutants of CPO using *A. niger* as the host. By studying the function and mechanism of the mutants, I further elucidated the structure of CPO's active site and its role in regulating CPO's catalytic activities and enantioselectivity. A very interesting and promising CPO mutant F103A was successfully produced and studied as part of my research. In addition, possible industrial applications of CPO were explored and examined. An attempt to obtain a CPO triple mutant C29H/C79H/C87H was made; however, it failed to produce active form of protein, probably a result of the instability of the triple mutant.

Chapter II

Optimization of *Aspergillus niger* expression system and NMR study of recombinant CPO

2.1 Material and methods

2.1.1 Strains and reagents

Recombinant CPO (rCPO) expressing *A. niger* strain pCPO3.1#5, which had been co-transformed with CPO expression vector pCPO3.1-amds and assistant plasmid pAB4.1, was kindly provided by Dr. Punt (TNO Nutrition and Food Research Institute, The Netherlands). Rabbit anti-CPO polyclonal IgG was also provided by Dr. Punt. Unless otherwise noted, all other chemicals and reagents were obtained from commercial sources and used without further purification.

2.1.2 Genomic DNA extraction and sequencing

Spores of *A. niger* were inoculated and cultured for 2 d in minimal medium. The mycelia sample were collected by centrifuge and re-suspended in an isosmotic buffer (1 g/20 mL). The cell wall was then partially digested by incubating with a lysing enzyme from *Trichoferma harziannum* (10 mg/20 mL, Sigma L-1412) for 4 h. The mycelia were again collected by centrifuge. The DNA extraction was performed with a QIAGEN plant DNA mini kit (QIAGEN, CA). The extracted DNA was then used as a template and amplified with primers (5'-cgc gga tcc atg ttc tcc aag gtc c -3' & 5'- ccg gaa ttc aag gtt gcg ggc-3') that flanked the CPO coding region. Co-transformants containing the expression cassettes were confirmed by the presence of a band at 1122 bp. The extension temperature for the PCR reaction was optimized to 56.3 °C.

2.1.3 Expression of rCPO

Fungal culturing was carried out in 2-L Erlenmeyer flasks containing 1 L of *A. niger* minimal growth medium with 5% maltose and supplemented with 0.5% casein amino acids. Cultures were inoculated with a whole Petri dish of conidia. After incubation in a rotary shaker revolving at 225 rpm for 24 h at 25 °C, the temperature was lowered to 22 °C and the shaking was continued for 6 d. Hemin (500 mg/L) was added either at the time of or 48 h after inoculation. Crude medium was checked for chlorination activity (MCD assay), using the MCD assay to monitor for the production of rCPO, on a daily base.

2.1.4 Purification of rCPO

Aspergillus niger crude medium samples were collected by filtering the fungal culture through Miracloth and then centrifuging at 9500 rpm for 1 h, followed by filtration through 0.8 µm filters to further remove mycelia debris. The crude culture medium containing the secreted enzyme was concentrated about 200 to 400 fold using a high output ultrafiltration cell (10 kDa cut off membrane, Millipore). The condensed medium sample (20 mL) was dialyzed twice against 25 mM potassium phosphate buffer (4 L) at pH 5.9 for at least 24 h to adjust the pH value and to obtain the proper conductivity. The sample was then applied to a DEAE Sepharose fast flow (Amersham) column (2.6 × 20 cm). After an initial wash to remove the unbounded protein, the mutant enzyme was eluted from the column by using a stepwise ionic strength gradient of 25 mM potassium phosphate buffer at pH 5.9 containing 0-0.5 M sodium chloride. The flow rate was adjusted to 1 mL/min. The Reinheitszahl value (Abs_{400 nm}/Abs_{280 nm}) was used to check the purity of each fraction. Fractions having an Rz value greater than 0.9 were collected, then concentrated using a Centriprep-YM30 concentrator (Amicon). Further

purification was done by gel filtration on a Sephadex G-75 (Amersham) column (2.6 × 100 cm) with 50 mM potassium phosphate buffer (pH 4.6, 0.5 mL/min). All purification steps were done either on ice or in a cold box at 4 °C.

2.1.5 Western blotting procedure

The SDS-PAGE gel was placed next to a nitrocellulose membrane. At room temperature, the protein samples were transferred from the SDS-PAGE gel to the nitrocellulose membrane using 50 V, and 164 mA for 1 h. The membrane was then incubated with blocking buffer (5% non-fat milk in Tris buffered saline with tween (TBST) for 1 h at room temperature with agitation. The membrane was washed 3 times for 5 minutes each with TBST and incubated with rabbit anti-CPO polyclonal IgG antibody in the same buffer with 5% BSA for 16 h at 4 °C with agitation. After incubation, the membrane was washed and then incubated with horseradish peroxidase-conjugated anti-rabbit IgG antibody for 1 h. After this secondary antibody incubation step, the membrane was washed and 3 mL of SuperSignal (1.5 mL Luminol/Enhancer, 1.5 mL 2x Hydrogen Peroxide) was added. After 1 min of gentle agitation, images were recorded by using X- ray film with an exposure time of 5 to 60 s.

2.1.6 Circular Dichroism spectrum study

Far-UV-CD (Circular Dichroism) spectra were recorded on a JASCO J-720 spectropolarimeter at room temperature. Spectrum was recorded from 190 to 250 nm at 0.1-nm intervals with a spectral bandwidth of 1 nm. The path length was 1 cm.

2.1.7 UV-visible absorption spectrum study

All UV-visible (UV-vis) absorption measurements were determined in a VARIAN Cary 300 spectrophotometer using a 1-cm path length quartz cuvette.

2.1.8 Enzyme activity assays

Chlorination Assay (MCD assay) — the chlorination rate of monochlorodimedone (MCD) was used to measure the chlorination activity of CPO (Yi, Conesa et al. 2003). The 3 mL reaction mixture contained 100 mM potassium phosphate buffer at pH 2.75, 20 mM KCl, 0.17 mM monochlorodimedone, 2 mM H₂O₂, and a suitable aliquot of CPO. The reaction was initiated by the addition of H₂O₂, and the decrease in absorbance at 278 nm was monitored at room temperature. One unit of chlorination activity was defined as the conversion of 1 μmole of MCD per minute.

2.1.9 NMR spectroscopy

The NMR samples of rCPO (~1.5 mM) were prepared in 100 mM potassium phosphate buffer at pD/pH 5.5 in either D₂O buffer or 90% H₂O/10% D₂O buffer. In D₂O the pH meter reading was adjusted by 0.4 units to account for solvent isotope effects. In 90% H₂O/10% D₂O buffer no adjustment was made. Preparation of rCPO in D₂O involved four buffer exchanges with D₂O buffer at pD 5.5 starting from solutions of rCPO in H₂O. The exchanges were accomplished at 4°C using a Centricon or Centriprep from Amicon. The protein concentration was determined from its absorbance at 398 nm ($\epsilon = 91.2 \times 10^3 \text{ M}^{-1}\text{cm}^{-1}$). The rCPO-CN adduct was prepared by addition of a 1.1-1.2 molar equivalents of KCN in D₂O, from a freshly made KCN stock solution (0.5 M).

Proton NMR spectra were recorded on a Bruker Avance 600 (Ultrashield) NMR spectrometer operating at a proton frequency of 599.97 MHz. The residual solvent signal was suppressed with pre-saturation during relaxation delay. Chemical shift values were referenced to the residual HDO signal at 4.76 ppm. All NMR spectra were acquired at 298 K unless otherwise noted. For variable temperature experiments the chemical shift of

the residual HDO signal was assigned a value according the relationship of $\delta_T = \delta_{25} - 0.012 (T - 25)$, where δ_T is the chemical shift of HDO at temperature T in °C, and δ_{25} is the chemical shift of HDO at 25 °C (Satterlee, Erman et al. 1983); The value of 4.76 ppm instead of the usual 4.81 ppm was selected to be consistent with previous experimental work on CPO (Wang, Tachikawa et al. 2003).

All two-dimensional data were processed on an HP Workstation with a Pentium 4 processor using Topspin 1.3 (Bruker). Various apodization functions were employed to emphasize protons with different relaxation properties. The spin-lattice relaxation times (T1) were determined from 16 spectra obtained at 25 °C with delay times ranging from 0.1 to 500 ms. After processing with Topspin each spectrum was downloaded into Microsoft Excel to determine peak heights and the resulting data curve fit using Sigma Plot.

2.2 Results and discussion

2.2.1 Optimization of rCPO production and purification procedure for rCPO

One obstacle presented in a previous report using the *A. niger* expression system was the very low production of the purified enzyme, at most 10 mg/L compared to 300 mg/L for Wt CPO produced by *C. fumago*; in addition, the heme incorporation rate of the enzyme was very low. While pure CPO has an Rz value higher than 1.44, the purified rCPO only had an Rz value of 0.54. These two shortcomings plus a low-yield purification procedure made it impractical to obtain sufficient protein for detailed structure and mechanistic studies. Thus, improved production yields, heme incorporation rates, and purification procedures were essential for the success of the project.

First, heme and heme precursor were added, as previous studies on the expression of other fungal peroxidase in *A. niger* had demonstrated that incomplete incorporation with prosthetic group was a major issue (Conesa, van De Velde et al. 2001). For example, Conesa has reported that rCPO produced by MGG029 was only partially (40%) incorporated with heme even after heme supplementation (Conesa, van De Velde et al. 2001). Table 2.1 shows the comparison between rCPO yield, and culture media with and without heme supplementation. When 500 mg of hemin was added at inoculation, protein production levels were similar to those reported previously. However, when hemin was added 48 h after inoculation, protein production was increased by 5-10 fold. Interestingly, the highest protein production (30.42 mg/L) was achieved without hemin addition at all, and protein production levels could be increased by 4-29 fold. Therefore, it seems that addition of heme to medium may have a toxic effect on the growth of *A. niger*.

Table 2.1 Optimized condition for production of rCPO after 72 h culture

Culture of <i>Aspergillus niger</i>	rCPO activity (unit/mL)	Estimated rCPO production yield (mg/L)
Reported in reference	1.60	1.14
Hemin (500 mg/L) added at inoculation	1.63	1.16
Hemin (500 mg/L) added after culture reach plateau (48 h)	8.52~19.7	6.08~14.07
No heme addition	6.28~42.6	4.49~30.42

Two additional factors were examined to improve rCPO production yield: pH stability and culture time. *Aspergillus niger* strains are known to produce large amount of organic acids that acidify the culture media. Overly acidic crude media will denature the secreted protein before it is folded and processed to the functional protein. Readjusting the pH with greater than 1 M KOH, might further denature the protein locally as well, and lower concentrations of KOH are impractically as they significantly dilute the media due to the high concentration of organic acids. Thus, over acidification might have a profound effect on expression level. In order to minimize acidification, different carbon sources were added into the culture media. The mycelia of a hyper productive CPO3.1#5 strain were used to inoculate one batch of 3x1 L cultures containing 5% maltose and no glucose, and another batch of 3x1 L cultures with maltose (5%) and glucose (1%). The pH values of the crude media were checked daily and the pH value was readjusted to 5 using 1 M KOH if necessary. After 7 days, flasks without glucose, had rCPO production yields of 7, 13, and 15 mg/L, and the flasks with glucose, had rCPO production yields of 36, 46, and 48 mg/L as determined by the MCD assay. In addition, the flasks without glucose reached to pH 3 after only two days, while the flasks with glucose never reached pH 3 during the course of the experiment. The pH values stayed between 4 and 5 for over 7 days, and there was no need to adjust the pH.

In previous work using *A. niger* as a heterologous expression host to express heme-containing proxidase, all culture media were collected either 48 h or 72 h after inoculation, probably because of factors such as the intrinsic stability of the enzyme and the denaturation effect of over acidification. Since CPO is very stable under acidic conditions, prolonged culture times could benefit the production of rCPO. The results of

rCPO production yields versus culture time are showed in figure 2.1. The rCPO production yields after 3, 4, 5, 6, and 7 days of inoculation, were 16, 29, 40, 48, and 56 mg/L, respectively. Further improvements in production efficiency were achieved by controlling the temperature. The initial culture temperature was increased from 22 °C to 25 °C to help *A. niger* reach its maximum biomass faster, then the temperature was lowered to facilitate the secretion of rCPO. In addition, lower temperatures would help to stabilize the secreted enzyme. By increasing the incubation time and adjusting the temperature, the rCPO production yield was further increased to 85 mg/ L.

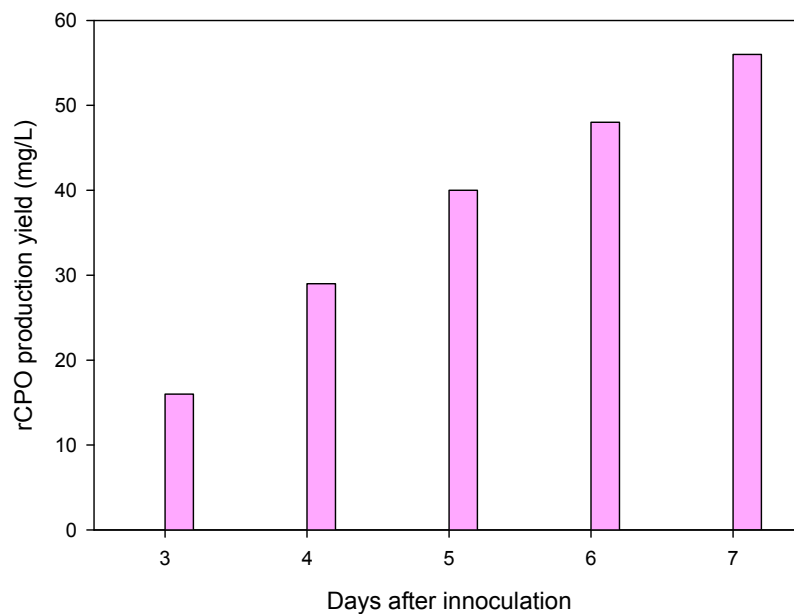


Figure 2.1 rCPO production yields versus days after inoculation.

A few modifications were also made to the rCPO purification procedure. A stepwise rather than a linear ion strength gradient was used in the ion-exchange chromatography step. In the gel filtration chromatography step, a smaller sample volume (<0.5% column volume) and slower flow rate (0.5 mL/min instead of 1 mL/min) were found to improve

the resolution. The chromatography results of rCPO purification are shown in Fig. 2.2 & Fig. 2.3. Compared to the published rCPO purification table (Conesa, van De Velde et al. 2001), the results (Table 2.2) demonstrated an approximately 2.5 times higher recovery rate and 2.6 times higher purity, thus enabling us to carry out an NMR study. Ultimately, I increased the overall production of pure rCPO to 85 mg/L and the Rz value of purified rCPO was up to 1.4. Wt CPO with an Rz value greater than 1.44 is considered pure. The ability to produce rCPO in high yield and purity opens the door to a greater understanding of the mechanism of CPO and the commercial application of mutants of CPO via protein engineering.

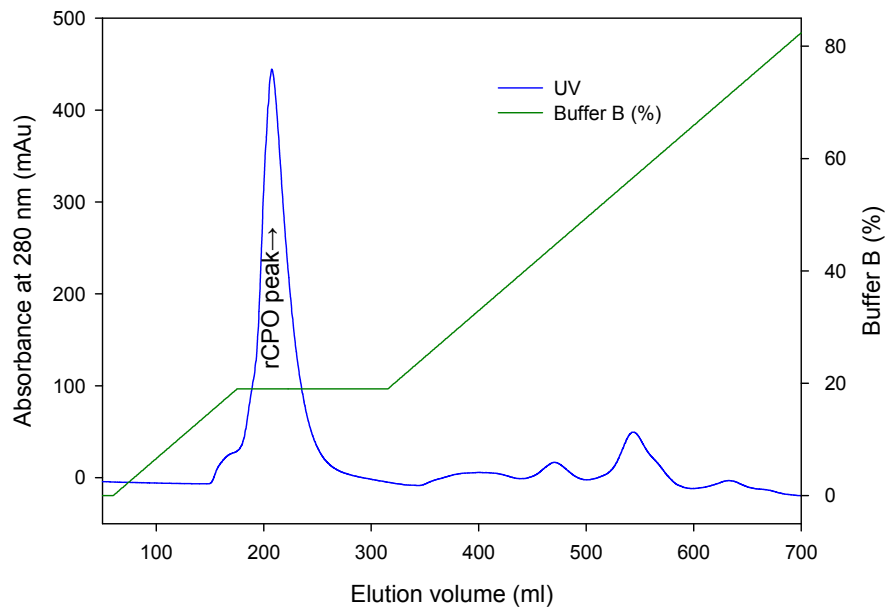


Figure 2.2 Chromatogram of ion exchange chromatography of rCPO.

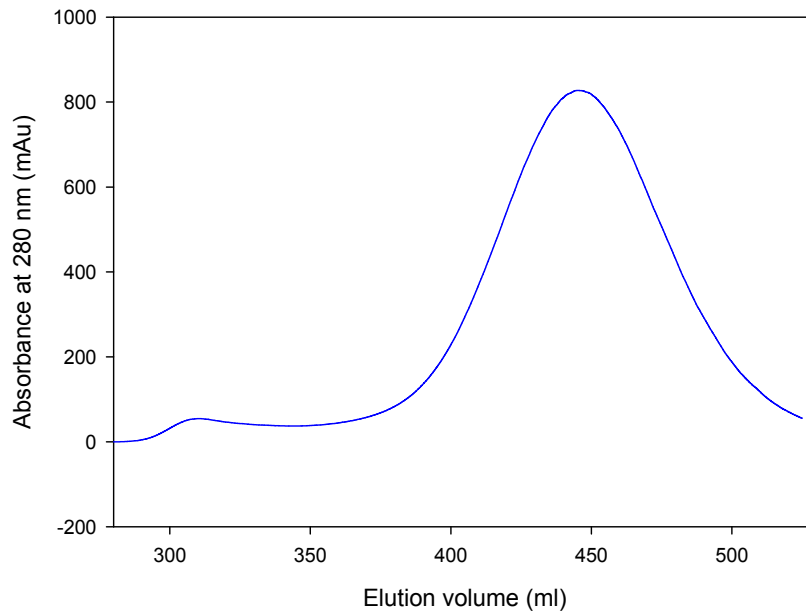


Figure 2.3 Chromatogram of gel filtration chromatography of rCPO

Table 2.2 Purification result of rCPO from *A. niger* culture

	Volume mL	Activity units/mL	Enzyme units	Yield %	Rz <i>A400/A280</i>
Crude media	580	29	16820	100	ND
Ultrafiltration	45	309	13888	82	ND
DEAE-Sephrose	90	109	9797	58	~1
Sephedex G-75	40	112	4480	26	1.4

2.2.2 Validation of rCPO

Validation of rCPO was done by SDS-PAGE (Fig. 2.4) and western blotting (Fig. 2.5). The results verified that the molecular weight of purified rCPO is slightly larger than that of Wt CPO. The western blot results showed the positive reaction of rCPO with

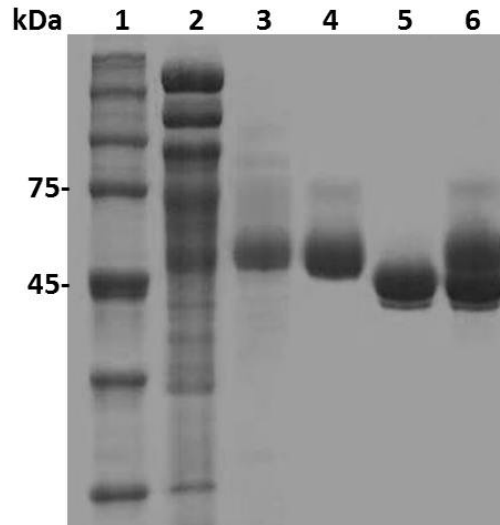


Figure 2.4 12% SDS-PAGE result of rCPO. Lane 1 is protein molecular weight markers. Lanes 2 to 4 are rCPO samples from crude media, and ion exchange and gel filtration purification steps, respectively. Lane 5 is a sample of Wt CPO and lane 6 is a mixed sample of Wt CPO and purified rCPO. According to the gel results, the molecular weight of the rCPO is 50 kDa and is slightly bigger than that of Wt CPO.

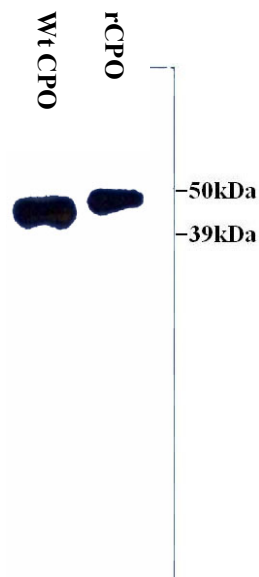


Figure 2.5 Western blotting results of Wt CPO and rCPO. Proteins were detected with an anti-CPO polyclonal antiserum. The antibody was diluted to 1:10000 for Wt and recombinant CPO.

polyclonal antibodies, despite the different glycosylation profiles of *A. niger* and *C. fumago*.

2.2.3 UV-vis & CD spectroscopic study of rCPO

After rCPO was verified, the UV-vis spectra of rCPO and Wt CPO (Fig. 2.6) were compared. The spectrum of rCPO was almost identical to that of Wt CPO in all regions except that the Soret band of Wt CPO was at 398 nm, but that of rCPO was at 400 nm. The activity assay also confirmed the validity of the rCPO (data not shown). The CD spectra (Fig. 2.7) also showed an essentially identical pattern between rCPO and Wt CPO indicating the presence of a similar secondary structure for the two proteins.

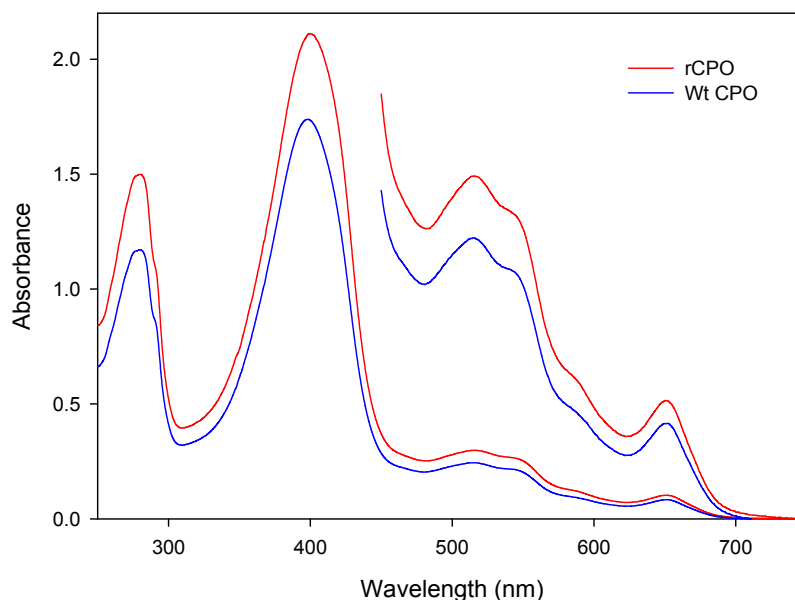


Figure 2.6 UV-vis spectra of rCPO and Wt CPO (in 0.05 M potassium phosphate buffer, pH 5.0, at room temperature).

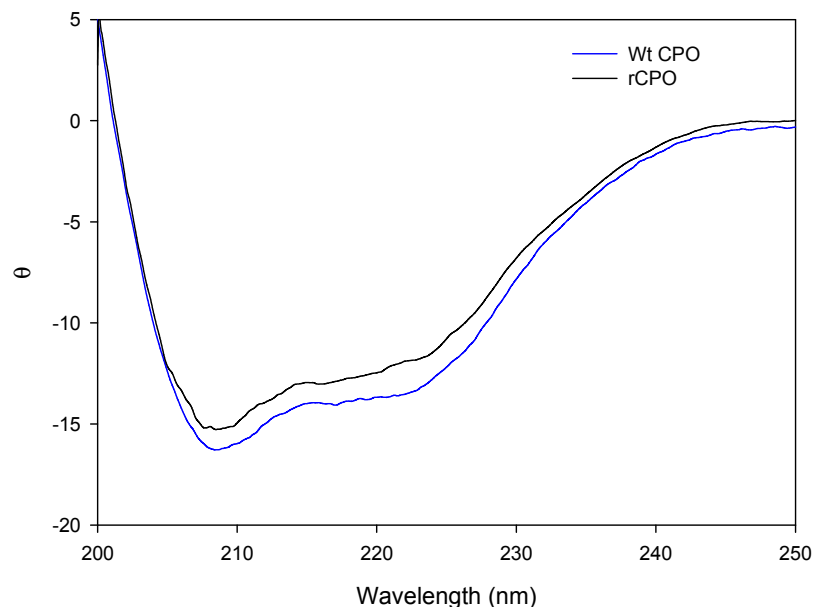
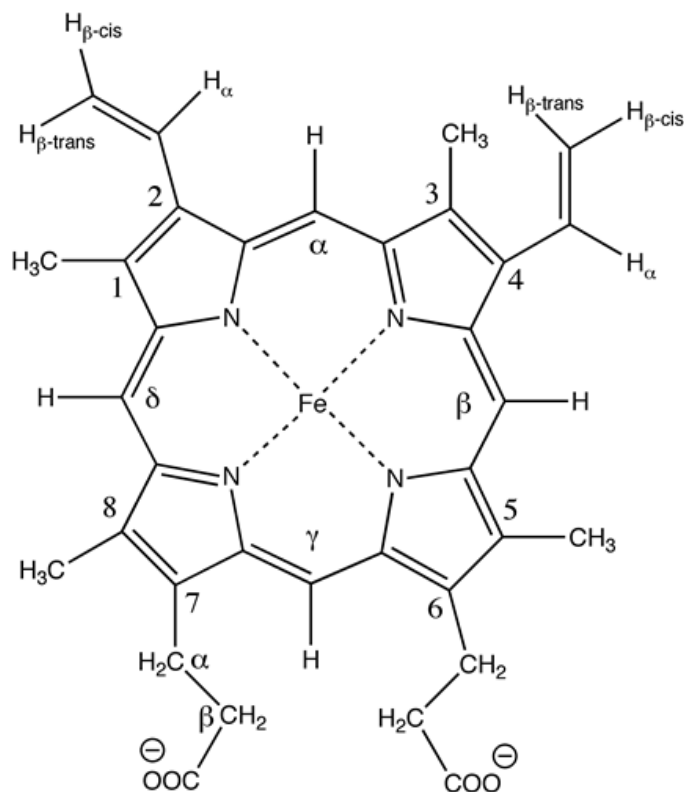


Figure 2.7 The CD spectra of rCPO (0.4 μM in 10 mM phosphate buffer, pH=6) and Wt CPO (0.35 μM in 10 mM phosphate buffer, pH=6). The experiments were carried out at room temperature and recorded from 190 to 250 nm. The path length was 1 cm.

2.2.4 NMR spectroscopic study of rCPO

The proton NMR spectrum of the rCPO-CN adduct displayed only one set of signals, indicating the presence of only one isozyme (Fig. 2.8). In contrast, the proton NMR spectrum of the Wt CPO-CN adduct has pairwise signals because of the presence of two isozymes (Wang, Tachikawa et al. 2003), which complicates spectral interpretation. The rCPO-CN adduct was in the ferric low spin state and provided relatively sharp NMR signals (Fig. 2.8). Although, the adduct is not physiologically active, it is the most favored system for paramagnetic NMR investigation as it provides the most information about the magnetic, electronic and structural properties of the active site and is also a good mimic of reaction intermediates Cpd I and Cpd II (Satterlee, Erman et al. 1983; Thanabal, Deropp et al. 1987; Satterlee, Erman et al. 1990; Banci, Bertini et al. 1992).

The structure of the active site of rCPO was investigated using spin-lattice relaxation times and Curie plots, as well as a NOESY spectrum (Table 2.3 and Scheme 1).



Scheme 1 Iron protoporphyrin IX in CPO

Comparisons were made with the comprehensive NMR results previously reported for Wt CPO (Wang, Tachikawa et al. 2003). The spin-lattice relaxation time of each paramagnetically shifted resonance in rCPO-CN was determined by measuring peak intensities as a function of relaxation times (Fig. 2.9) and then the results were curve fit to peak intensity = $I_0 - 2 * a * e^{-t/T1}$, where I_0 and a are variables corresponding approximately to the maximum peak intensity, t is time, and $T1$ is the spin-lattice relaxation constant (Fig. 2.10). The spin-lattice relaxation times provide information about the distance between

the proton and the iron center (Table 2.4). The Curie plots involved plotting the chemical shift of a proton as a function of $1/T$, where T is the temperature in Kelvin (Fig. 2.11). The intercept of the plot estimates the chemical shift of the proton in the absence of paramagnetic effects from the iron. Resonances were assigned based on analogy with the well-studied Wt CPO spectrum and the heme resonance was partially assigned based on off diagonal peaks in the COSY spectrum (Fig 2. 12) (Wang, Tachikawa et al. 2003).

The NOESY (Fig. 2.13) spectrum of rCPO possesses many of the same off diagonal peaks as that of Wt CPO. On the basis of the analogy with the Wt CPO spectrum, twenty four of the 37 crosspeaks observed in Wt CPO for isozyme B were identified in rCPO and the missing crosspeaks tended to be of lower intensity in the Wt CPO NOESY spectrum or may correspond to isozyme A. Off diagonal peaks between the heme hydrogens of rCPO and Pro28, Ala31, Phe57, Ile63, Val67, Ile68, Leu97, and Phe186 were observed. Unlike Wt CPO, no off diagonal peak was observed between the heme protons and Phe57, although this is a very weak signal in the Wt CPO NOESY spectrum (Wang, Tachikawa et al. 2003).

In summary, on the basis of the NMR data, rCPO and Wt CPO have very similar active site structures. The 1D and 2D spectra are nearly identical, as are the T_1 values and the intercepts of the Curie plots. The chemical shifts of the paramagnetically shifted resonances in isozyme B of Wt CPO and the corresponding resonances in rCPO are at most 0.4 ppm apart with the exception of the resonance at approximately 39 ppm, which is broad and has a poorly defined peak, Table 2.3. For comparison, when yeast cytochrome *c*, a non-glycosylated heme protein was expressed in *E. coli*, the chemical shifts of the paramagnetically shifted resonance of wild type and recombinant proteins

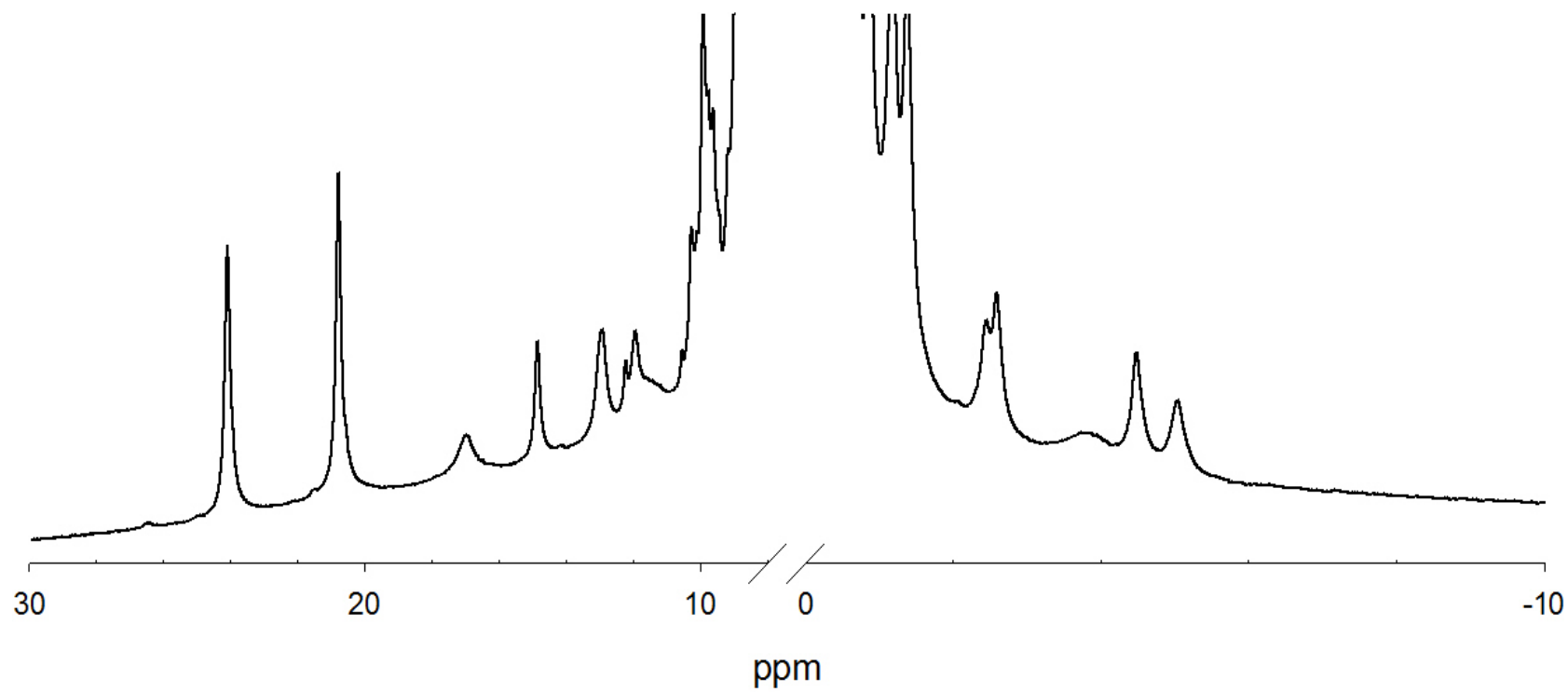


Figure 2.8 NMR spectrum of rCPO at 25 °C in 0.1 M potassium phosphate buffer

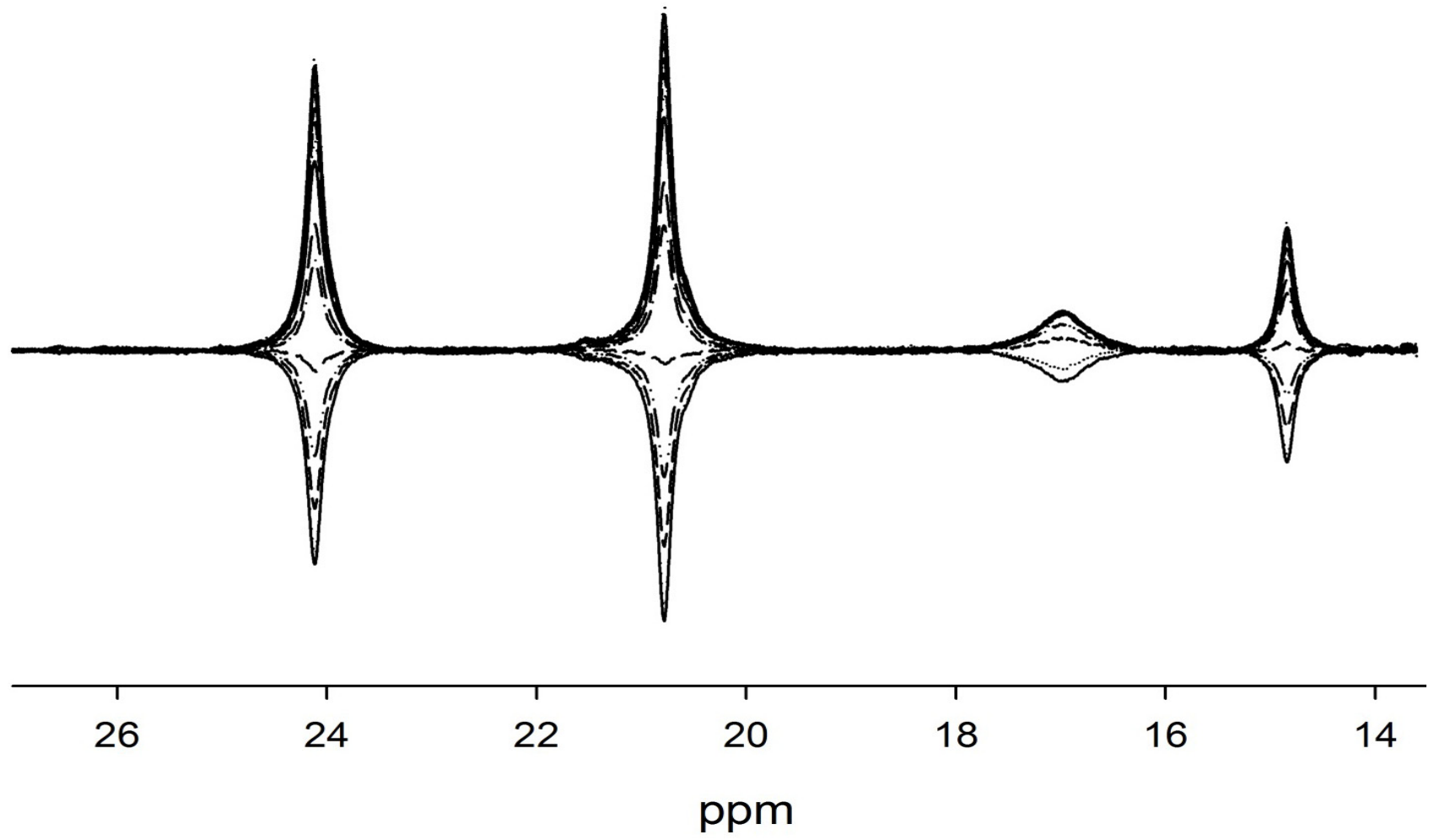


Figure 2.9 Selected signals from the NMR spectra of rCPO at various relaxation times at 25 °C and pD 5.5.

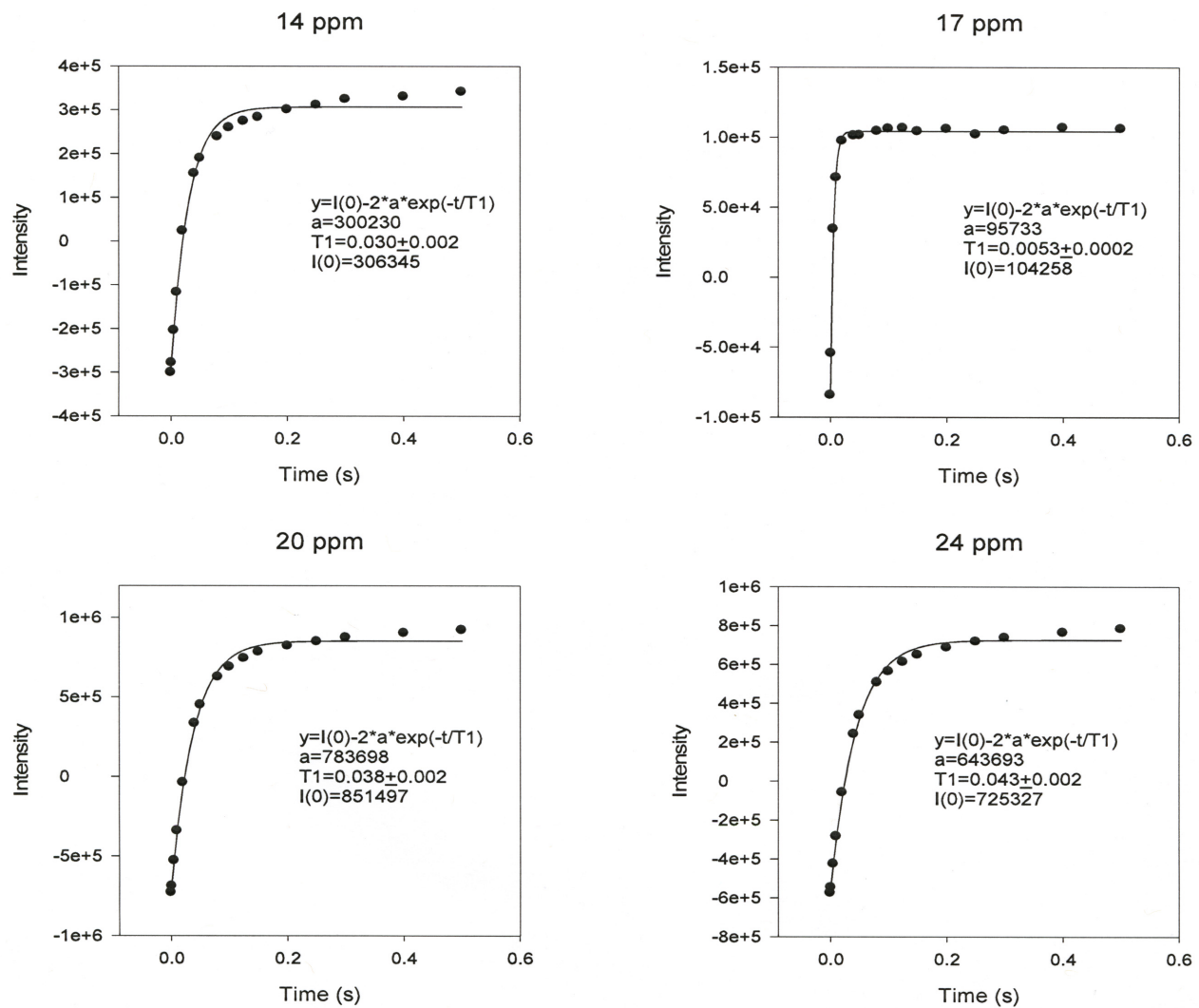


Figure 2.10 Determination of the spin-lattice relation times from peak intensities versus delay times.

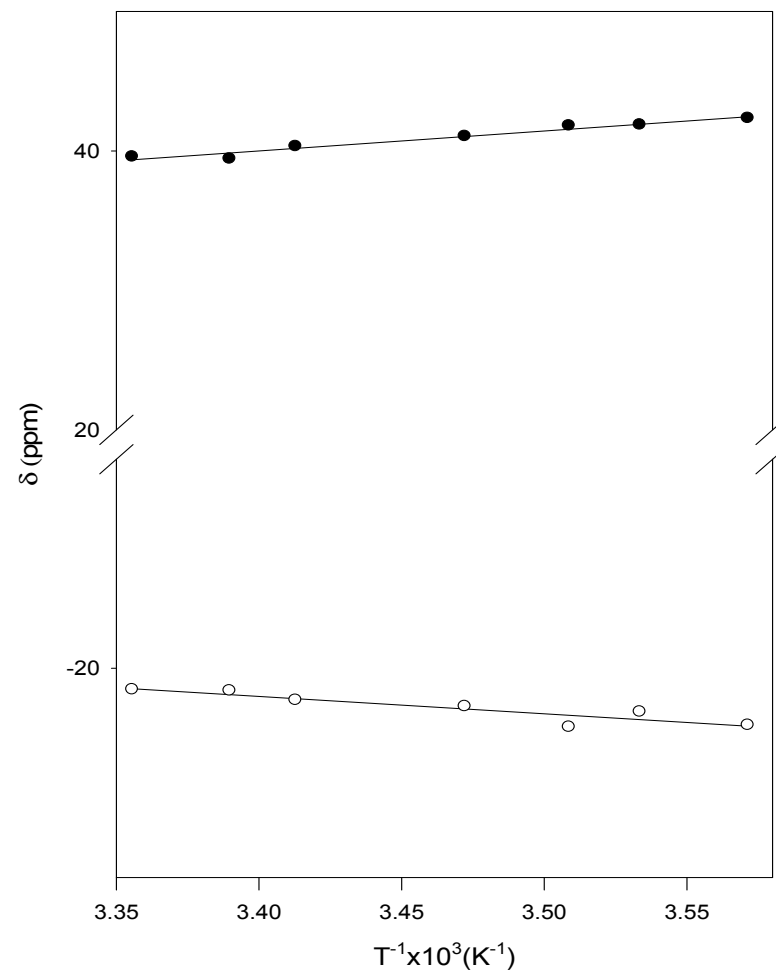
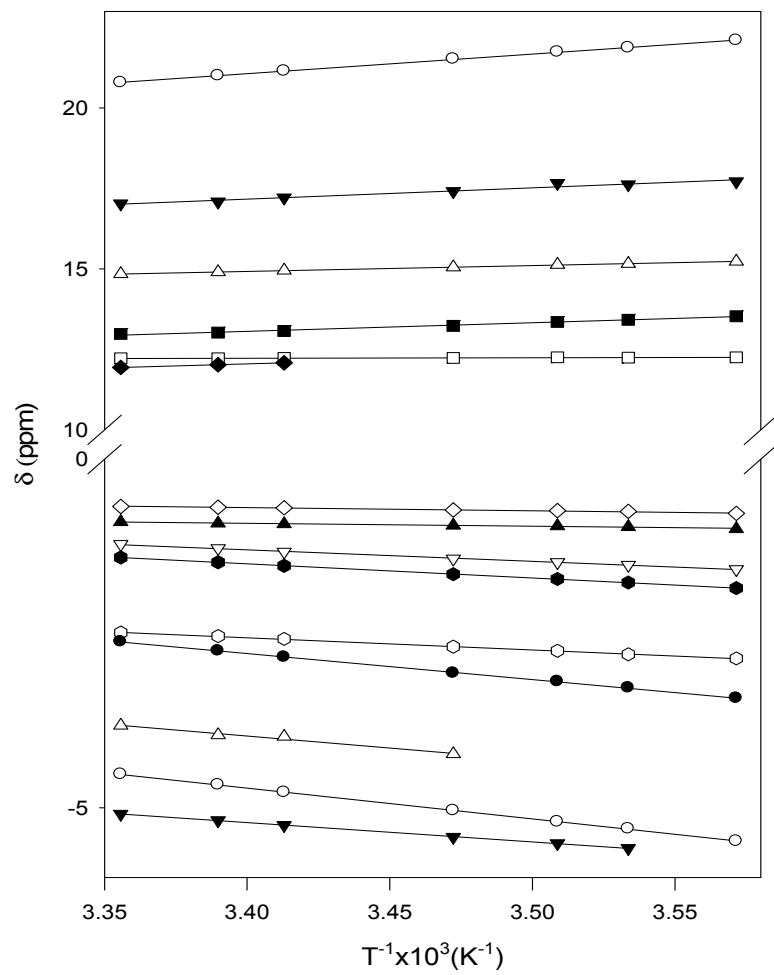


Figure 2.11 Curie plots for selected signals of rCPO.

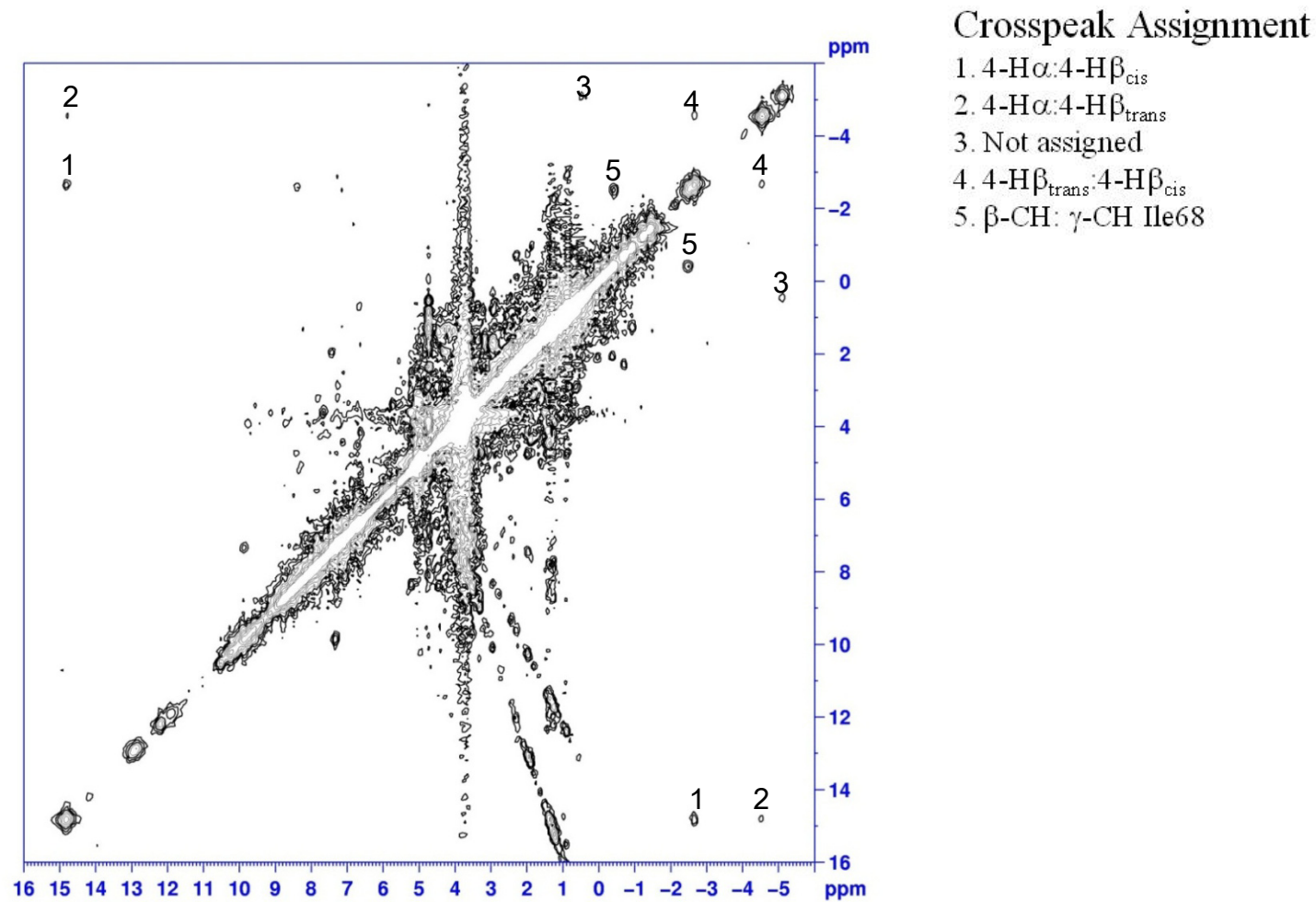
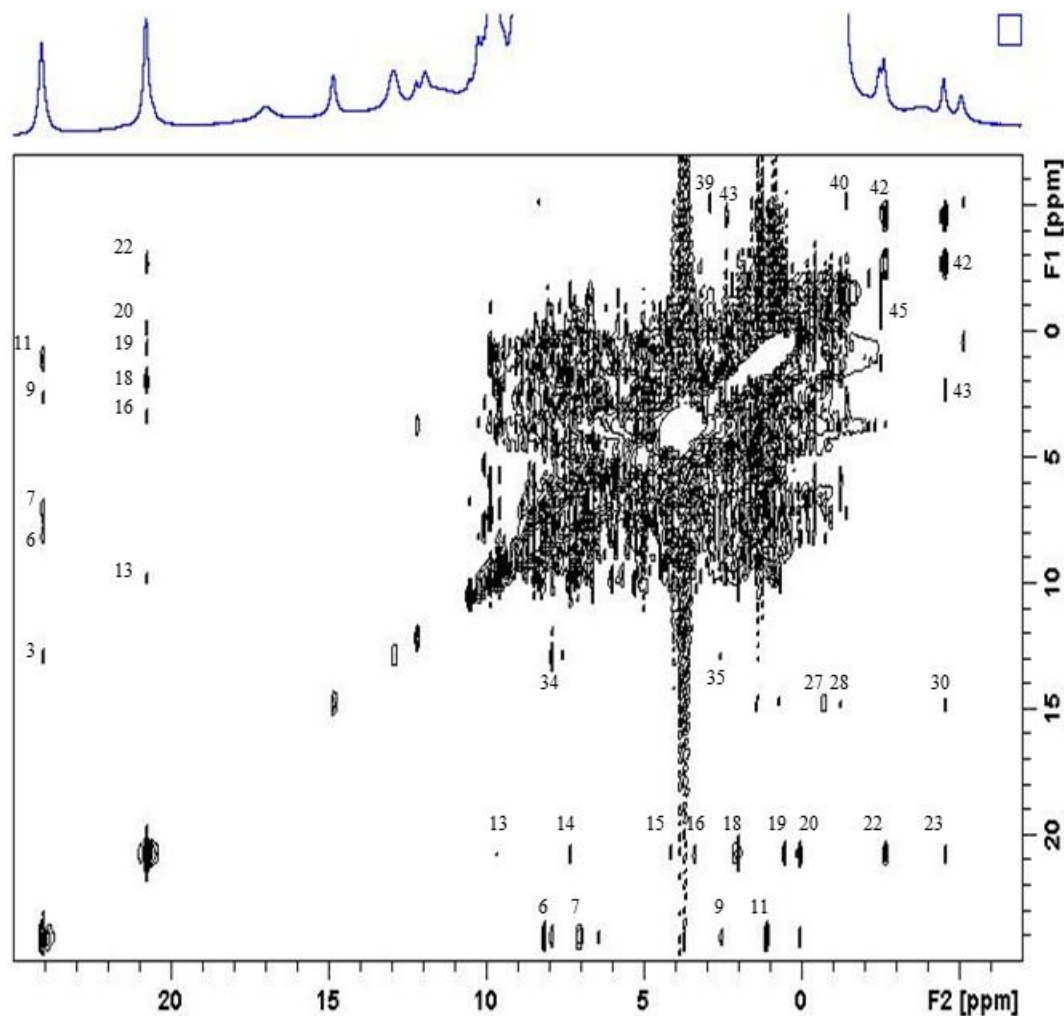


Figure 2.12 rCPO COSY plot.



Crosspeak Assignment

- 3. 8-CH₃:7H α
- 6,7. not assigned
- 9. 8-CH₃:7H β
- 11. 8-CH₃: δ -CH₃ Leu⁹⁷
- 13. 3-CH₃:He₁ Phe⁵⁷
- 14. 3-CH₃:Hd₁ Phe⁵⁷
- 15. 3-CH₃:Hy Ile⁶³
- 16. 3-CH₃: β -CH₃ Ala³¹
- 18. 3-CH₃: γ -CH₃ Ile⁶³
- 19. 3-CH₃: γ -CH₃ Ile⁶⁸
- 20. 3-CH₃: γ 1-CH₃ Val⁶⁷
- 22. 3-CH₃:4-H β_{trans}
- 23. 3-CH₃:4-H β_{cis}
- 27, 28. not assigned
- 30. 4-H α :4-H $\beta_{\chi_{1\sigma}}$
- 34. 7-H α : γ -CH₂ Pro²⁸
- 35. 7-H α :7-H β
- 39. 2-H α :2-H β_{cis}
- 40. 2-H α :2-H β_{trans}
- 42. 4-H β_{trans} :4-H β_{cis}
- 43. β -CH₂ Phe¹⁸⁶:4-H β_{trans}
- 45. β -CH₂: γ -CH₃ Ile⁶⁸

Figure 2.13 rCPO NOESY plot and crosspeak assignments based on analogy with Wt CPO (Wang, Tachikawa et al. 2003). The same numbering system was used as in Wt CPO, which has additional peaks, in part, due to the presence of two isozymes.

Table 2.3 Spin lattice relaxation times (T1) of paramagnetic shifted resonances for rCPO and Wt CPO in 0.1 M phosphate buffer, pD 5.5 and 25 °C.

rCPO			Wt CPO ^a			
Chemical shift (ppm)	T1 (ms)	Intercept (ppm)	Chemical shift (ppm)	T1 (ms)	Intercept (ppm)	Assignment
39.6		-8.5	39.0/38.3		-10.6/-9.6	H β -Cys29
24.1	43	1.8	24.0/23.8	33/35	0.1/0.4	8-CH ₃
20.8	38	0.4	20.7/20.4	30/34	-0.7/-0.6	3-CH ₃
17.0	5	5.3	17.4/17.0	6/6	3.1/3.0	NA ^c
			16.3 (H ₂ O) ^b	200		His105
14.8	30	8.7	14.8	29	8.7	4- H α
12.9	33	4.0	14.1/12.9	35/35	3.3/2.4	7- H α
12.2	265	11.7	12.3/11.9	220/NR ^d	NR/NR ^d	CH ₂ -Pro28
11.9	10	3.8	12.2/11.8	NR/NR ^d	NR/NR ^d	CH-Phe186
			11.6 (A) ^a	30 (A) ^a	3.5 (A) ^a	7- H α ' (A) ^a
-1.2	52	4.4				
-1.4	54	5.4	-1.4	NR ^d	5.8	2- H β _{trans}
-2.5	81	3.4	-2.5	NR ^d	3.4	β -CH-Ile68
-2.6	65	9.9	-2.7	70	9.7	4-H β _{trans}
-3.8	7	7.7	-3.8	7	5.5	NA ^c
-4.5	72	10.3	-4.4	80	10.8	4-H β _{cis}
-5.1	62	4.2	-5.2	58	4.6	2-H β _{cis}
-21.0	1.4	0.8	-20.7	1.5	6.4	H β '-Cys29

^aPairwise signals were observed for Wt CPO, the first number corresponds to isozyme A and the second number corresponds to isozyme B. One number corresponds to both isozymes unless indicated otherwise (Wang, Tachikawa et al. 2003).

^bSignal observed in H₂O but not D₂O.

^cNot assigned in Wt CPO due to several possibilities or undetermined

^dNot reported

Table 2.4 Distance between the selected protons and the heme iron in rCPO based upon spin-lattice relaxation values and from the X-ray structure of Wt CPO (Sundaramoorthy, Ternier et al. 1995).

Chemical Shift (ppm)	T1 (ms)	Assignment	Predicted Distance (Å)	X-ray (Å) of Wt CPO
24.1	43	8-CH ₃	6.1	6.1
20.8	38	3-CH ₃	5.9	6.0
17.0	5	Meso-H	4.2	4.6
14.8	30	4-H α	5.7	5.5
12.9	33	7-H α	5.8	6.3
12.2	265	CH ₂ , Pro28	8.2	7.9
11.9	10	CH, Phe186	4.7	3.9
-2.6	65	4- H β _{trans}	6.5	6.8
-4.5	72	4-H β _{cis}	6.6	6.8

^aThe predicted distances were determined from the T1 values assuming that the average distance between the three protons of 8-CH₃ and the heme iron was 6.05 Å and that T1 varies with 1/r⁶.

differed by up to 0.6 ppm (Satterlee, Erman et al. 1990). The chemical shifts of the paramagnetically shifted resonance of the two isozymes of Wt CPO listed in Table 2.3 also differed by slightly more than 1 ppm (Wang, Tachikawa et al. 2003). Based on the chemical shifts of the 7-H α protons, rCPO is slightly closer in structure to isozyme B of Wt CPO than to isozyme A.

2.3. Conclusion

Expression level is an important feature for a recombinant protein system. Structural and mechanistic studies requires large quantities of protein and under laboratory condition, it is impractical to increase the fermentation volume to compensate for low

production yields. It is also a very important factor for economic reasons, if future industrial applications of the protein are under consideration. Needless to say, high purity is also critical for structural and other in-depth studies of protein function. My optimization of the expression and purification procedure of CPO not only allows the production of protein with adequate purity for structural studies, but also increases the production efficiency of active enzyme by 7 fold. Although, addition of either heme-precursor or heme was proposed to increase the production yield and heme incorporation rate, the current work proved it to be unnecessary. My work showed that an Rz value of up to 1.40 can be achieved for rCPO without the use of either heme or heme precursor during protein expression, demonstrating at least 97% heme incorporation rate. The rCPO produced by *A. niger* was both structurally and functionally very similar to Wt CPO, although the glycosylation degree was different. The UV-vis, CD, and 1D and 2D NMR spectra were almost identical between rCPO and WtCPO. The CD data suggested only minor changes in the secondary structure and the NMR data suggested that the structure of the active site was essentially the same. Importantly, rCPO also possessed efficient catalytic activity as Wt CPO does.

My work proved that *A. niger* is an efficient and effective system for heterologous expression of CPO. In addition, the results suggested that *A. niger* may be used to express heme-containing proteins from other source which have proven difficult to express otherwise (Zong 1997; Aburto, Correa-Basurto et al. 2008; Lubertozzi and Keasling 2009). The results also laid a solid foundation for future studies on CPO using site-directed mutagenesis as demonstrated in Chapter 3 of this dissertation.

Chapter III

F103A CPO mutant preparation and properties

3.1 Material and methods

3.1.1 Strains and reagents

Escherichia coli strains *DH5α* and *Novablue* were used for the construction and propagation of vectors. *E. coli* strain XL Gold-10 was purchased from the quik-change II XL kit (Stratagene, CA) to propagate the nicked and mutagenesis induced CPO expression vector. The *A. niger* strain MGG029 (*prtT*, *gla::fleo^r*, *pyrG*) was obtained from TNO Nutrition and Food Research Institute, The Netherlands and was employed as recipient strain in the transformation experiments. High fidelity DNA polymerase *pfu* ultra and Phusion were obtained from Stratagene (San Diego, CA) and New England Biolabs, respectively. Rabbit anti-CPO polyclonal IgG was provided by Dr. Punt. Purified oligonucleotide primers were synthesized by MWG-Biotech. Unless otherwise noted, all other chemicals and reagents were obtained from commercial sources and used without further purification.

3.1.2 CPO mutant gene construction

The rCPO expression vector pCPO3.I-AmdS, a plasmid containing the CPO genomic clone, was purchased from TNO Nutrition and Food Research Institute, The Netherlands. In vector pCPO3.I-AmdS, the cDNA sequence encoding the full-length CPO precursor (1122 bp, GenBankTM accession #.AJ300448) is placed under the control of the *A. niger* glucoamylase promoter and *A. nidulans trpC* terminator. The *A. nidulans* AmdS selection marker was introduced at a unique *NotI* site. The AmdS selection marker encodes acetamidase as a dominant nutritional marker. The mutation was prepared by the

QuikChange II XL site-directed mutagenesis kit (Stratagene, CA), and introduced via PCR amplification of pCPO3.I-AmdS with mutagenic oligonucleotide primers encoding an F103A mutation (5' gcc gag ccc cac gct GCC gag cac gac cac tcc 3'). The PCR reactions were carried out in a Eppendorf Mastercycler gradient thermal cycler (Eppendorf, North American) using the following parameters: initial denaturation at 95 °C for 2 min followed by 18 cycles of 95 °C for 1 min (denaturation), 60 °C for 1 min (annealing) and 68 °C for 15 min (elongation). The final touch up PCR step was 68 °C for 7 min. The desired mutation was confirmed by DNA sequencing and the expression vector pCPO3.I-AmdS containing the F103A mutation was denoted as pCPO-F103A-AmdS.

3.1.3 Plasmid transformation into *Aspergillus niger* protoplast

Fungal co-transformation was carried out as described (Punt 1992) using each of the expression vectors and pAB4.1 plasmids containing the *A. niger pyrG* selection marker in weight ratio of 10:1. Because the original lysing enzyme Novozym 234 was no longer commercially available, the lysing enzyme from *Trichoferma harziannum* (Sigma S-1412) was used. For protoplast production, 1 g of wet *A. niger* mycelia was incubated with 150 mg lysing enzyme for 4.5 h in 20 mL of isosmotic buffer. Transformants were selected on minimal medium plates containing acetamide as the sole nitrogen source. Transformants were further selected for multicopy integration of the expression cassettes on acrylamide plates. Extracellular peroxidase activity was screened on *o*-anisidine plates using 0.05% H₂O₂ in 0.1 M potassium phosphate (pH=3) as developing buffer.

3.1.4 Genomic DNA extraction and sequencing

Spores of *A. niger* were inoculated and cultured for 2 days in minimal medium. The mycelia were collected by centrifugation at 3500 rpm for 20 minutes and re-suspended in an isosmotic buffer (1 g/20 mL). The cell wall was then partially digested by incubating with lysing enzyme (10 mg/20 mL, Sigma L-1412) for 4 h. The mycelia were again collected by centrifugation. DNA extraction was performed with a QIAGEN plant DNA mini kit (QIAGEN, CA). The extracted DNA was then used as the template and amplified with primers (5'-cgc gga tcc atg ttc tcc aag gtc c -3' & 5'- ccg gaa ttc aag gtt gcg ggc-3') which flanked the CPO coding region. Co-transformants containing the expression cassettes were confirmed by the presence of a band at 1122 bp. The extension temperature for the PCR reaction was optimized to 56.3 °C.

3.1.5 Expression of F103A mutant

Fungal culturing was carried out in 2-L Erlenmeyer flasks containing 1 L of *A. niger* minimal growth medium with 5% maltose and supplemented with 0.5% casein amino acids. Cultures were inoculated with a whole Petri dish of conidia. After incubation in a rotary shaker revolving at 225 rpm for 24 h at 25 °C, the temperature was lowered to 22 °C and the shaking was continued for 6 days.

3.1.6 Purification of F103A mutant

Aspergillus niger crude medium was collected by filtering the fungal culture through Miracloth and then centrifuging at 9500 rpm for 1 h, followed by filtration through 0.8 µm filters, to further remove mycelia debris. The crude culture medium containing the secreted enzyme was concentrated about 200 ~ 400 fold by using a high output ultrafiltration cell (10 kDa cut off membrane, Millipore). The condensed medium was

dialyzed twice against 25 mM potassium phosphate buffer (4 L) at pH 5.9 for at least 24 h to adjust the pH and to obtain the proper conductivity. The sample was then applied to a DEAE Sepharose fast flow (Amersham) column (2.6 × 20 cm). After an initial wash to remove the unwanted protein, the mutant enzyme was eluted from the column by using a linear ionic strength gradient of 25 mM potassium phosphate buffer at pH 5.9 containing 0-0.5 M sodium chloride in 15 bed volumes. The flow rate was adjusted to 1 mL/min. The Rz value was used to check the purity of each fraction. Fractions having an Rz value greater than 0.6 were collected, then concentrated using a Centriprep-YM30 concentrator (Amicon). Further purification was done by gel filtration on a Sephadex G-75 (Amersham) column (2.6 × 100 cm) with 50 mM potassium phosphate buffer (pH 4.6, 0.5 mL/min). All purification steps were done either using on ice or in a cold box at 4 °C.

3.1.7 Western blotting procedure

The same procedure was used as described for rCPO in section 2.1.5.

3.1.8 Circular Dichroism spectrum study

The same procedure was used as described for rCPO in section 2.1.6.

3.1.9 UV-Visible absorption spectrum study

All UV-visible absorption measurements were determined in a VARIAN Cary 300 spectrophotometer using a 1-cm path length quartz cuvette.

3.1.10 Determination of extinction coefficients of CPO mutant

In order to determine the extinction coefficient of the Soret band of the F103A mutant, both the Wt CPO and the F103A mutant were denatured and then reduced in the presence of pyridine and the absorbance of the free ferrous heme complex bound with pyridine at 555 nm measured. The mixture contained 166 µL enzyme solution, 600 µL

NaOH solution (0.066 N), and 400 μL pyridine. After careful mixing, 10 μL of 1 M $\text{Na}_2\text{S}_2\text{O}_4$ was then added to reduce the heme from ferric to ferrous state. On the basis of the known extinction coefficient of Wt CPO ($\epsilon_{398\text{nm}} = 91200 \text{ M}^{-1}\text{cm}^{-1}$), the extinction coefficient of the free ferrous heme-pyridine complex was determined ($\epsilon_{555\text{nm}} = 33.8 \text{ M}^{-1}\text{cm}^{-1}$), which was then used to calculate the extinction coefficient of the F103A mutant.

3.1.11 Activity assays

1). Chlorination Assay (MCD assay) — the same procedure was used as described for rCPO.

2). Peroxidase Assay (ABTS assay) — the peroxidase's activity was measured by using 2,2'-azino-bis-3-ethyl-benzthiazoline-6-sulfonic acid (ABTS) as the electron donor (Yi, Conesa et al. 2003). The 3 mL reaction mixture contained 50 mM phosphate-citrate buffer, pH 5.0, 0.01% H_2O_2 , 100 mg/L ABTS, and a suitable aliquot of the enzyme. The reaction was initiated by the addition of H_2O_2 , and the increase in absorbance at 405 nm was monitored at room temperature. One unit will oxidize 1.0 μmole of ABTS per minute at pH 5.0 at 25°C.

3). Catalase Assay — The 3 mL reaction mixture contained 50 mM phosphate buffer, pH 5.0, 4 μL of 35 % H_2O_2 , and a suitable aliquot of the enzyme. The reaction was initiated by the addition of enzyme, and the decrease in absorbance at 240 nm was monitored at room temperature.

4). Epoxidation activity and enantioselectivity study — The initial epoxidation rate of styrene or its derivatives was determined by monitoring the decrease in absorption at 242~252 nm with time. The exact wavelength depended on the derivative being analyzed.

The 3-mL reaction mixture contained approximately 5 µg of native or mutant CPO, 2 mM H₂O₂, and 300 µM substrate in 100 mM, pH= 5.5 citrate buffer at room temperature (Yi, Mroczko et al. 1999). Product yields and enantioselectivity of native and mutant CPOs with styrene and its derivatives were determined by HPLC. For these assays, a mixture containing 70 µL of styrene or its derivatives, 100 µL of *tert*-butyl hydrogen peroxide, and 400 µL of *tert*-butanol was first prepared. Then, 250 µL of the above mixture was added to 1 mg of wild-type or mutant CPO in 375 µL of 100 mM citrate buffer, pH 5.5. The reaction mixture was agitated at room temperature. After 45 min, the reaction was stopped by the addition of 50 µL of 1 M Na₂S₂O₃ in a saturated solution of NaHCO₃. The reaction mixture was extracted with 300 µL of isooctane. The HPLC analysis of the extracted organic phase was conducted on a Pirkle Concept WhelkO-1-SS column (2% isopropyl alcohol in hexane, 1 mL/min, and UV detector at 214 nm) to determine the yield of the reaction and the enantiomeric excess of epoxides (Geigert, Lee et al. 1986).

5). *N*-demethylation activity — the reaction mixtures (Kedderis, Koop et al. 1980) contained sodium/potassium phosphate buffer (0.5 M), pH 6.0, *N,N*-dimethylaniline (0.53 mM), and *tert*-butyl hydroperoxide (2.1 mM) in a final volume of 3 mL. The reactions were initiated by the addition of the enzyme, incubated at 25 °C for 15 min, and terminated by the addition of 0.75 mL of 60% trichloroacetic acid. The incubation mixtures were extracted twice with ethyl acetate (5 mL) to remove the violet color formed during the course of the reaction at higher protein concentrations. To 1 mL of the extracted aqueous phase, 0.5 mL of Nash reagent (30 g of ammonium acetate and 0.4 mL of 2, 4-pentanedione per 50 mL volume) was added and the solutions were mixed and incubated at 25 °C for 45 min. The absorbance of the resulting conjugate was read at 421

nm. All experiments were carried out in duplicate or triplicate and included controls in which the enzyme was omitted. The data presented are average values.

3.1.12 Optimum pH for the chlorination activity

The relationship between activity and pH was examined from pH 2.5 to 7.0 using the MCD assay. The phosphate buffer contained 20 mM KCl at each pH value.

3.1.13 Ligand binding study

The apparent dissociation constant (K_d) of enzyme and substrate binding was determined by the titration method (Dawson, Sono et al. 1983). Enzyme solution (5 μ M) was prepared in 100 mM phosphate buffer at the appropriate pH and added to a cuvet, which was then placed inside a UV-vis spectrometer. A stock solution of the ligand was made in the same buffer and added in equal volume to the enzyme solution and the blank, which initially contained only the phosphate buffer. The UV-vis spectrum was recorded at the beginning and every time an aliquot of the ligand was added until the spectrum stopped changing. The K_d was calculated using the formula:

$$K_d = [L] (1-v)/v$$

K_d is the apparent dissociation constant, $[L]$ is the free ligand concentration and v is the ratio of ligand bound enzyme concentration to total enzyme concentration.

To obtain the ferrous-CO complex of CPO, the $[Fe^{+3}]$ was first reduced to $[Fe^{+2}]$ with dithionite and then bubbled for 1 min with carbon monoxide.

To evaluate the affinity of CPO for a sixth axial ligand, ligands such as cyanide and azide, that are known to bind strongly to the heme iron atom, were used and UV-vis spectra of the enzyme-ligand complexes were obtained. These ligands would induce a change of the heme iron from high spin to low spin (Sono, Dawson et al. 1986).

3.2. Results and discussion

3.2.1 Preparation and purification of F103A mutant

After successfully expressing rCPO, I prepared a new mutant of CPO, F103A employing the same system. Using Stratagene QuikChange II XL site-directed mutagenesis kit, a 34 base primer containing the intended mutation was introduced into the pCPO3.1-Amds plasmid. After amplification and purification, the PCR product was analyzed by agarose gel electrophoresis to verify the vector size and was sequenced to verify that the mutation was indeed introduced at the correct location. The new plasmid was named pCPOF103A3.1 and was transformed into *A. niger* strain MGG029 as described in Chapter 2. After two rounds of screening based on the uridine dependence, ability to use acrylamide and extracellular peroxidase activity, several colonies were picked for further investigation. As with rCPO, DNA sequencing was used to confirm the presence of the mutant gene in each colony after several rounds of passage of the transformed strain to eliminate possible transient transformation.

One colony was then selected and cultured to produce the mutant protein and the mutant protein was purified by the procedure mentioned above for rCPO. The chromatography results of purification are shown in Fig. 3.1 & Fig. 3.2. The fractions were collected based on the UV-vis absorption at 418 nm (for Soret band) and 280 nm (for protein absorption). The fourth peak in Fig. 3.1 and the second peak in Fig. 3.2 were identified as heme-proteins and the fractions corresponding to these peaks were collected and combined. The purification results are summarized in Table 3.1. With this method, more than 8 mg/L active protein can be obtained. Strikingly, the purified F103A CPO mutant displayed an Rz value of 1.25, which matched the theoretically calculated value

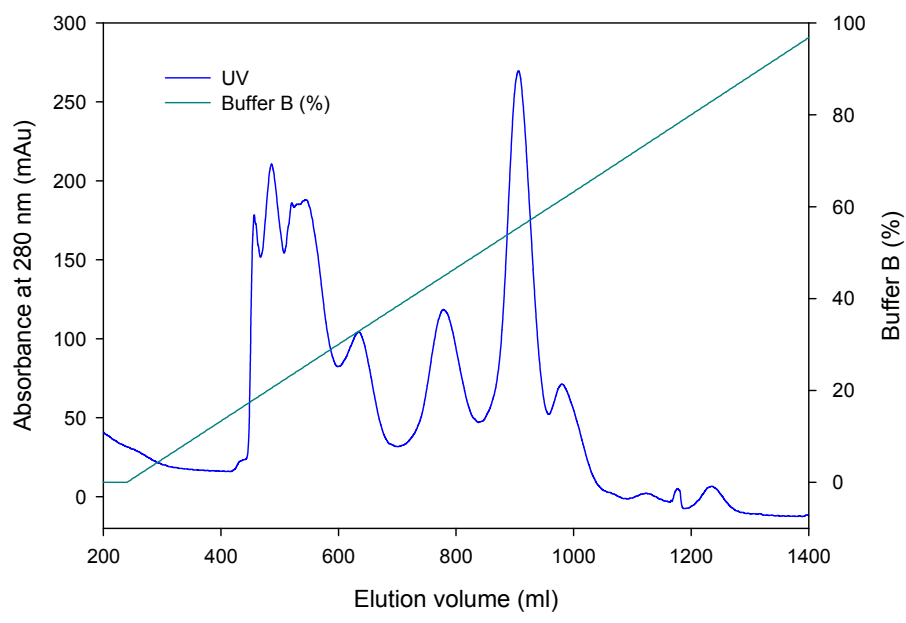


Figure 3.1 Chromatogram of ion exchange chromatography of F103A.

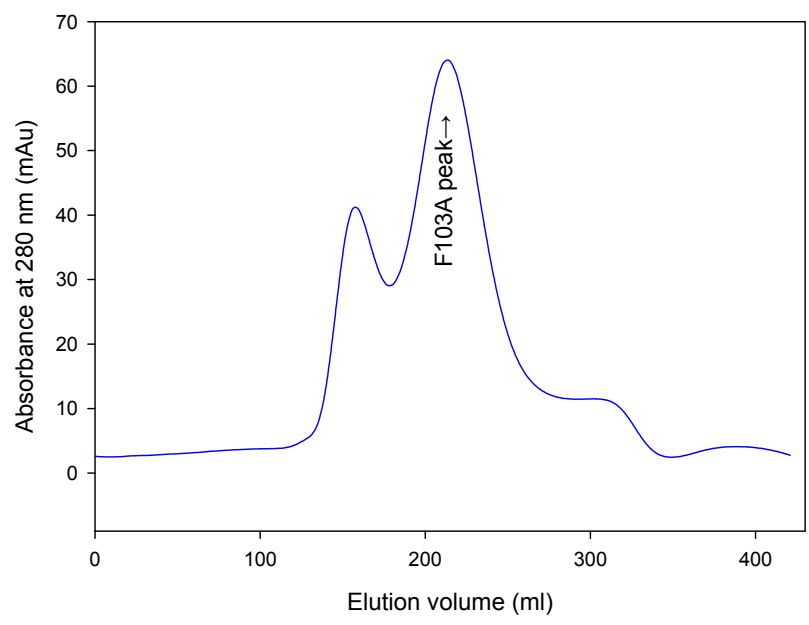


Figure 3.2 Chromatogram of gel filtration chromatography of F103A

Table 3.1 F103A purification result

	Volume mL	Absorbance at 418 nm	Enzyme mg	Yield %	Rz <i>A418/A280</i>
Crude media (condensed)	43	1.934	44.1	100	ND
Dialysis	27	2.223	31.8	72	ND
DEAE-Sepharose	60	0.4174	13.3	30	~0.9
Sephadex G-75	40	0.3588	7.6	17	~1.25

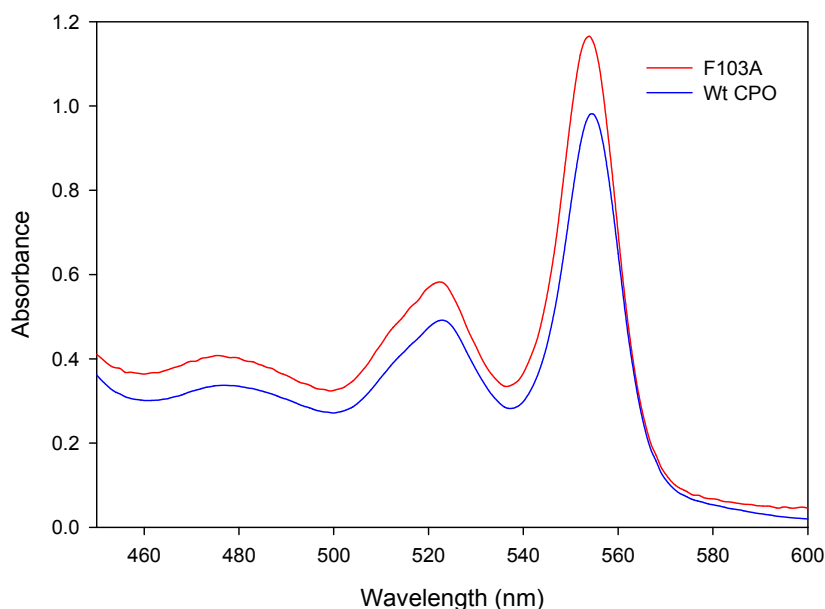


Figure 3.3 Visible spectra of the free ferrous heme-pyridine complex of F103A mutant and Wt CPO. The Soret bands are located at 555, 523, and 478 nm. Based on the known extinction coefficient of Wt CPO ($\epsilon_{398 \text{ nm}} = 91200 \text{ M}^{-1}\text{cm}^{-1}$) and the calculated extinction coefficient of free ferrous heme-pyridine complex ($\epsilon_{555 \text{ nm}} = 33.8 \text{ M}^{-1}\text{cm}^{-1}$), the extinction coefficient for the F103A mutant was determined. For F103A mutant, $\epsilon_{418 \text{ nm}} = 79200 \text{ M}^{-1}\text{cm}^{-1}$, and the Rz value = 1.25.

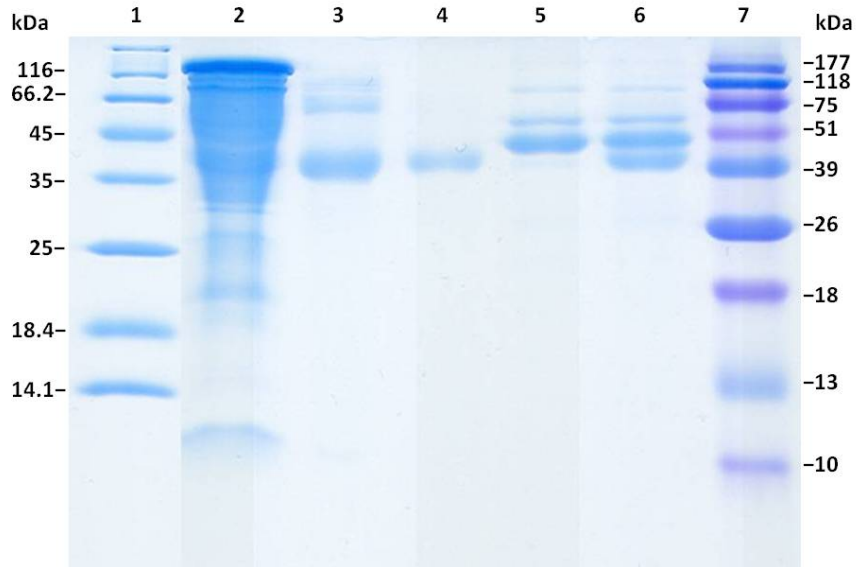


Figure 3.4 15% SDS-PAGE result of F103A purification. Lanes 1&7 are protein molecular weight markers. Lanes 2 to 4 are F103A samples from crude media, and ion exchange and gel filtration purification steps, respectively. Lane 5 is the sample of Wt CPO and lane 6 is a mixed sample of Wt CPO and purified F103A. According to the gel result, the molecular weight of the F103A mutant is slightly smaller than that of Wt CPO.

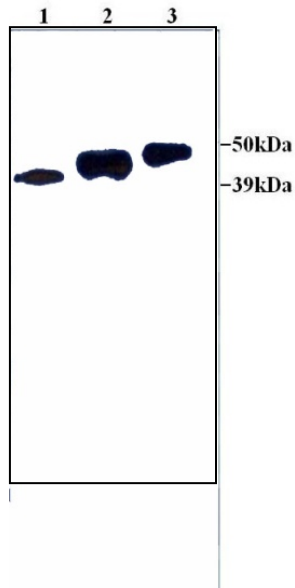


Figure 3.5 Western blotting analysis result: Lanes 1 to 3 are F103A, Wt CPO, and rCPO respectively. Proteins were detected with an anti-CPO polyclonal antiserum. The antibody was diluted 1:10K for F103A, and 1:100K for Wt and rCPO.

for F103A using the pyridine hemochromagen method (Fig. 3.3). The calculated extinction coefficient for F103A at 418 nm equals to $79200 \text{ M}^{-1} \text{ cm}^{-1}$, and the pure form of protein is supposed to has an Rz value equals to 1.25. The protein fractions from each purification step and the final product were analyzed by SDS-PAGE to determine its purity (Fig. 3.4). In addition, the authenticity of the product was examined by western blotting (Fig. 3.5). As seen in the SDS-PAGE and western blotting, the molecular weight of F103A is apparently smaller than that of either rCPO or Wt CPO, probably because of a different glycosylation profile. The molecular difference may indicate a possible conformational change causing the amino acid side chains exposed on the protein surface to have changed, thus altering the glycosylation profile. However, due to the difficulty caused by the heavy glycosylation with both N- and O-glycosylation, I was unable to identify the differences in glycosylation. Nonetheless, the western blotting with rabbit anti-CPO polyclonal antibody confirmed that the purified protein is indeed a CPO mutant.

3.2.2 Structure and function study of F103A mutant

Heme proteins have characteristic visible Soret absorption bands that convey significant information about the structure and coordination state of their active sites. The UV-vis spectrum of F103A, Wt CPO, and P450 camphor were examined and compared in Fig. 3.6. The UV-vis spectrum of F103A was quite different from that of Wt CPO, yet resembled that of camphor free P450cam (CYP101). The major Soret band for Wt CPO is at 398 nm and the corresponding band for the mutant is at 418 nm. The α and β bands of Wt CPO are at 514 nm and 539 nm; the corresponding bands for the mutant are at 539 nm and 573 nm. Both the major Soret band and the minor bands of F103A mutant are

all at the positions that are very similar to P450cam, which has bands at 417, 536, and 569 nm.

One similarity between Wt CPO and P450cam is that they have a cysteine as the proximal ligand for the heme center. To verify that such a structural feature was retained in the F103A mutant, the UV-vis spectral properties of the protein-CO complex of these enzymes under reducing condition were studied (Fig. 3.7). The ferrous-CO complex of heme containing enzymes with a thiol group as the proximal ligand shows a distinctive Soret band near 450 nm. The spectrum of F103A CPO-CO complex was essentially identical to that of Wt CPO-CO and P450-CO, confirming that F103A also has a thiol proximal ligand.

These spectral features are summarized in Table 3.2 and indicate that although F103A has the same proximal ligand as Wt CPO; F103A has different structural features around the heme center. It is most probable that these differences are caused by change on the distal side. The close resemblance of F103A and P450cam indicates that F103A may have a water molecule as the sixth ligand, like P450cam. Unlike in Wt CPO, the water molecule in the active center does not bind to the ferrous center directly, but only binds with Glu183 by hydrogen bond. These changes will affect ligand binding, substrate selection, as well as catalytic behavior of the enzyme; it makes F103A a much better model for p450. The structural basis for this change is worth further exploration. There is a slight possibility that the changes were the result of an overall structural reconfiguration. A nearly identical CD spectrum (Fig. 3.8) showed that, like rCPO, there is no significant secondary structural change in F103A compared to Wt CPO.

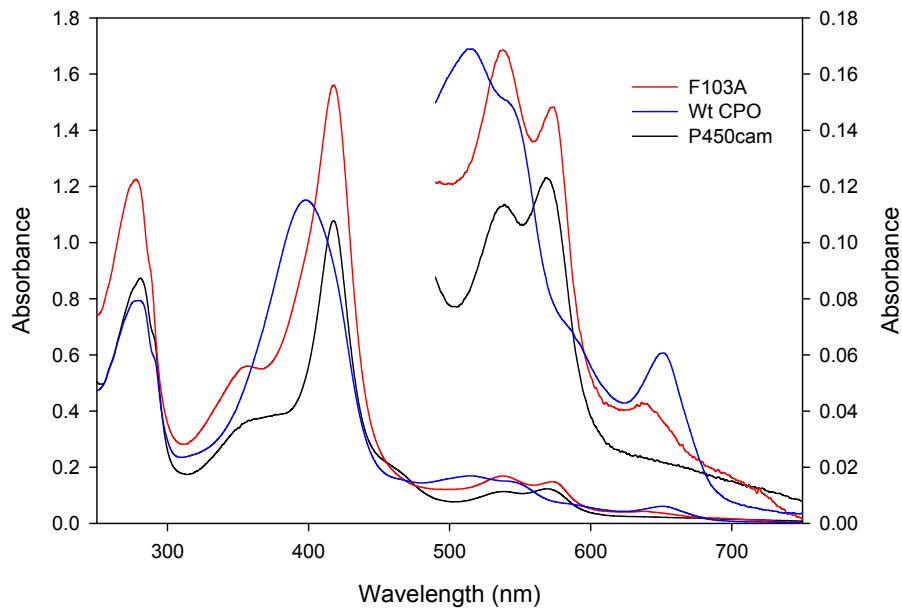


Figure 3.6 UV-vis spectra of Wt CPO, and its F103A mutant in 0.05 M potassium phosphate buffer, pH 5.0, and P450cam in 0.05 M potassium phosphate buffer, pH 7.4.

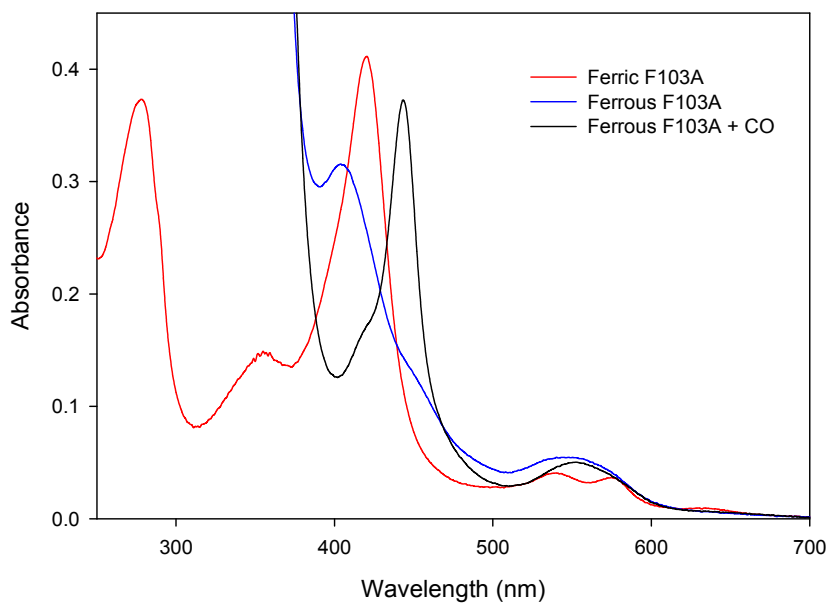


Figure 3.7 UV-vis spectra of the ferric, ferrous, and ferrous-CO complexes of the F103A mutant in 0.05 M potassium phosphate buffer, pH 5.0

Table 3.2 Spectral properties of heme thiolate proteins (P450cam, Wt CPO and CPO F103A mutant) and their ligand complexes

Protein	λ_{\max} , nm (ϵ , $\text{mM}^{-1}\cdot\text{cm}^{-1}$)					reference
	δ	Soret	β	α	CT	
Ferric substrate free						
CPO F103A	356	418 (79.2)	538 (8.5)	572 (7.5)	637 (2.2)	this work
Wt CPO		398 (91.2)	514 (13.0)	543 (11.5)	651 (4.4)	
Wt P450cam	365	417 (115)	536 (10.6)	569 (11.1)	na	(Dawson, Andersson et al. 1982)
Ferrous ligand free						
CPO F103A		405 (60.6)	547 (10.5)			This work
Wt CPO		408 (79.3)	550 (12.7)			This work
Wt P450cam		408 (87.1)	540 (15.8)			This work
Ferrous-CO complex						
CPO F103A		443 (71.7)	552 (9.7)			This work
Wt CPO		446(124.8)	550 (11.2)			This work
Wt P450cam		446(130.6)	550 (16.3)			This work

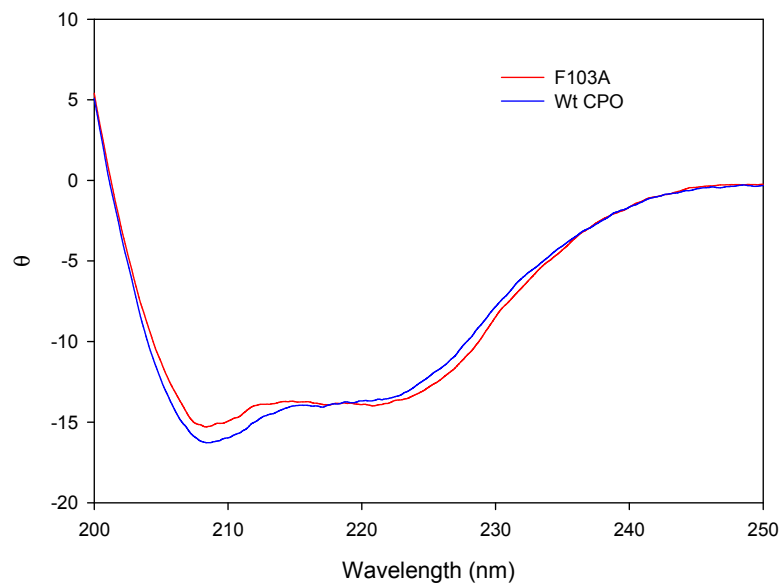


Figure 3.8 The CD spectra of F103A mutant (0.375 μ M in 10 mM phosphate buffer pH=6) and Wt CPO (0.3 μ M in 10 mM phosphate buffer, pH=6). The experiments were carried out at the room temperature and recorded from 190 to 250 nm. The path length was 1cm.

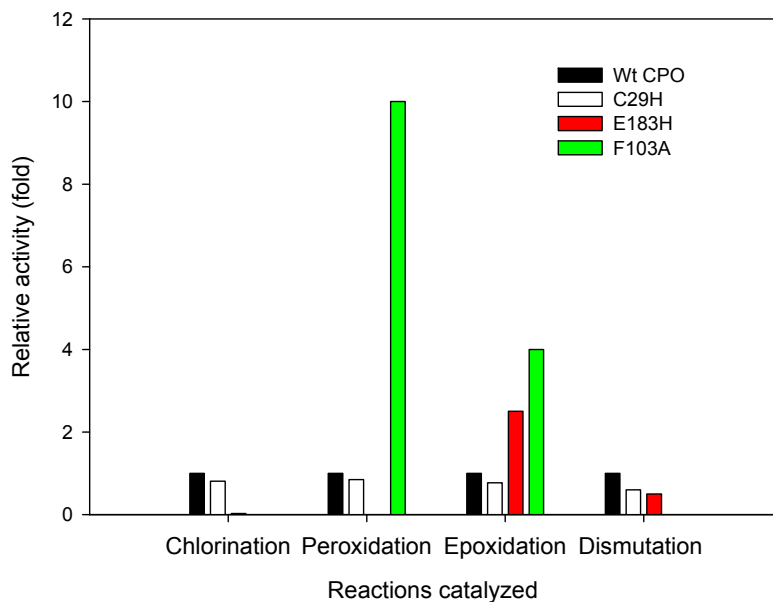


Figure 3.9 Relative activities of Wt CPO, C29H, F103A and E183H mutants.

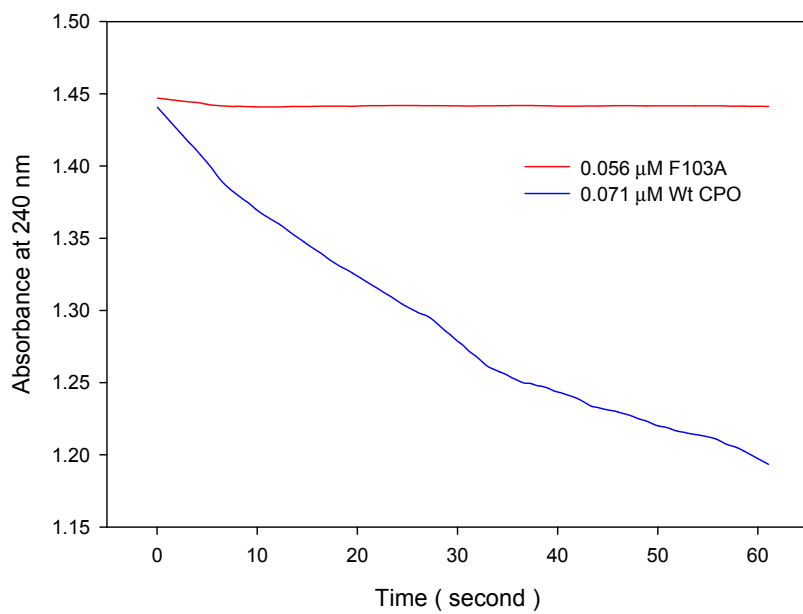


Figure 3.10 Catalase activity assays of Wt CPO and F103A.

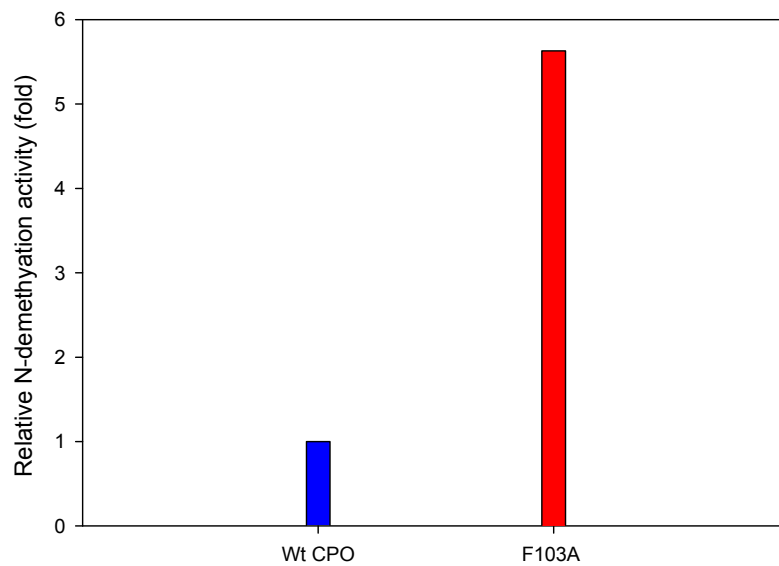


Figure 3.11 *N*-demethylation activities of Wt CPO and its F103A mutant.

Naturally, I am interested in understanding how these structural changes affect the protein's catalytic properties. A comparison of the chlorination, epoxidation, peroxidation and dismutation activity of the wild type, F103A mutant, and other CPO mutants is shown in Fig. 3.9. The chlorination activity of the mutant enzyme decreased to 1% of the wild type activity, so did the dismutation activity, and the catalase activity decreased to an undetectable level (Fig. 3.10). Peroxidation and epoxidation activity, however, unexpectedly increased by 10-fold, and 4-fold, respectively. Similarly, an increase of 5.6 fold in the *N*-demethylation activity was observed for this mutant CPO (Fig. 3.11).

These data show that the F103→A mutation changes the catalytic activity of CPO dramatically. As mentioned in the introduction, once the CPO reacts with hydrogen peroxide and forms Cpd I, it has three pathways to return to the resting state: (1) react with another molecule of polar substrate with high redox potential like peroxide or chloride, generating O₂ or a reactive oxygen species like HOCl; (2) return to resting state by two one-electron steps, lose one redox equivalent and be reduced to Cpd II, a nonradical oxoferryl species, then oxidize another substrate and return to the resting state; (3) lose two electron equivalents by inserting its oxoferryl oxygen into a suitable acceptor in a P450 type reaction.

After examination of the catalytic activities of F103A, it becomes evident that pathway (1) is inhibited, whereas pathways (2) and (3) are enhanced as reflected by the decrease in catalase and chlorination activity but an increase in peroxidase, epoxidation and *N*-demethylation activity. Two plausible explanations for the results are that F103A Cpd I has a lower redox potential, and thus is unable to oxidize reactants with higher redox potentials; and that the F103A catalytic center does not react with polar substrates

favorably, thus lowering the reactivity with hydrogen peroxide and chloride ion. A combination of both is also possible; however, further studies are required.

The dramatic changes in the activity profile of F103A CPO actually make it a better industrial catalyst than Wt CPO. Epoxidation of alkenes, chloroalkenes, styrene, and other chemicals is an important type of reactions used in drug synthesis (Neidleman and Geigert 1983; Lakner and Hager 1996). Higher activity will certainly preferred for a catalyst used in these areas. In Wt CPO, the epoxidation pathway has to compete with catalytic pathway; a lower catalase activity will help to improve the epoxidation activity and conversion rate especially with higher hydrogen peroxide concentration (Manoj and Hager 2001)

To gain insight into the structural changes of the active site, the UV-vis spectrum of F103A was acquired at each of several pH values. As the pH is lowered down to 3, a shoulder peak at 400 nm became more prominent (Fig. 3.12), indicating the presence of a high spin ferric center, similar to that found in Wt CPO from pH 2 to 7. The five coordinate high spin state of F103A could be produced by the loss of water from the six-coordinate low spin state. As the pH is lowered, water has a lower binding affinity for F103A and tends to disassociate from the heme center converting the ferric center of F103A from a six coordinate low spin state to a five coordinate high spin or mixed spin state. In the mixed spin state some of the iron atoms are high. This further proves that the F103A CPO mutant, like P450cam, has a water molecule served as the sixth ligand of the heme center at its resting state. Similar spectral changes are also observed when P450 binds a molecule of camphor, which results in the loss of water as the sixth ligand completely (Dawson, Andersson et al. 1982).

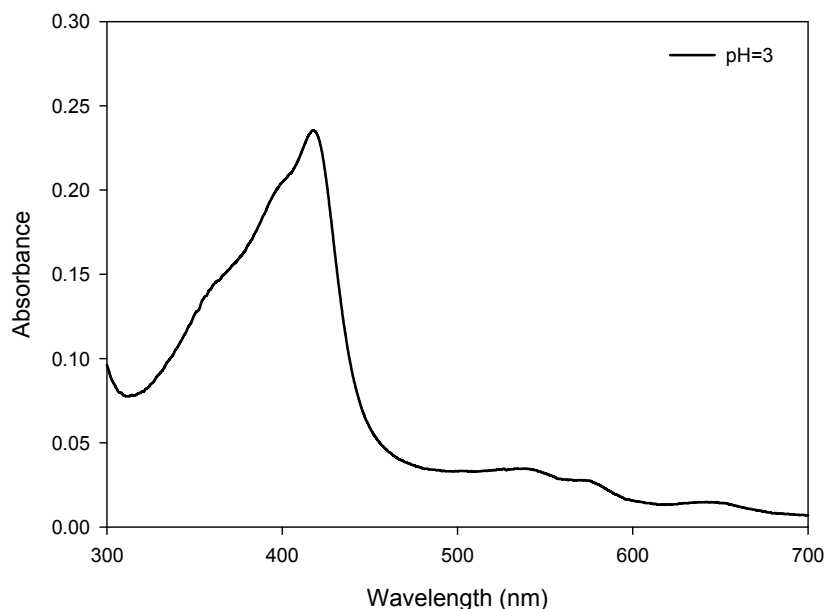


Figure 3.12 UV-vis spectra of F103A in 0.1 M potassium phosphate buffer at pH 3. At pH=3, the F103A mutant has a shoulder peak around 400 nm.

The ligand binding properties of F103A with a variety of ligand were investigated to probe the chemical environment of the heme center in this CPO mutant. A wide range of ligands with different pK_a values and different coordinating atoms were employed. The spectrums of each F103A-ligand and Wt CPO-ligand complex are presented here: cyanide (Fig. 3.13), azide (Fig. 3.14), imidazole (Fig. 3.15), thiocyanate (Fig. 3.16), formate (Fig. 3.17), and acetate (Fig. 3.18). Both Wt CPO and its F103 mutant showed very similar absorption spectrum when binding to the same ligand, indicating the heme center in F103A has a similar configuration to Wt CPO when binds to a ligand, thus it may adopt similar intermediates and mechanism during catalysis. The only exception is acetate; unlike in Wt CPO, it binds to the ferric center and gives a mixed spin state for the heme center (Sono, Dawson et al. 1986), in F103A, the heme center remains its original low spin state, in addition to no shift in Soret band position shift was observed.

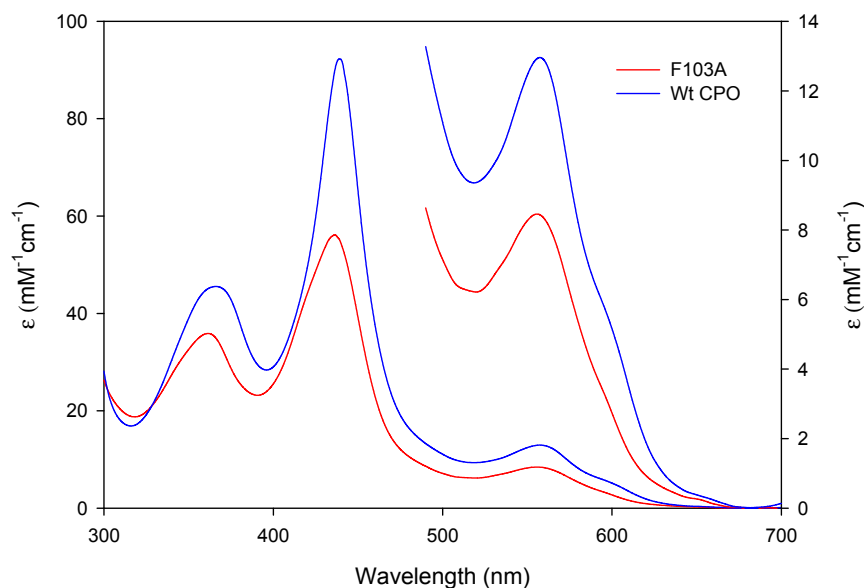


Figure 3.13 UV-vis absorption spectra of the cyanide complexes of ferric Wt CPO and F103A. The spectra were obtained at pH=3 in 0.1 M potassium phosphate buffer at room temperature with 5 μ M enzyme concentration. The ligand concentrations were 0.2 M for F103A mutant, and 20 mM for Wt CPO

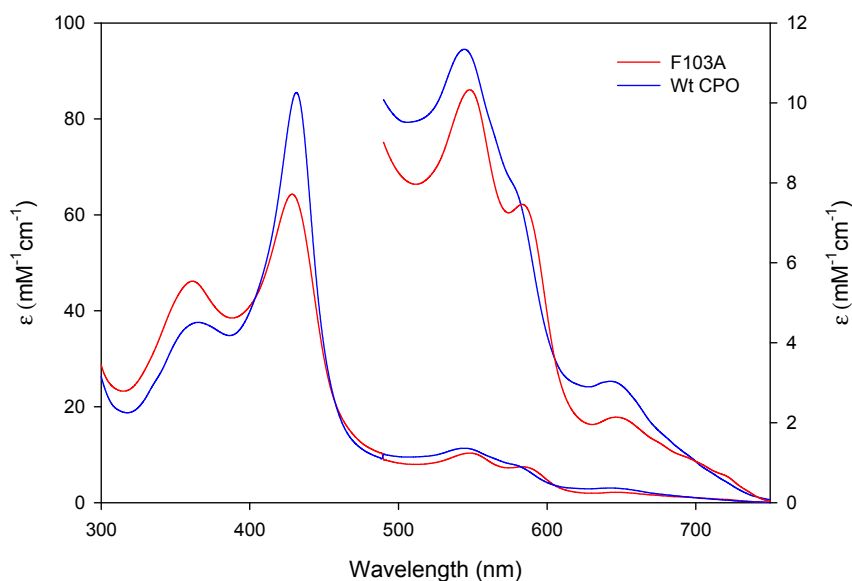


Figure 3.14 UV-vis absorption spectra of the azide complexes of ferric Wt CPO and F103A. The spectra were obtained at pH=3 in 0.1 M potassium phosphate buffer at room temperature with 5 μ M enzyme concentration. The ligand concentrations were 35 mM for F103A mutant, and 13 mM for Wt CPO.

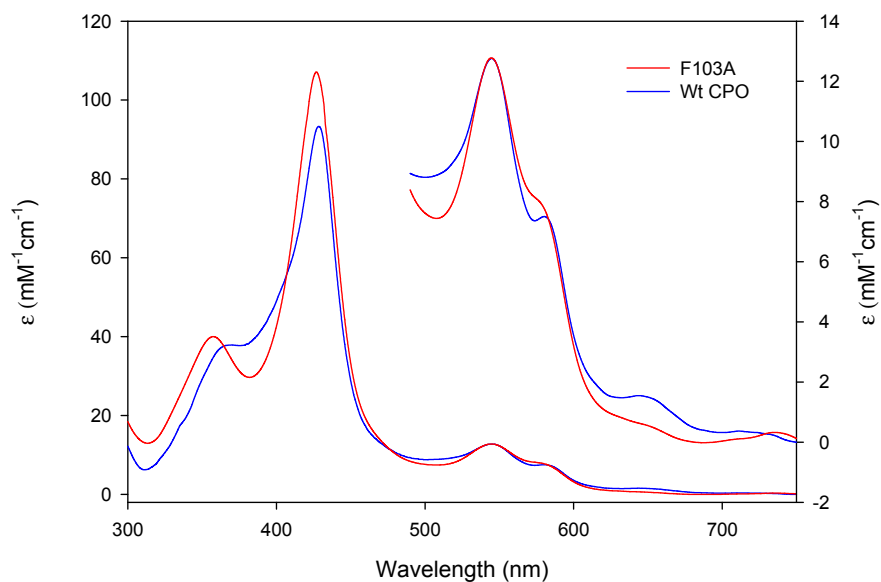


Figure 3.15 UV-vis absorption spectra of the imidazole complexes of ferric Wt CPO and F103A. The spectra were obtained at pH=6 in 0.1 M potassium phosphate buffer at room temperature with 5 μ M enzyme concentration. The ligand concentrations were 2 M for F103A mutant, and 4 M for Wt CPO.

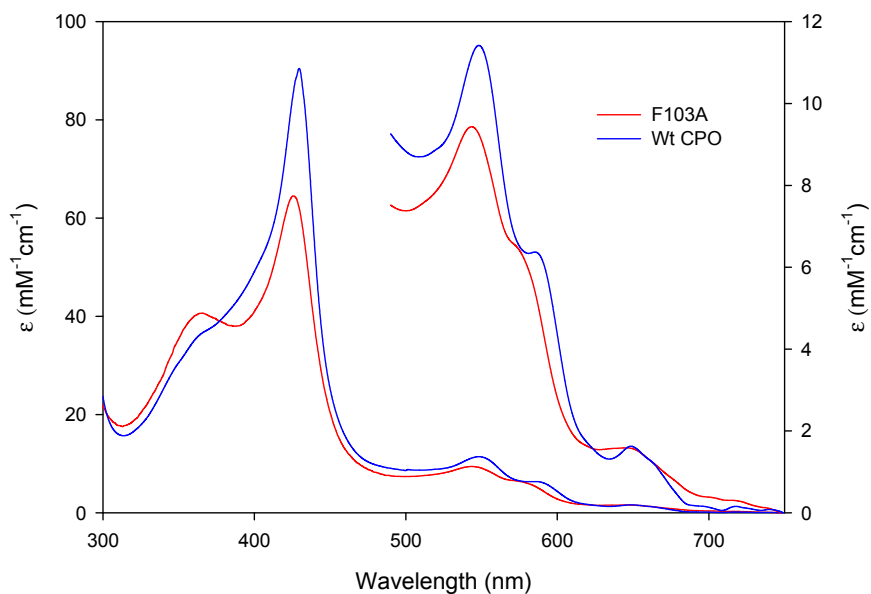


Figure 3.16 UV-vis absorption spectra of the thiocyanate complexes of ferric Wt CPO and F103A. The spectra were obtained at pH=3, in 0.1 M potassium phosphate buffer at room temperature with 5 μ M enzyme concentration. The ligand concentration was 100 mM for F103A mutant, and 15 mM for Wt CPO.

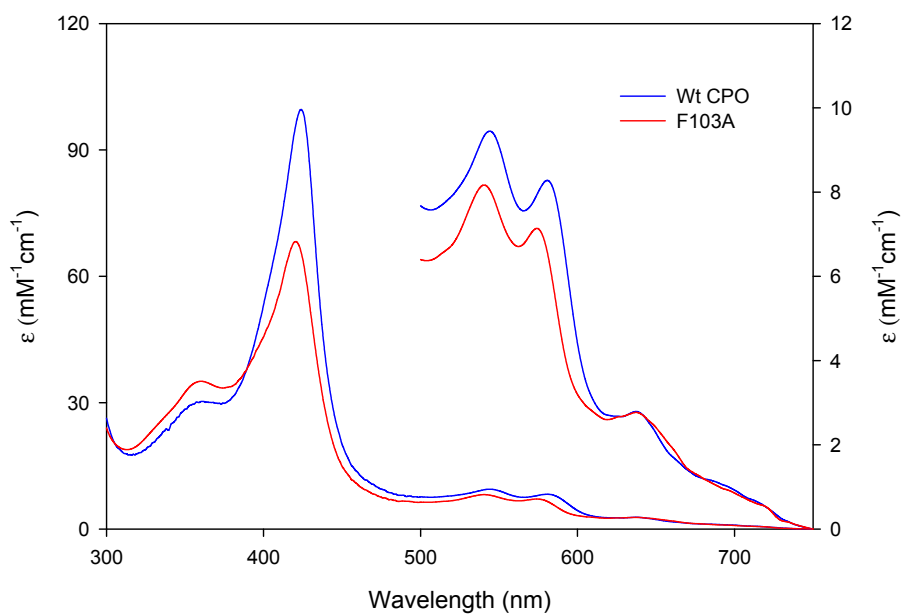


Figure 3.17 UV-vis absorption spectra of the formate complexes of ferric Wt CPO and F103A. The spectra were obtained at pH=3 in 0.1 M potassium phosphate buffer at room temperature with 5 μ M enzyme concentration. The ligand concentration was 1.5 M.

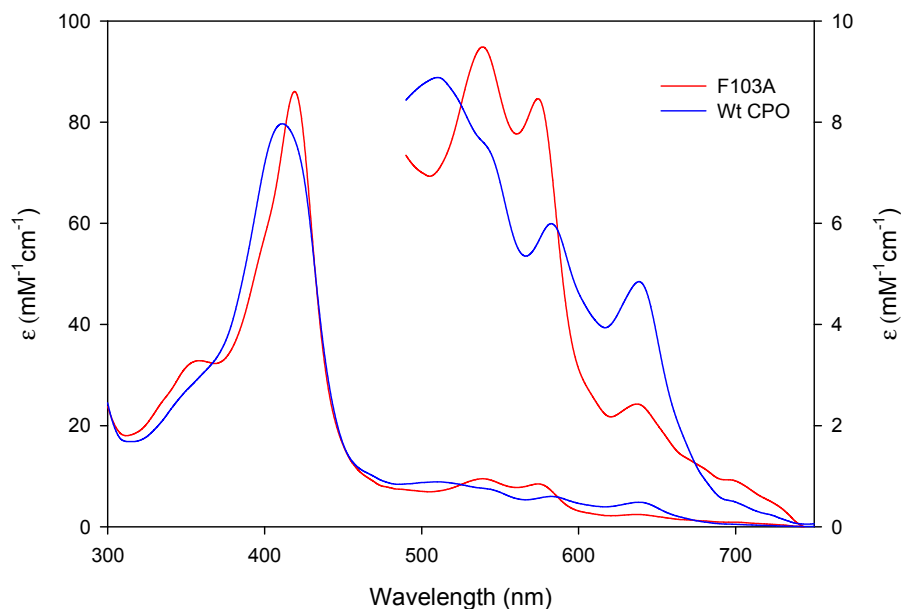


Figure 3.18 UV-vis absorption spectra of the acetate complexes of ferric Wt CPO and F103A. The spectra were obtained at pH=3 in 0.1 M potassium phosphate buffer at room temperature with 5 μ M enzyme concentration. The ligand concentration was 2 M.

Table 3.3 Optical absorption data, dissociation constants, and spin states of ferric Wt CPO & ferric F103A CPO mutant ligand complexes^a

Ligand	Enzyme name	P _{k_a} of Ligand ^b	absorption maxima ^c [λ (ϵ_{mM})]				K _d ^{app} (mM) pH=3	K _d ^{int^d} (mM)	spin state	
			δ	Soret	β	α				
KCN	Wt CPO		366 (45.4)	439 (92.3)	557 (13.0)		0.14	0.14	low	
	F103A CPO	9.14	361 (35.9)	436 (56.1)	556 (8.5)		0.27	0.27	low	
KN ₃	Wt CPO		365 (37.6)	431 (85.5)	544 (11.3)	580 (7.8)	642 (3.0)	1.3 \pm 0.2	1.3	low
	F103A CPO	4.72	360 (46.1)	428 (64.3)	548 (10.3)	583 (7.5)	647 (2.1)	2.9 \pm 1.4	1.8	low
KSCN	Wt CPO		365 (36.8)	430 (90.3)	548 (11.4)	585 (6.4)	649 (1.4)	0.09 \pm 0.01	<i>e</i>	low
	F103A CPO	-1.90	366 (40.6)	426 (64.5)	543 (9.4)	575 (6.4)	646 (1.6)	6 \pm 4	<i>e</i>	low
Imidazole	Wt CPO		367 (37.8)	428 (93.3)	545 (12.8)	580 (7.5)	644 (1.5)	<i>e</i>	<i>e</i>	low
	F103A CPO	7.00	358 (40.0)	427 (107.1)	545 (12.8)	575 (8.1)		<i>e</i>	<i>e</i>	low
HCOOK	Wt CPO		358 (30.1)	424 (99.6)	544 (9.4)	581 (8.3)	637 (2.9)	0.62	0.53	low
	F103A CPO	3.75	360 (35.1)	421 (68.3)	541 (8.2)	574 (7.1)	637 (2.8)	102	87	low
CH ₃ COOK	Wt CPO			411 (79.7)	540 (7.6)	583 (6.0)	638 (4.8)	<i>e</i>	<i>e</i>	mix
	F103A CPO	4.77	358 (32.8)	419 (86.1)	538 (9.5)	574 (8.5)	638 (2.4)	<i>e</i>	<i>e</i>	low

^a All data were obtained in 0.1 potassium phosphate buffer at pH 6 or pH 3 at room temperature. ^b *pK_a* values for the ligands are taken from the following literature: (i) (Danehy and Parameswaran 1968); (ii) (Perrin, Dempsey et al. 1981); (iii) (Streitwieser 1981). ^c The λ and ϵ_{mM} expressed in nm and mM⁻¹cm⁻¹, respectively. ^d Intrinsic (int) affinity for the neutral form of the ligands (see text). ^e Not determined.

Table 3.4 Apparent K_d for cyanide binding of Wt CPO and F103A at various pH

pH value	F103A	Wt CPO
pH=3	268.0 μM	141.5 μM
pH=4	298.0 μM	151.7 μM
pH=5	4236.8 μM	165.7 μM
pH=6	4481.7 μM	90.33 μM

The apparent K_d values (K_d) for ligand binding of several ligands were derived from the ligand binding studies (Table 3.3). Generally F103A shows lower affinity for ligands than Wt CPO, an effect that can be accounted for by a more opened active center allowing more freedom of the ligand in F103A, plus the ligand has to compete with a H_2O molecule that served as the sixth ligand, while in Wt CPO, a H_2O is 3.5 Å away from the heme center. The binding affinity of the F103A for cyanide and azide decreased 2 fold, and for two of the more acidic ligand, thiocyanate, and formate decreased dramatically (100 fold). The extent of decrease was hard to determine for acetate because it has a very low affinity for Wt CPO and any significant decrease will cause its binding with F103A to become undetectable. However the extent of the decrease is not correlated with pK_a values, it is possible that the structure of the ligand may also play a role here.

The effect of pH on the ligand binding of the F103A mutant to one of the strongest ligands, cyanide (Table 3.4). Compared to Wt CPO, which has a small increase in the ligand affinity between pH 5~6, F103A actually showed an abrupt decrease in ligand affinity between pH 4~5. A similar effect was observed when studying the chlorination

activity of F103A, unlike Wt CPO that has an optimum pH=2.75, F103A mutant has an optimum pH=3 (Fig. 3.19).

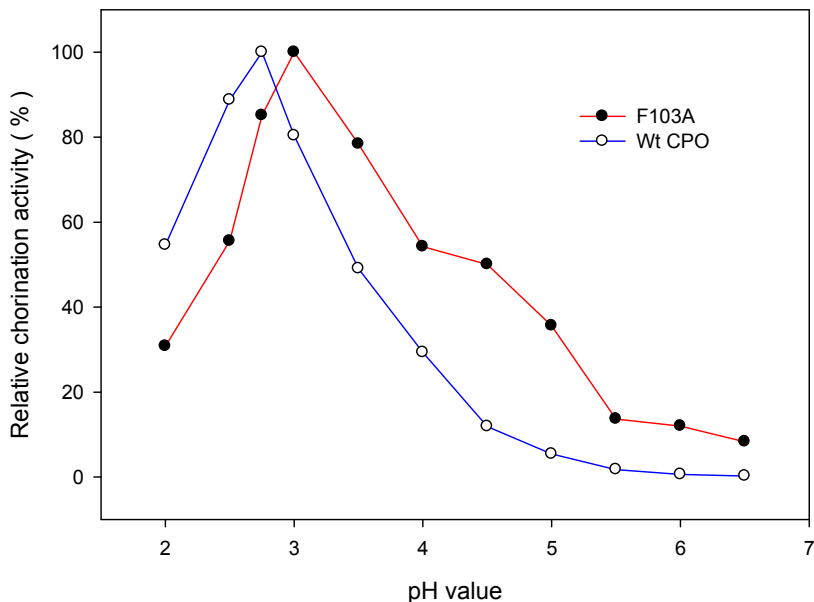


Figure 3.19 pH profiles for chlorination activity of Wt CPO and F103A.

One possible explanation for such changes could be changes of the distal ligand state. It had been well established that Glu183 plays an important role in stabilizing the ligand-ferric heme iron complex (Sundaramoorthy, Terner et al. 1998; Kuhnel, Blankenfeldt et al. 2006). It is possible that Glu183 may not be suitably close enough to the ferric center to form a hydrogen bond with the ligand, or the hydrogen bond network formed by Glu183, His105 and Asp106 had been interrupted. Thus instead of Glu183, Ser 184 is placed close to the ferric center, adopting a similar configuration to P450cam. Another possible scenario is that the F103A mutation causes a slight twist of the peptide backbone where F103 is located, disrupting the nearby hydrogen bond between His105

and Glu183, resulting in the formation of a new hydrogen bond between Asp106 and Glu183. On the basis of significant decrease in cyanide binding between pH 4-5 and the decrease in optimum pH of chlorination, the latter hypothesis is more plausible.

3.2.3 F103A mutant as a possible industrial catalyst

As mentioned in the introduction, one drawback of Wt CPO is its limited ability to accept larger substrate, thus substituting the Phe103 with a smaller amino acid, Ala, should change the structure of the active center to allow access of larger substrate. To evaluate this approach, a series of styrene derivatives were used to study the catalytic activity of the F103A mutant.

Although Wt CPO can catalyze the epoxidation of α -methylstyrene and α -ethylstyrene (Dexter, Lakner et al. 1995), with high enantioselectivity, the turnover number decreased dramatically as the substituent group was changed from methyl to ethyl; a similar phenomenon was also observed when comparing α -methylstyrene and styrene. It is proposed that repositioning the methyl or larger substituent group on the double bond of the styrene might offer insights into the steric control of both reactant size and reaction enantioselectivity. Furthermore, styrene and its derivatives are an important group of compounds for industrial applications, yet are challenging to modify with enzymes. In addition, the aromatic group will enable assessment of the reaction with UV-vis spectroscopy.

The epoxidation behavior of F103A on styrene derivatives with increasing size of the substituent on alpha carbon of the double bond was investigated: α -methylstyrene, α -ethylstyrene, and α -propylstyrene. An increase in catalytic activity with both α -ethylstyrene and α -propylstyrene (Fig. 3.20) was observed for F103A, both substrate

react very slow with Wt CPO and required prolonged time (~1 h) for a noticeable change to occur by UV-vis. Styrene derivatives with a more highly substituted group on the double bond was also used as substrates. While Wt CPO reacts poorly with tri-substituted styrene, F103A can accept such substrates with higher turnover rates. However, tetra-substituted styrene was accepted as a substrate by neither Wt CPO nor F103A (Fig. 3.21). The next structural feature we studied was the conformation of the substrate. *Trans* derivatives of styrene and *trans* olefins, in general, were found to be poor substrates for Wt CPO, as is usually the case in epoxidation reactions catalyzed by heme proteins and their synthetic models (Groves and Nemo 1983). However, F103A can catalyze the epoxidation of *trans*- β -methylstyrene (Fig. 3.22), and *trans*-substrates with larger substituent, such as *trans*-1-phenyl-1-pentene and *trans*-1-phenyl-1-butene.

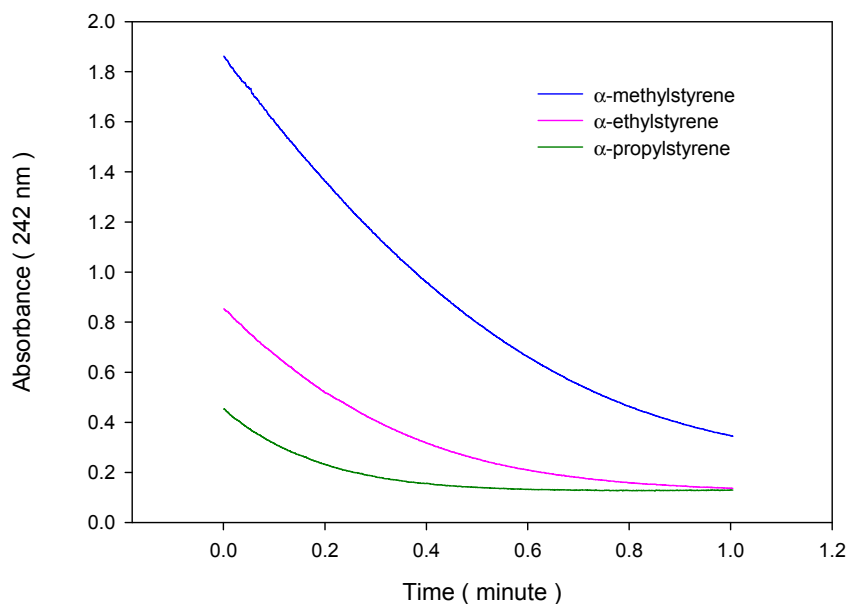


Figure 3.20 UV absorbance decrease at 242 nm profiles for F103A (39 nM) catalysis of the epoxidation of α -methylstyrene, α -ethylstyrene, and α -propylstyrene (300 μ M) in 100 mM citrate buffer, pH = 5.5.

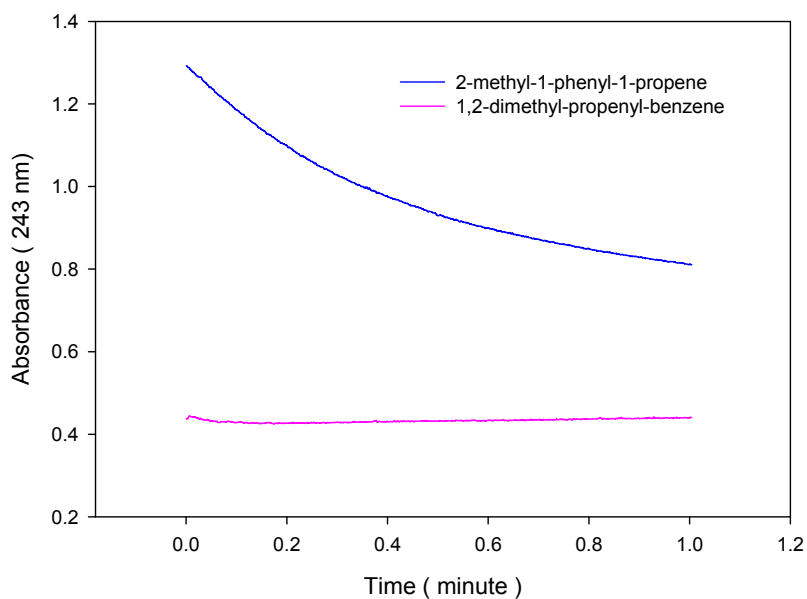


Figure 3.21 UV absorbance decrease at 243 nm profiles for F103A (39 nM) catalysis of the epoxidation of 2-methyl-phenyl-1-propene and 1,2-dimethyl-propenyl-benzene (300 μ M) in 100 mM citrate buffer, pH = 5.5.

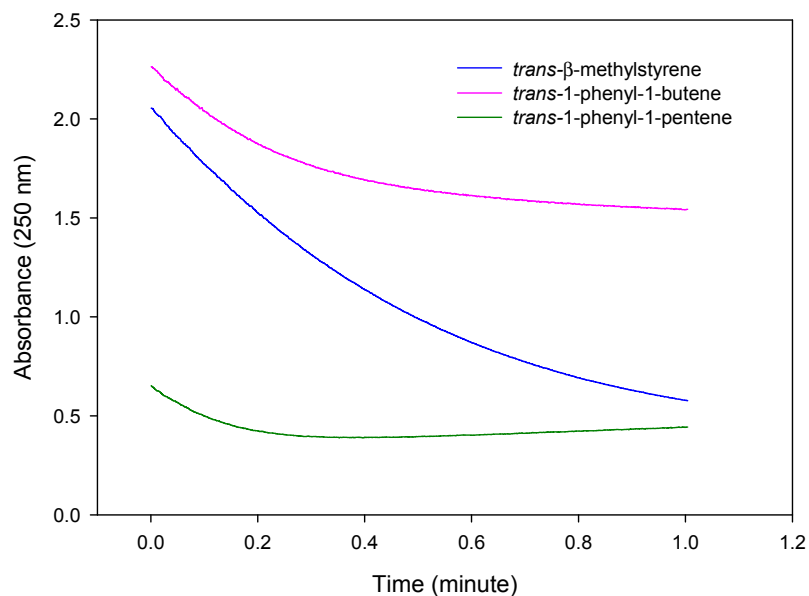


Figure 3.22 UV absorbance decrease at 250 nm profiles for F103A (39 nM) catalysis of the epoxidation of *trans*- β -methylstyrene, *trans*-1-phenyl-1-butene, and *trans*-1-phenyl-1-pentene (300 μ M) in 100 mM citrate buffer, pH = 5.5.

Lastly, the enantioselectivity of F103A with these substrates was examined. Chiral HPLC with an UV detector was used to study the epoxidation products of various styrene derivatives. A sample HPLC trace is shown in Fig. 3.23 & Fig. 3.24. In these figures, It can be seen that the F103A mutant has almost completely lost its enantioselectivity when catalyzing styrene epoxidation, in contrast to Wt CPO which has an ee% of 49. For other substrates that can be accepted by both Wt CPO and F103A, F103A showed a distinctive enantioselectivity profile (Table 3.5). Similar to styrene, F103A almost lost its enantioselectivity when catalyzing the epoxidation of *cis*- β -methylstyrene. However, when catalyzing another substrate that reacts readily with Wt CPO, α -methylstyrene, F103A showed high enantioselectivity but with a different configurational In summary, on the basis of the NMR data, rCPO and Wt CPO have very similar active site structures. The 1D and 2D spectra are nearly identical, as are the T1 values and the intercepts of the Curie plots. The chemical shifts of the paramagnetically shifted resonances in isozyme B of Wt CPO and the corresponding resonances in rCPO are at most 0.4 ppm apart with the exception of the resonance at approximately 39 ppm, which is broad and has a poorly defined peak, Table 2.3. For comparison, when yeast cytochrome *c*, a non-glycosylated heme protein was expressed in *E. coli*, the chemical shifts of the paramagnetically shifted resonance of wild type and recombinant proteins differed by up to 0.6 ppm preference. When catalyzing larger, more branched substrates, *trans*- β -methylstyrene, *trans*-1-phenyl-1-butene, and 2-methyl-phenyl-1-propene, F103A exhibited higher enantioselectivities and higher conversion rate.

The new enantioselectivity profile can be explained by the steric control of substrate access to the ferric center and the configuration inside the heme pocket. When F103 is

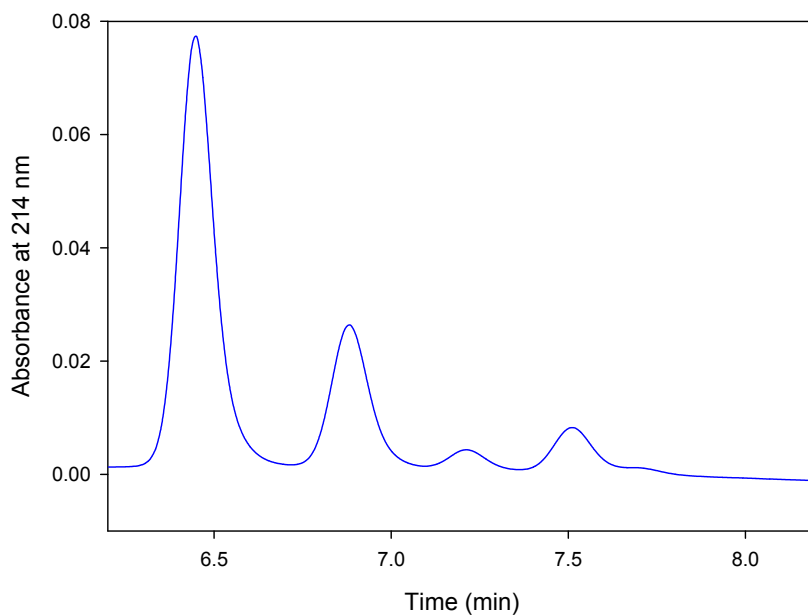


Figure 3.23 Chiral HPLC trace of the products obtained from the epoxidation of styrene catalyzed by Wt CPO.

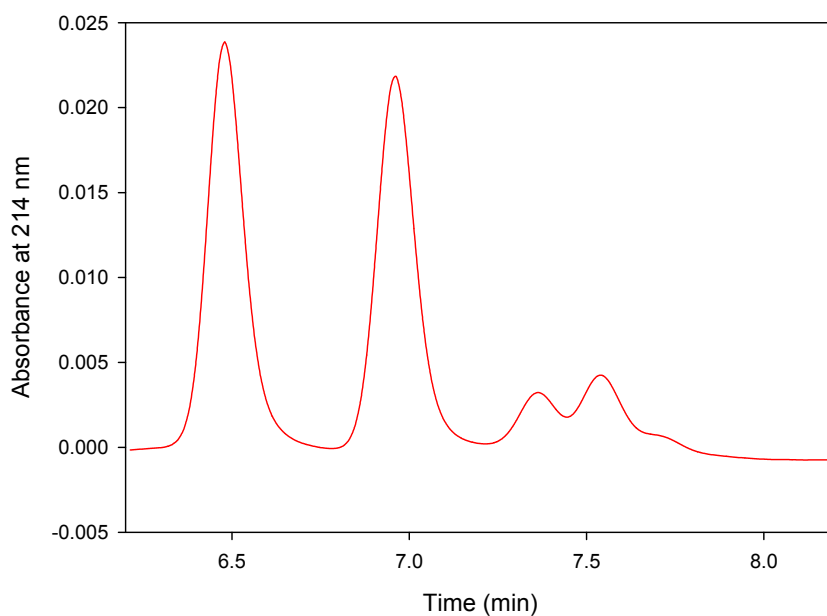
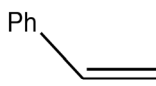
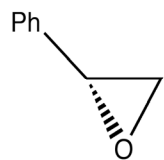
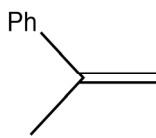
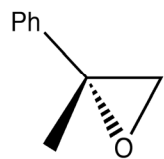
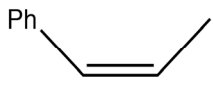
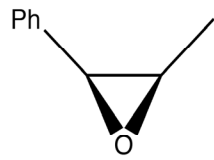
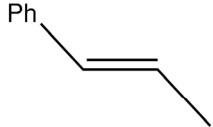
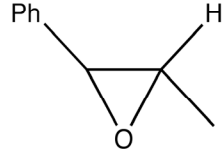
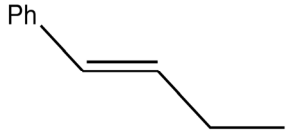
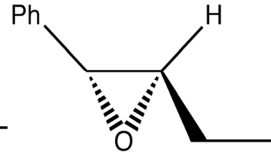
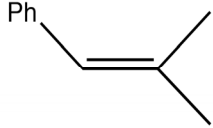
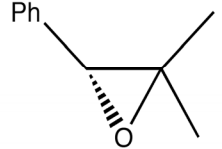


Figure 3.24 Chiral HPLC trace of the products obtained from the epoxidation of styrene catalyzed by F103A.

Table 3.5 Enantioselectivity study of F103A catalyzed of epoxidation reactions

Substrate	Major product	ee (%) ^a	Yield (%)	
		49	86	CPO
		2	95	F103A
		80 (R)	52	CPO
		66 (S)	45	F103A
		99	85	CPO
		5	86	F103A
		5	15	CPO
		50	75	F103A
		2	12	CPO
		34	47	F103A
		8 (S-R)	8	CPO
		69	53	F103A

^a enantiomeric excess (ee%)

replaced by Ala, it creates a larger opening within the heme pocket. Thus, when styrene derivatives enter the heme pocket of F103A, the substrates have more freedom compared to Wt CPO. A model of styrene binding to Wt CPO indicates close proximity between the alpha-carbon of styrene and F103. Therefore, the alpha-substituted styrenes have to adapt

a configuration that allows them to avoid Phe103 and Phe186, resulting in a lower reaction rate and a different orientation of the double bond next to the catalytic center. Other more branched styrene derivatives can enter the heme pocket in F103A, but have a much greater difficulty entering the Wt CPO heme pocket. Once the styrene derivative enters the heme pocket, a conformation that allows it to be in a close proximity to the ferric-oxo catalytic center has to be adapted, thus leading to enantioselective oxygen insertion reactions.

Furthermore, the heme pocket of F103A must be wider and maybe deeper than that of Wt CPO, as it can accommodate *trans*-substituted styrenes and other styrene derivatives with larger or more substituted double bonds. This may be because the alpha-helix where the F103 is located adopts a slightly different orientation when F103 is substituted with Ala.

3.3 Conclusion

In F103A mutant, a Phe located at the opening of the heme pocket was replaced by a small hydrophobic amino acid, Ala. The mutant displayed very desirable features compared to Wt CPO. One significant improvement is F103A's lack of catalase activity. Catalase pathway compete with monooxygenase pathway in CPO, lower catalase activity will help to improve the desired activities like epoxidation increased; indeed, epoxidation activity of F103A increased by 4-fold. Another important change was F103A's ability to catalyze the epoxidation of many styrene derivatives with high enantioselectivity that are poor substrates for Wt CPO. Styrene and its derivatives are an important group of substrates with important industrial applications (Hager, Lakner et al. 1998). F103A can

be served as a very promising candidate as an industrial catalyst due to its special substrate specificity and enantioselectivity.

It is very intriguing that a simple replacement of a single amino acid outside the catalytic center can cause such dramatic changes in the catalytic profile of CPO. Phenylalanine 103 was originally proposed to regulate substrate access to the catalytic center, although this hypothesis proved to be valid, by the study of its epoxidation of styrene derivatives, it is somewhat unexpected that it can act as a switch to turn on and off many of the Wt CPO's activities.

A look at the primary sequence and secondary structure of CPO tells us that Phe103 is located at the end of a hydrogen bonded turn and at the beginning of an undefined loop that consists of a series of polar amino acid ranging from Glu104 to Tyr114. It contains Glu104-His105-Asp106-His107-Ser108-Phe109-Ser110-Arg111-Lys112-Asp113-Tyr114 , and forms part of the wall and ceiling of the heme-pocket as revealed by the X-ray structure of Wt CPO (Sundaramoorthy, Turner et al. 1995). Two of these amino acids, His 105 and Asp106, were proposed to form a hydrogen bond network with Glu183 to facilitate the formation of Cpd I and ligand binding.

Since there are no significant structural changes in F103A as indicated by the CD spectroscopy study, one possible explanation for the importance of Phe103 is that the replacement of F103 by A caused subsequent conformation changes in this undefined loop structure, including perturbation of the hydrogen bonded network formed by His105, Asp 106 and Glu183. Since cyanide binding affinity undergoes significant decrease between pH 4-5, it is suspected that another acidic amino acid side chain is still involved with Glu183, if it remains in the same position as in Wt CPO. One possible candidate is

Asp106. Another possible scenario is that more dramatic changes have caused Glu183 to move away, and another amino acid side chain has repositioned to react with the water molecule. Judging from the optimal pH and ligand binding affinity of F103A, the amino acid would still be an acidic amino acid side chain like Glu or Asp. By analyzing the crystal structural of Wt CPO, such relocations would have caused significant overall structural changes, thus the latter scheme is unlikely to happen.

The F103A is a very interesting mutant as it provides greater enzymatic activities and several clues on how CPO regulates its catalytic activity. Since it has a greater resemblance to P450cam in its UV-vis spectrum; F103A is a better model to understand the long standing yet difficult question of P450 mechanism than CPO. Future studies on F103A, with more site-directed mutagenesis, spectroscopic and kinetic studies, will help us to elucidate the structural basis of its attractive features and the mechanism underlying them. It will also facilitate the study of P450cam and other related heme-containing peroxidase.

Chapter IV

C29H/C79H/C87H CPO Mutant Purification and Characterization

4.1 Material and methods

4.1.1 Strains and reagents

The same procedure was used as described for F103A in section 3.1.1; except that *A. niger* strain ATCC 62590 (*pyrG* deficiency) was bought from American type culture center (ATCC) and was used as the expression host. The strain carries a nonfunctional *pyrG* gene, which enables the use of the *pyrG* selection marker. Recombinant CPO was expressed successfully in our laboratory using *A. niger* strain ATCC 62590 as host strain.

4.1.2 CPO mutant gene construction of expression plasmid

The same procedure was used as described for F103A in section 3.1.2, except that three different primers were used to introduce the triplet mutation into CPO. The three primers were C29H-anti: gac tct cgt gct cct CAC cca gct ctg aac gct c, C79H-anti: c aac gcc ttc gtc gtc CAC gag tac gtt act ggc and C87H-anti: gtt act ggc tcc gac CAT ggt gac agc ctt gtc. After each mutation was confirmed by DNA sequencing, the resulting plasmid was then used as the template for the next mutation. The CPO expression vector with the triple mutations was named pCPO#3C.

4.1.3 Plasmid transformation into *A. niger* protoplast

Fungal co-transformation was carried out as described in section 3.1.3, using the CPO expression vector pCPO#3C and assistant plasmids pAB4.1, which contains the *A. niger pyrG* selection marker in a weight ratio of 10:1.

4.1.4 Genomic DNA extraction and sequencing

The same procedure was used as described for F103A in section 3.1.4

4.1.5 Expression of C29H/C79H/C87H CPO mutant

The same procedure was used as described for F103A in section 3.1.5

4.1.6 Total mRNA extraction and reverse transcription PCR

Aspergillus niger culture medium was collected after 48 h of growth then filtered. The *A. niger* mycelia were washed with sterile water and then grinded in liquid nitrogen to a fine power. The grinded power, 50 mg, was either stored in a -70°C freezer for further study or used directly. Total mRNA was extracted with a QIAGEN plant mRNA kit. The extracted total mRNA was then converted into cDNA via reverse transcription PCR (RT PCR). The RT PCR mixture contained, 5 µL of mRNA sample as template, 0.75 µL of a blend of random hexameric RNA primers, 0.25 µL of anchored oligo dT RNA primers, 1 µL of RT enhancer, 1 µL of reverse transcription DNA polymerase, 2 µL of dNTP mix, 4 µL of 5X PCR buffer and 4 µL of water. The extension PCR step was performed at 56 °C for 30 min. The cDNA sample was then used as the template to undergo a second PCR reaction using primers 5'-cgc gga tcc atg ttc tcc aag gtc c -3' and 5'- ccg gaa ttc aag gtt gcg ggc-3' to amplify the CPO coding region. A PCR fragment size of 1122 bp was used to confirm positive CPO mRNA transcription.

4.1.7 Western blotting procedures

The same procedure was used as described for F103A in section 3.1.7

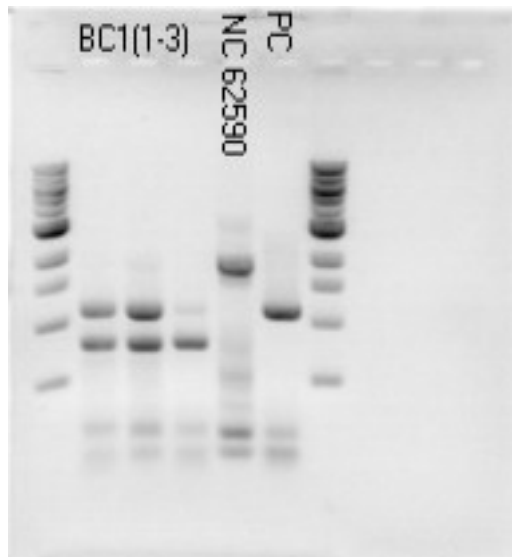
4.2 Results and discussion

One unique feature that separates CPO and P450 from other peroxidases is the proximal ligand, which is the fifth ligand to the ferric center of the heme. In CPO, the proximal ligand is a cysteine, instead of the usual histidine. A previous report about C29H expressed in *C. fumago* showed that replacement of the proximal amino acid Cys29 with

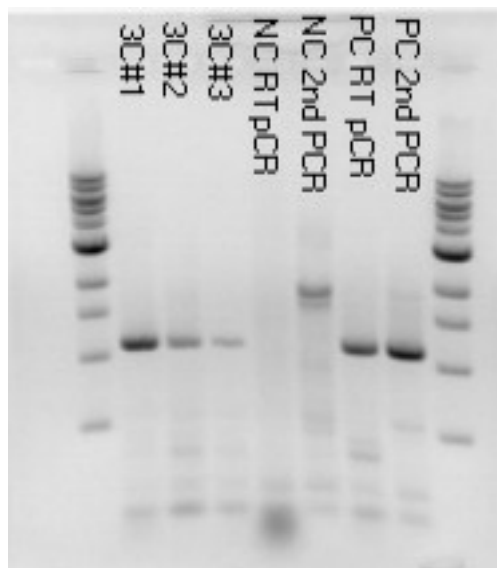
histidine had no significance effect on enzymatic activity (Yi, Mroczko et al. 1999) Given the surprising result, I suspected that another cysteine was involved as the proximal ligand or contamination from endogenous Wt CPO in the parental host. With these questions in mind, I attempted to create a new CPO mutant C29H/C79H/C87H in which all of the cysteines in CPO were replaced by histidine.

The experimental approach is basically the same as for the F103A CPO mutant. I designed the primers and introduced the three mutations to the transformation vector one by one. The vector was then sequenced to verify that the mutations were introduced correctly and that no other bases had been altered. The new vector was named pCPO#3C. I then proceeded to co-transform of pCPO#3C and pAB4.1 into *A. niger* strain ATCC 62590, the parent strain of MGG029. The MGG029 strain was used to produce rCPO and F103A as described in earlier chapters. After uridine and acrylamide selection, PCR confirmed that a positive clone had been selected and RT-PCR was then undertaken to confirm that the CPO gene was transformed and transcribed (Fig. 4.1).

However, when I proceeded to purify the mutant protein, I found neither detectable extracellular peroxidase activity nor a visible protein band between 40 to 50 kDa on the SDS-PAGE gel. Therefore I extracted not only the extracellular protein secreted by *A. niger*, but also the cellular protein of *A. niger* as well for immunizing detection. A western blot showed no reaction between the polyclonal CPO antibody and a protein of the correct size (Fig. 4.2), although, some broad bands did appear. I reasoned that the three mutations had dramatically changed the protein conformation, thus, the product protein lost structural similarity to CPO and maybe also the ability to incorporate heme, since no peroxidase activity was detected. Other possible explanation are that the mutant



A



B.

Figure 4.1 Confirmation of positive transformation and transcription of C29H/C79H/C87H mutant. A. PCR results on extracted genomic DNA sample to confirm positive transformation. *A.niger* strain ATCC 62590 was transformed with plasmids pCPO#3C and pAB4.1. B. RT-PCR & cDNA PCR results. RT-PCR was done on extracted mRNA sample of *A. niger* strain B3C#1-3. The second PCR were done on the cDNA sample synthesized in the RT-PCR to confirm positive CPO gene transcription. NC and PC are the abbreviation of negative and positive control respectively.

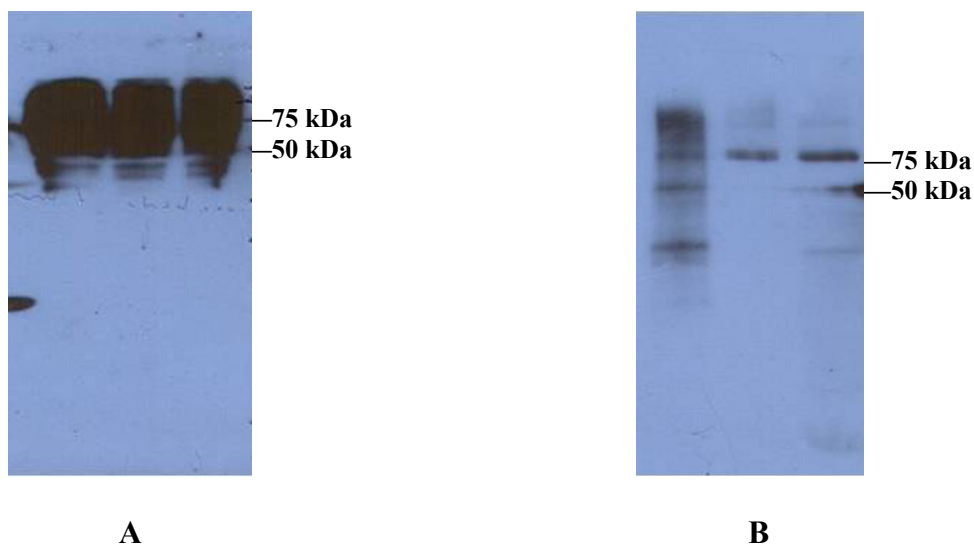


Figure 4.2 Western blotting analysis on extracted both cellular and extracellular protein samples from *A. niger* strain (ATCC 62590) transformed with CPO expression vector pCPO#3C to detect CPO mutant expression. A. Total extracellular protein; B. Total cellular protein.

protein was expressed but partially digested by protease or wrongly folded, which caused the unclear, broaden bands in the western blot. Similar phenomenon were observed with a CPO mutant with a truncated C-terminal gene (Conesa, Weelink et al. 2001).

4.3 Conclusion

Although, successful transformation and transcription was confirmed for the C29H/C79H/C87H mutant, no active protein could be isolated or detected in the culture media, indicating that a complete structural rearrangement have taken place in this mutant. Cystine 29 is undoubtedly an important amino acid served as the proximal ligand for the ferric heme center in Wt CPO. Surprisingly no dramatic change but some decrease (about 20%) in activity was observed in the C29H mutant (Yi, Mroczko et al. 1999) My results suggest that Cys79 and Cys87 are critical to maintaining the structural scaffold of CPO. According the CPO crystal structure (Sundaramoorthy, Terner et al. 1995), Cys79

and Cys87 are close enough to form a disulfide bond and are located in the middle of an alpha-helix. Apparently disrupting the disulfide bond, results in the collapse of the protein scaffold and loss of its active conformation. Thus, it is very unlikely that in C29H mutant, another Cys was recruited as the proximal ligand for the heme-center. Therefore my results supports the findings made in the C29H study that cysteine is not required for Wt CPO activity although its ligation to ferric center facilitates the cleavage of O-O bond to form Cpd I. It will be interesting to see if replacement of C29 with another amino acid like tyrosine would cause a different scenario. Ultimately, the distal amino acid forming the substrate binding pocket above the heme center may play a significant role in regulation CPO's enzymatic activities.

Chapter V

In *vitro* biodegradation of carbon nanotube by CPO

5.1 Material and Methods

5.1.1 Reagents

Electric arc discharge single wall nanotubes (SWNTs) were purchased from Carbon Solutions, Inc. All other reagents were purchased from Sigma-Aldrich. Wt CPO was purified in Dr. Xiaotang Wang's laboratory.

5.1.2 Nanotube biodegradation by CPO and H₂O₂

Purchased SWNTs were further purified by oxidative treatment with H₂SO₄ /H₂O₂ to remove residual metal catalyst, to impart carboxylic acid groups, and to break down the size of the SWNTs to shorter pieces (500~600 nm), thus improving solubility in aqueous media.

Nanotubes (2 mg) were suspended in 4.5 mL of 0.1 M phosphate buffer at pH 3 or 5 using an ultrasonic bath for 1 min (Branson 1510, frequency 40 kHz). Purified CPO (1 mg/mL) was dissolved in 0.1 M phosphate buffer (pH 3 or 5), and then 4.0 mL was added to the carboxylated nanotubes suspended in the same buffer. The entire suspension was then statically incubated for 24 h at 4 °C in the dark. Hydrogen peroxide, 10.0 mL of a 160 μM solution in 0.1 M phosphate buffer at the corresponding pH, either 3 or 5, was added to the bulk sample to start the catalytic biodegradation of carbon nanotubes in the presence of CPO. Static incubation with H₂O₂ was performed at 4 °C in the dark to avoid enzyme denaturation and photolysis of H₂O₂.

Over the incubation period, daily measurements of H₂O₂ concentration were performed, and fresh H₂O₂ was added to bring the total concentration back to the initial

concentration. Furthermore, the absorbance of the mixture at 398 nm was determined biweekly and fresh CPO was added to maintain the CPO concentration, if necessary.

5.1.3 Measurement of H₂O₂ concentration

I prepared FOX-2 reagent (Nourooz-Zadeh 1999) by dissolving xylenol orange and ammonium ferrous sulfate in 250 mM H₂SO₄ to final concentrations of 1 and 2.5 mM, respectively. One volume of this concentrated reagent was added to 9 volumes of HPLC grade methanol containing 4.4 mM BHT (butylated hydroxytoluene) to make the working reagent which comprised of 250 μM ammonium ferrous sulfate, 100 μM xylenol orange, 25 mM H₂SO₄, and 4 mM BHT in 90% v/v methanol. A mixture containing 100 μL of sample and 900 μL of FOX-2 reagent was incubated at room temperature for 30 min and then the absorbance at 560 nm was measured. The working reagent has an extinction coefficient of $4.3 \times 10^4 \text{ M}^{-1} \text{ cm}^{-1}$ for hydroperoxide. The FOX-2 reagent was prepared in bulk and stored in the dark at 4 °C (good for 6 months). The reagent was calibrated with known concentrations of H₂O₂ before each use.

5.1.4 Scanning electron microscope (SEM)

The SEM in the Physics Department was used to follow the degradation of the SWNTs. Samples (250 μL) of CPO treated SWNTs were centrifuged (3400 rpm) and then the supernatant was decanted off. The pellet of SWNTs was washed with water twice and ethanol three times. For SEM sample preparation, the SWNTs were resuspended in approximately 1 mL of *N,N*-dimethylformamide (DMF) via sonication.

5.2 Results and discussion

Another possible application for CPO is the catalytic biodegradation of hazardous waste, especially aromatic substrates, which represent a difficult task for many

biodegradation reagents. Given the recent surge in nanowaste, single wall nanotubes (SWNTs) represented an ideal target. Another peroxidase, horseradish peroxidase (HRP), was recently shown to catalytically degrade SWNTs (Allen, Kichambare et al. 2008).

The degradation of SWNTs at pH 3 and 5 in the presence of 80 μM H_2O_2 and CPO was evaluated by SEM. However, no significant change in the morphology of the SWNTs was detected, suggesting that CPO has little or no effect on the degradation of SWNTs under these conditions. Some SEM images are shown below:

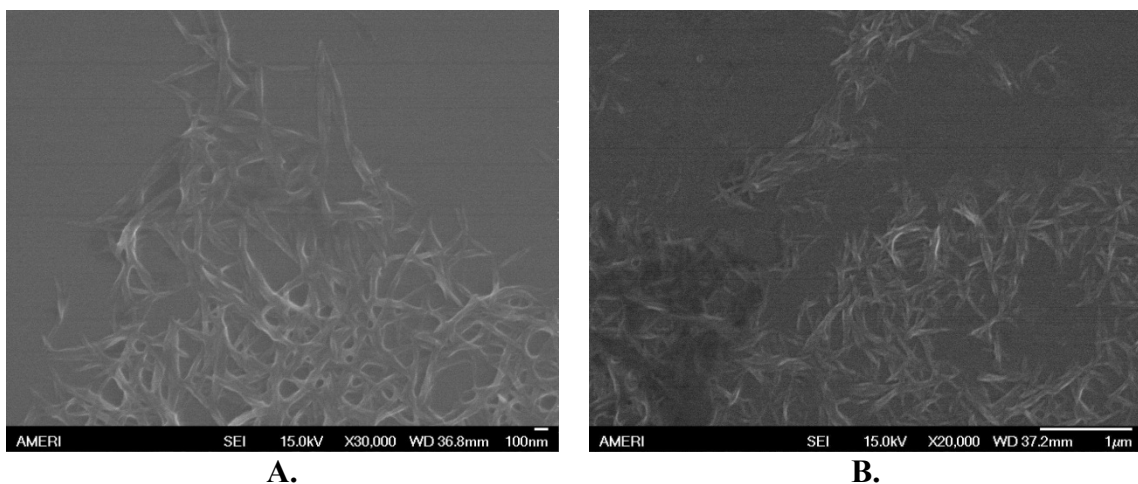


Figure 5.1 SEM images of SWNTs treated with CPO for 8 weeks. A. pH=3; B. pH=5

5.3 Conclusion

Unlike HRP, which facilitate the degradation of SWNTs *in vitro*, CPO seems have no effect on their degradation. This may due to the structure and mechanism differences of these two enzymes: HRP has a more open active site, and produces reactive oxygen species (ROS) during its catalytic cycle while CPO has restricted access to its activity site, and does not generate ROS during its catalytic cycle, except for during some halogenation reactions. Thus, the ROS produced during the catalytic cycle of HRP may

be responsible for the degradation of the SWNTs. Therefore, in the presence of high halide concentrations, CPO might facilitate the degradation of SWNTs.

Chapter VI

Perspectives

For rCPO expression, a detailed analysis can be done to determine which factors affecting the production yield of heme-proteins, such as the copy number of the gene, the level of transcription of mRNA, the ratio of apo to holo secreted protein. Co-expressing with foldases, molecular chaperones can be done as well, to see if they could help to increase production yield of rCPO further.

The production of partially deuterated rCPO can be attempted by letting the host strain growing in culture media made from D₂O. NMR spectrum of deuterated rCPO should be less complex than that of its fully protonated analog and offers the possibility of assigning additional resonances with concomitant structural information.

The dramatic catalytic behavioral changes of the F103A mutant suggest that not only the major amino acids, which actually take part in the catalysis, but also that the distal heme microenvironment plays an important in regulating catalytic behavior. Additional mutations of amino acids close to the heme center should be constructed and expressed, based on the current hypothesis. Targets should include V182 and F186.

The structure of F103A should be elucidated so that the kinetic and ligand binding results can be placed in context. Because the enantioselectivity profile changed with the F103 to A mutation, other large amino acids in the active site should be mutated to alanine as well, such as V182 and F186. Furthermore, mutants that might improve upon the enantioselectivity of WT CPO for styrene should also be constructed such as F103V, F103Y, and F103W.

REFERENCES

- Aburto, J., J. Correa-Basurto, et al. (2008). "Atypical kinetic behavior of chloroperoxidase-mediated oxidative halogenation of polycyclic aromatic hydrocarbons." Arch Biochem Biophys **480**(1): 33-40.
- Allen, B. L., P. D. Kichambare, et al. (2008). "Biodegradation of single-walled carbon nanotubes through enzymatic catalysis." Nano Lett **8**(11): 3899-3903.
- Araiso, T., R. Rutter, et al. (1981). "Kinetic analysis of compound I formation and the catalytic activity of chloroperoxidase." Can J Biochem **59**(4): 233-236.
- Banci, L., I. Bertini, et al. (1992). "H-1-Nmr Investigation of Manganese Peroxidase from Phanerochaete-Chrysosporium - a Comparison with Other Peroxidases." Biochemistry **31**(41): 10009-10017.
- Boddupalli, S. S., C. A. Hasemann, et al. (1992). "Crystallization and preliminary x-ray diffraction analysis of P450terp and the hemoprotein domain of P450BM-3, enzymes belonging to two distinct classes of the cytochrome P450 superfamily." Proc Natl Acad Sci U S A **89**(12): 5567-5571.
- Brown, F. S. and L. P. Hager (1967). "Chloroperoxidase. IV. Evidence for an ionic electrophilic substitution mechanism." J Am Chem Soc **89**(3): 719-720.
- Casella, L., M. Gullotti, et al. (1992). "Mechanism of enantioselective oxygenation of sulfides catalyzed by chloroperoxidase and horseradish peroxidase. Spectral studies and characterization of enzyme-substrate complexes." Biochemistry **31**(39): 9451-9459.
- Casella, L., S. Poli, et al. (1994). "The chloroperoxidase-catalyzed oxidation of phenols. Mechanism, selectivity, and characterization of enzyme-substrate complexes." Biochemistry **33**(21): 6377-6386.
- Chakraborty, B. N., N. A. Patterson, et al. (1991). "An electroporation-based system for high-efficiency transformation of germinated conidia of filamentous fungi." Can J Microbiol **37**(11): 858-863.
- Champion, P. M., E. Munck, et al. (1973). "Mossbauer investigations of chloroperoxidase and its halide complexes." Biochemistry **12**(3): 426-435.
- Conesa, A., D. Jeenes, et al. (2002). "Calnexin overexpression increases manganese peroxidase production in *Aspergillus niger*." Appl Environ Microbiol **68**(2): 846-851.
- Conesa, A., P. J. Punt, et al. (2002). "Fungal peroxidases: molecular aspects and applications." J Biotechnol **93**(2): 143-158.

- Conesa, A., P. J. Punt, et al. (2001). "The secretion pathway in filamentous fungi: a biotechnological view." Fungal Genet Biol **33**(3): 155-171.
- Conesa, A., F. van De Velde, et al. (2001). "Expression of the *Caldariomyces fumago* chloroperoxidase in *Aspergillus niger* and characterization of the recombinant enzyme." J Biol Chem **276**(21): 17635-17640.
- Conesa, A., C. A. van den Hondel, et al. (2000). "Studies on the production of fungal peroxidases in *Aspergillus niger*." Appl Environ Microbiol **66**(7): 3016-3023.
- Conesa, A., G. Weelink, et al. (2001). "C-terminal propeptide of the *Caldariomyces fumago* chloroperoxidase: an intramolecular chaperone?" FEBS Lett **503**(2-3): 117-120.
- Corbett, M. D., B. R. Chipko, et al. (1980). "The action of chloride peroxidase on 4-chloroaniline. N-oxidation and ring halogenation." Biochem J **187**(3): 893-903.
- Daboussi, M. J., A. Djeballi, et al. (1989). "Transformation of seven species of filamentous fungi using the nitrate reductase gene of *Aspergillus nidulans*." Curr Genet **15**(6): 453-456.
- Danehy, J. P. and K. N. Parameswaran (1968). "Acidic dissociation constants of thiols." Journal of Chemical & Engineering Data **13**(3): 386-389.
- Dawson, J. H., L. A. Andersson, et al. (1982). "Spectroscopic investigations of ferric cytochrome P-450-CAM ligand complexes. Identification of the ligand trans to cysteinate in the native enzyme." J Biol Chem **257**(7): 3606-3617.
- Dawson, J. H., M. Sono, et al. (1983). "Comparative studies of spectroscopic and ligand-binding properties of Chloroperoxidase and Cytochrome-P-450." Federation Proceedings **42**(7): 1900-1900.
- Denisov, I. G., J. H. Dawson, et al. (2007). "The ferric-hydroperoxo complex of chloroperoxidase." Biochem Biophys Res Commun **363**(4): 954-958.
- Doerge, D. R. (1986). "Oxygenation of organosulfur compounds by peroxidases: evidence of an electron transfer mechanism for lactoperoxidase." Arch Biochem Biophys **244**(2): 678-685.
- Dunford, H. B., A. M. Lambeir, et al. (1987). "On the mechanism of chlorination by chloroperoxidase." Arch Biochem Biophys **252**(1): 292-302.
- Fang, G. H., P. Kenigsberg, et al. (1986). "Cloning and sequencing of chloroperoxidase cDNA." Nucleic Acids Res **14**(20): 8061-8071.

- Frew, J. E. and P. Jones (1984). "Structure and functional properties of peroxidases and catalases Adv." Inorg. Bioinorg. Mech **3**: 175-212.
- Gebicka, L. and J. Didik (2007). "Kinetic studies of the reaction of heme-thiolate enzyme chloroperoxidase with peroxynitrite." J Inorg Biochem **101**(1): 159-164.
- Geigert, J., T. D. Lee, et al. (1986). "Epoxidation of alkenes by chloroperoxidase catalysis." Biochem Biophys Res Commun **136**(2): 778-782.
- Geigert, J., S. L. Neidleman, et al. (1983). "Novel haloperoxidase substrates. Alkynes and cyclopropanes." J Biol Chem **258**(4): 2273-2277.
- Gordon, C. L., V. Khalaj, et al. (2000). "Glucoamylase::green fluorescent protein fusions to monitor protein secretion in *Aspergillus niger*." Microbiology **146 (Pt 2)**: 415-426.
- Gouka, R. J., P. J. Punt, et al. (1996). "Analysis of heterologous protein production in defined recombinant *Aspergillus awamori* strains." Appl Environ Microbiol **62**(6): 1951-1957.
- Gouka, R. J., P. J. Punt, et al. (1997). "Efficient production of secreted proteins by *Aspergillus*: progress, limitations and prospects." Appl Microbiol Biotechnol **47**(1): 1-11.
- Green, M. T., J. H. Dawson, et al. (2004). "Oxoiron(IV) in chloroperoxidase compound II is basic: implications for P450 chemistry." Science **304**(5677): 1653-1656.
- Groves, J. T. and T. E. Nemo (1983). "Aliphatic Hydroxylation Catalyzed by Iron Porphyrin Complexes." J Am Chem Soc **105**(20): 6243-6248.
- Hager, L. P., F. J. Lakner, et al. (1998). "Chiral synthons via chloroperoxidase catalysis." Journal of Molecular Catalysis B-Enzymatic **5**(1-4): 95-101.
- Hager, L. P., D. R. Morris, et al. (1966). "Chloroperoxidase. II. Utilization of halogen anions." J Biol Chem **241**(8): 1769-1777.
- Hallenberg, P. F. and L. P. Hager (1978). "Purification of chloroperoxidase from *Caldariomyces fumago*." Methods Enzymol **52**: 521-529.
- Hanegraaf, P. P., P. J. Punt, et al. (1991). "Construction and physiological characterization of glyceraldehyde-3-phosphate dehydrogenase overproducing transformants of *Aspergillus nidulans*." Appl Microbiol Biotechnol **34**(6): 765-771.
- Hasemann, C. A., R. G. Kurumbail, et al. (1995). "Structure and function of cytochromes P450: a comparative analysis of three crystal structures." Structure **3**(1): 41-62.

- Hewson, W. D. and L. P. Hager (1979). "Oxidation of horseradish-peroxidase compound II to compound I." J Biol Chem **254**(9): 3182-3186.
- Hofrichter, M. and R. Ullrich (2006). "Heme-thiolate haloperoxidases: versatile biocatalysts with biotechnological and environmental significance." Appl Microbiol Biotechnol **71**(3): 276-288.
- Hollenberg, P. F. and L. P. Hager (1973). "The P-450 nature of the carbon monoxide complex of ferrous chloroperoxidase." J Biol Chem **248**(7): 2630-2633.
- Horner, O., J. M. Mouesca, et al. (2007). "Spectroscopic description of an unusual protonated ferryl species in the catalase from *Proteus mirabilis* and density functional theory calculations on related models. Consequences for the ferryl protonation state in catalase, peroxidase and chloroperoxidase." J Biol Inorg Chem **12**(4): 509-525.
- Hosten, C. M., A. M. Sullivan, et al. (1994). "Resonance Raman spectroscopy of the catalytic intermediates and derivatives of chloroperoxidase from *Caldariomyces fumago*." J Biol Chem **269**(19): 13966-13978.
- Juge, N., B. Svensson, et al. (1998). "Secretion, purification, and characterisation of barley alpha-amylase produced by heterologous gene expression in *Aspergillus niger*." Appl Microbiol Biotechnol **49**(4): 385-392.
- Kedderis, G. L. and P. F. Hollenberg (1984). "Peroxidase-catalyzed N-demethylation reactions. Substrate deuterium isotope effects." J Biol Chem **259**(6): 3663-3668.
- Kedderis, G. L., D. R. Koop, et al. (1980). "N-Demethylation reactions catalyzed by chloroperoxidase." J Biol Chem **255**(21): 10174-10182.
- Kenigsberg, P., G. H. Fang, et al. (1987). "Post-translational modifications of chloroperoxidase from *Caldariomyces fumago*." Arch Biochem Biophys **254**(2): 409-415.
- Kim, S. H., R. Perera, et al. (2006). "Rapid freeze-quench ENDOR study of chloroperoxidase compound I: the site of the radical." J Am Chem Soc **128**(17): 5598-5599.
- Kobayashi, S., M. Nakano, et al. (1987). "On the mechanism of the peroxidase-catalyzed oxygen-transfer reaction." Biochemistry **26**(16): 5019-5022.
- Kriechbaum, M., H. J. Heilmann, et al. (1989). "Cloning and DNA sequence analysis of the glucose oxidase gene from *Aspergillus niger* NRRL-3." FEBS Lett **255**(1): 63-66.

- Kuhnel, K., W. Blankenfeldt, et al. (2006). "Crystal structures of chloroperoxidase with its bound substrates and complexed with formate, acetate, and nitrate." J Biol Chem **281**(33): 23990-23998.
- Lakner, F. J. and L. P. Hager (1996). "Chloroperoxidase as Enantioselective Epoxidation Catalyst: An Efficient Synthesis of (R)-(-)-Mevalonolactone." J Org Chem **61**(11): 3923-3925.
- Libby, R. D. and N. S. Rotberg (1990). "Compound I formation is a partially rate-limiting process in chloroperoxidase-catalyzed bromination reactions." J Biol Chem **265**(25): 14808-14811.
- Libby, R. D., N. S. Rotberg, et al. (1989). "The chloride-activated peroxidation of catechol as a mechanistic probe of chloroperoxidase reactions. Competitive activation as evidence for a catalytic chloride binding site on compound I." J Biol Chem **264**(26): 15284-15292.
- Libby, R. D., A. L. Shedd, et al. (1992). "Defining the involvement of HOCl or Cl₂ as enzyme-generated intermediates in chloroperoxidase-catalyzed reactions." J Biol Chem **267**(3): 1769-1775.
- Libby, R. D., J. A. Thomas, et al. (1982). "Chloroperoxidase halogenation reactions. Chemical versus enzymic halogenating intermediates." J Biol Chem **257**(9): 5030-5037.
- Liu, L., J. Liu, et al. (2003). "Improving heterologous gene expression in *Aspergillus niger* by introducing multiple copies of protein-binding sequence containing CCAAT to the promoter." Lett Appl Microbiol **36**(6): 358-361.
- Lubertozzi, D. and J. D. Keasling (2009). "Developing *Aspergillus* as a host for heterologous expression." Biotechnol Adv **27**(1): 53-75.
- Makino, R., R. Chiang, et al. (1976). "Oxidation-reduction potential measurements on chloroperoxidase and its complexes." Biochemistry **15**(21): 4748-4754.
- Manoj, K. M. and L. P. Hager (2001). "Utilization of peroxide and its relevance in oxygen insertion reactions catalyzed by chloroperoxidase." Biochim Biophys Acta **1547**(2): 408-417.
- Miller, V. P., R. A. Tschirret-Guth, et al. (1995). "Chloroperoxidase-catalyzed benzylic hydroxylation." Arch Biochem Biophys **319**(2): 333-340.
- Mooibroek, H., A. G. Kuipers, et al. (1990). "Introduction of hygromycin B resistance into *Schizophyllum commune*: preferential methylation of donor DNA." Mol Gen Genet **222**(1): 41-48.

- Morris, D. R. and L. P. Hager (1966). "Chloroperoxidase. I. Isolation and properties of the crystalline glycoprotein." J Biol Chem **241**(8): 1763-1768.
- Nakajima, R., I. Yamazaki, et al. (1985). "Spectra of chloroperoxidase compounds II and III." Biochem Biophys Res Commun **128**(1): 1-6.
- Neidleman, S. L. and J. Geigert (1983). "Biological halogenation and epoxidation." Biochem Soc Symp **48**: 39-52.
- Ngiam, C., D. J. Jeenes, et al. (2000). "Characterization of a foldase, protein disulfide isomerase A, in the protein secretory pathway of *Aspergillus niger*." Appl Environ Microbiol **66**(2): 775-782.
- Nourooz-Zadeh, J. (1999). Ferrous ion oxidation in presence of xylenol orange for detection of lipid hydroperoxides in plasma. Methods Enzymol. P. Lester, Academic Press. **Volume 300**: 58-62.
- Ortiz de Montellano, P. R., Y. S. Choe, et al. (1987). "Structure-mechanism relationships in hemoproteins. Oxygenations catalyzed by chloroperoxidase and horseradish peroxidase." J Biol Chem **262**(24): 11641-11646.
- Osborne, R. L., G. M. Raner, et al. (2006). "C. fumago chloroperoxidase is also a dehaloperoxidase: oxidative dehalogenation of halophenols." J Am Chem Soc **128**(4): 1036-1037.
- Palcic, M. M., R. Rutter, et al. (1980). "Spectrum of chloroperoxidase compound I." Biochem Biophys Res Commun **94**(4): 1123-1127.
- Pelletier, I., J. Altenbuchner, et al. (1995). "A catalytic triad is required by the non-heme haloperoxidases to perform halogenation." Biochim Biophys Acta **1250**(2): 149-157.
- Penner-Hahn, J. E., T. J. McMurry, et al. (1983). "X-ray absorption spectroscopic studies of high valent iron porphyrins. Horseradish peroxidase compounds I and II and synthetic models." Journal of Biological Chemistry **258**(21): 12761-12764.
- Penner-Hahn, J. E., K. Smith Eble, et al. (1986). "Structural characterization of horseradish peroxidase using EXAFS spectroscopy. Evidence for Fe=O ligation in compounds I and II." J Am Chem Soc **108**(24): 7819-7825.
- Perrin, D. D., B. Dempsey, et al. (1981). pKa Prediction of Organic Bases. New York Chapman and Hall.

- Punt, P. J., N. van Biezen, et al. (2002). "Filamentous fungi as cell factories for heterologous protein production." Trends Biotechnol **20**(5): 200-206.
- Punt, P. J., G. Veldhuisen, et al. (1994). "Protein targeting and secretion in filamentous fungi. A progress report." Antonie Van Leeuwenhoek **65**(3): 211-216.
- Punt, P. J. v. d. H., C. A. (1992). "Transformation of filamentous fungi based on hygromycin B and phleomycin resistance markers." Methods Enzymol **216**: 447-457.
- Roth, A. H. F. J. and P. Dersch (2010). "A novel expression system for intracellular production and purification of recombinant affinity-tagged proteins in *Aspergillus niger*." Applied Microbiology and Biotechnology **86**(2): 659-670.
- Rubin, B., J. VanMiddlesworth, et al. (1982). "Crystallization and preliminary X-ray data for chloroperoxidase." J Biol Chem **257**(13): 7768-7769.
- Ruiz-Diez, B. (2002). "Strategies for the transformation of filamentous fungi." J Appl Microbiol **92**(2): 189-195.
- Satterlee, J. D., J. E. Erman, et al. (1983). "Assignment of Hyperfine-Shifted Resonances in Low-Spin Forms of Cytochrome-C Peroxidase by Reconstitutions with Deuterated Hemins." J Am Chem Soc **105**(8): 2099-2104.
- Satterlee, J. D., J. E. Erman, et al. (1990). "Comparative Proton Nmr Analysis of Wild-Type Cytochrome-C Peroxidase from Yeast, the Recombinant Enzyme from *Escherichia-Coli*, and an Asp-235-]Asn-235 Mutant." Biochemistry **29**(37): 8797-8804.
- Schulz, C. E., P. W. Devaney, et al. (1979). "Horseradish-peroxidase compound I .1. Evidence for spin coupling between the heme iron and a free-radical " Febs Letters **103**(1): 102-105.
- Silverstein, R. M. and L. P. Hager (1974). "The chloroperoxidase-catalyzed oxidation of thiols and disulfides to sulfenyl chlorides." Biochemistry **13**(25): 5069-5073.
- Sono, M., J. H. Dawson, et al. (1986). "Ligand and halide binding properties of chloroperoxidase: peroxidase-type active site heme environment with cytochrome P-450 type endogenous axial ligand and spectroscopic properties." Biochemistry **25**(2): 347-356.
- Sono, M., K. S. Eble, et al. (1985). "Preparation and properties of ferrous chloroperoxidase complexes with dioxygen, nitric oxide, and an alkyl isocyanide. Spectroscopic dissimilarities between the oxygenated forms of chloroperoxidase and cytochrome P-450." J Biol Chem **260**(29): 15530-15535.

- Spencer, A., L. A. Morozov-Roche, et al. (1999). "Expression, purification, and characterization of the recombinant calcium-binding equine lysozyme secreted by the filamentous fungus *Aspergillus niger*: comparisons with the production of hen and human lysozymes." Protein Expr Purif **16**(1): 171-180.
- Stone, K. L., R. K. Behan, et al. (2006). "Resonance Raman spectroscopy of chloroperoxidase compound II provides direct evidence for the existence of an iron(IV)-hydroxide." Proc Natl Acad Sci U S A **103**(33): 12307-12310.
- Streitwieser, A., Jr. Heathcock, C. H., Ed. (1981). Introduction to Organic Chemistry. New York, Macmillan.
- Suh, Y. J. and L. P. Hager (1991). "Chemical and transient state kinetic-studies on the formation and decomposition of horseradish-peroxidase compound-X(I) and compound-X(II)." J Biol Chem **266**(33): 22102-22109.
- Sun, W., T. A. Kadima, et al. (1994). "Catalase activity of chloroperoxidase and its interaction with peroxidase activity." Biochem Cell Biol **72**(7-8): 321-331.
- Sundaramoorthy, M., J. Turner, et al. (1995). "The crystal structure of chloroperoxidase: a heme peroxidase--cytochrome P450 functional hybrid." Structure **3**(12): 1367-1377.
- Sundaramoorthy, M., J. Turner, et al. (1998). "Stereochemistry of the chloroperoxidase active site: crystallographic and molecular-modeling studies." Chem Biol **5**(9): 461-473.
- Swart, K., A. J. Debets, et al. (2001). "Genetic analysis in the asexual fungus *Aspergillus niger*." Acta Biol Hung **52**(2-3): 335-343.
- Turner, J., V. Palaniappan, et al. (2006). "Resonance Raman spectroscopy of oxoiron(IV) porphyrin pi-cation radical and oxoiron(IV) hemes in peroxidase intermediates." J Inorg Biochem **100**(4): 480-501.
- Thanabal, V., J. S. Deropp, et al. (1987). "Identification of the Catalytically Important Amino-Acid Residue Resonances in Ferric Low-Spin Horseradish-Peroxidase with Nuclear Overhauser Effect Measurements." J Am Chem Soc **109**(24): 7516-7525.
- Thomas, J. A. and L. P. Hager (1968). "The peroxidation of molecular iodine to iodate by chloroperoxidase." Biochem Biophys Res Commun **32**(5): 770-775.
- Thomas, J. A., D. R. Morris, et al. (1970). "Chloroperoxidase. 8. Formation of peroxide and halide complexes and their relation to the mechanism of the halogenation reaction." J Biol Chem **245**(12): 3135-3142.

- Thomas, J. A., D. R. Morris, et al. (1970). "Chloroperoxidase. VII. Classical peroxidatic, catalatic, and halogenating forms of the enzyme." J Biol Chem **245**(12): 3129-3134.
- Turnbull, I. F., D. R. Smith, et al. (1990). "Expression and secretion in *Aspergillus nidulans* and *Aspergillus niger* of a cell surface glycoprotein from the cattle tick, *Boophilus microplus*, by using the fungal amdS promoter system." Appl Environ Microbiol **56**(9): 2847-2852.
- Verdoes, J. C., P. J. Punt, et al. (1993). "Glucoamylase overexpression in *Aspergillus niger*: molecular genetic analysis of strains containing multiple copies of the glaA gene." Transgenic Res **2**(2): 84-92.
- Verdoes, J. C., A. D. van Diepeningen, et al. (1994). "Evaluation of molecular and genetic approaches to generate glucoamylase overproducing strains of *Aspergillus niger*." J Biotechnol **36**(2): 165-175.
- Visser, J., H. J. Bussink, et al. (1995). "Gene expression in filamentous fungi. Expression of pectinases and glucose oxidase in *Aspergillus niger*." Bioprocess Technol **22**: 241-308.
- Wang, X., H. Tachikawa, et al. (2003). "Two-dimensional NMR study of the heme active site structure of chloroperoxidase." J Biol Chem **278**(10): 7765-7774.
- Withers, J. M., R. J. Swift, et al. (1998). "Optimization and stability of glucoamylase production by recombinant strains of *Aspergillus niger* in chemostat culture." Biotechnol Bioeng **59**(4): 407-418.
- Yi, X., A. Conesa, et al. (2003). "Examining the role of glutamic acid 183 in chloroperoxidase catalysis." J Biol Chem **278**(16): 13855-13859.
- Yi, X., M. Mroczko, et al. (1999). "Replacement of the proximal heme thiolate ligand in chloroperoxidase with a histidine residue." Proc Natl Acad Sci U S A **96**(22): 12412-12417.
- Zhang, R., N. Nagraj, et al. (2006). "Kinetics of two-electron oxidations by the compound I derivative of chloroperoxidase, a model for cytochrome P450 oxidants." Org Lett **8**(13): 2731-2734.
- Zong, Q. (1997). "Expression of recombinant chloroperoxidase." University of Illinois at Urbana-Champaign Ph.D Thesis
- Zong, Q., P. A. Osmulski, et al. (1995). "High-pressure-assisted reconstitution of recombinant chloroperoxidase." Biochemistry **34**(38): 12420-12425.

APPENDICES

Table A1 Primers used to conduct the research in FIU

Figure B1 Plasmid pCPO3.1-amds sequencing results by primer walking (12.2k bp)

Figure B2 Map of assistant plasmid pAB4.1.

APPENDIX A

Table A1 Primers used to conduct the research in FIU

Primer name	Primer's sequence
C29H-anti:	5'-gac tet cgt gct cct CAC cca gct ctg aac gct c-3'
C79H-anti:	5'-c aac gcc ttc gtc gtc CAC gag tac gtt act ggc-3'
C87H-anti:	5'-gtt act ggc tcc gac CAT ggt gac agc ctt gtc-3'
C29H-sense:	5' -gag cgt tca gag ctg ggt gag cac gag agt-3'
C79H-sense:	5' -gcc agt aac gta ctc gtg gac gac gaa ggc gtt-3'
C87H-sense:	5' -gac aag gct gtc acc atg gtc gga gcc agt aac-3'
F103A-anti:	5'-gcc gag ccc cac get GCC gag cac gac aca tcc -3'
F103A-sense:	5' -gga tgt gtc gtg ctc ggc agc gtg ggg ctc ggc-3'
CPO-anti:	5'-ccg gaa ttc aag gtt gcg ggc ctt gtt-3'
CPO-sense:	5' -cgc gga tcc atg ttc aag gtc ctt ccc-3'

APPENDIX B

Figure B1 Plasmid pCPO3.1-amds sequencing results by primer walking (12.2k bp)

G A G G A C G G A T T T G G T G A A G A G G C G G A G G T C T A A C A T A C T T C A T C A G T G A C
T G C C G G T C T C G T A T A T A G T A T A A A A A G C A A G A A A G G A G G A C A G T G G A G G C
C T G G T A T A G A G C A G G A A A A G A A G G A A G A G G C G A A G G A C T C A C C C T C A A C A
G A G T G C G T A A T C G G C C C G A C A A C G C T G T G C A C C G T C T C C T G A C C C T C C A T
G C T G T T C G C C A T C T T T G C A T A C G G C A G C C G C C C A T G A C T C G G C C T T A G A C
C G T A C A G G A A G T T G A A C G C G G C C G G C A C T C G A A T C G A G C C A C C G A T A T C C
G T T C C T A C A C C G A T G A C G C C A C C A C G A A T C C C A A C G A T C G C A C C C T C A C C
A C C A G A A C T G C C G C C G C A C G A C C A G T T C T T G T T G C G T G G G T T G A C G G T G C
G C C C G A T G A T G T T G T T G A C T G T C T C G C A G A C C A T C A G G G T C T G C G G G A C A
G A G G T C T T G A C G T A G A A G A C G G C A C C G G C T T T G C G G A G C A T G G T T G T C A G
A A C C G A G T C C C C T T C G T C G T A C T T G T T T A G C C A T G A G A T G T A G C C C A T T G
A T G T T T C G T A G C C C T G G T G G C A T A T G T T A G C T G A C A A A A G G G A C A T C T A
A C G A C T T A G G G G C A A C G G T G T A C C T T G A C T C G A A G C T G G T C T T T G A G A G A
G A T G G G G A G G C C A T G G A G T G G A C C A A C G G G T C T C T T G T G C T T T G C G T A G T
A T T C A T C G A G T T C C C T T G C C T G C G C G A G A G C G G C G T C A G G G A A G A A C T C G

TGGGCGCAGTTTGTCTGCACAGAAGCCAGCGTCAGCTTGATAGTCCCATA
AGGTGGCGTTGTTACATCTCCCTGAGAGGTAGAGGGGACCCTACTAACTG
CTGGGCGATTGCTGCCCGTTTACAGAATGCTAGCGTAACTTCCACCGAGG
TCAACTCTCCGGCCGCCAGCTTGGACACAAGATCTGCAGCGGAGGCCTCT
GTGATCTTCAGTTCGGCCTCTGAAAGGATCCCCGATTTCTTTGGGAAATC
AATAACGCTGTCTTCCGCAGGCAGCGTCTGGACTTTCCATTTCATCAGGGA
TGGTTTTTTCGAGGCGGGCGCGCTTATCAGCGGCCAGTTCTTCCCAGGAT
TGAGGCATTCTGTGTTAGCTTATAGTCAGGATGTTGGCTCGACGAGTGTA
AACTGGGAGTTGGCATGAGGGTTATGTAGGCTTCTTTAGCCCCGCATCCC
CCTCATTCTCCTCATTGATCCCGGGGGAGCGGATGGTGTGATAAGAGAC
TAATTATAGGGTTTAGCTGGTGCCTAGCTGGTGATTGGCTGGCTTCGCCG
AATTTTACGGGCCAAGGAAAGCTGCAGAACC GCGGCACTGGTAAACGGTA
ATTAAGCTATCAGCCCCATGCTAACGAGTTTAAATTACGTGTATTGCTGA
TAAACACCAACAGAGCTTTACTGAAAGATGGGAGTCACGGTGTGGCTTCC
CCACTGCGATTATTGCACAAGCAGCGAGGGCGAACTTGA CTGTCTCGCT
GAGCAGCCTGCAGTCAAACATACATATATATCAACCGCGAAGACGTCTGG
CCTTGTAGAACACGACGCTCCCTAGCAACACCTGCCGTGTCAGCCTCTAC
GGTTGTTACTTGCATTTCAGGATGCTCTCCAGCGGGCGAGCTATTCAAAT
ATTCAAAGCAGGTATCTCGTATTGCCAGGATTCAGCTGAAGCAACAGGTG
CCAAGGAAATCTGCGTTCGGTTCTCATCTGGGCTTGCTCGGTCCTGGCGTA
GATCTAGAAACCGCAATCTCTATGAAATGATAAGGTGCTTGACCAATTCT
AATATCGGTGTGGTGGACTGTCCTAACAAAACCCGGCTATATTGGACCCA
TCAGAGCTCTCTTTGATCTTCATATCCAGCGAATGCAGTCGCAGCATTTA
CATCAGGCTTGATTGAGTATACATCAGCGTTTGCAGTTGGACTGGATCAG
GAGGCAACACCTCATGTTGTAGTTCATCATCTAGGTCTTTTGA AACGGAC
TACTGGGCTTGT CATACCAAGTGCATCTTAGCGCTTGT TTTGTGTGACCTA
TTGTATCATGGGTAACATGTTGATGTCATTTCAGGCTGAGTAATCTGCCTA
TCCAATGATGACTAGTTAAAGATGGATATACGTCGTACATCCGACCTTCA
GGGCCGGATGCATTCTTCAGCATA CGAACTGGTGTTATAACTTTGAATC
CCATCAATGGTTATCGGGTTGGTCCCATAATAAACA AAAAGAGGCTGCAT
TGCCCTATGGCATGCCATTCTTGACGCGGCATGCCGAGTTAGCCGAAATT
GGGCCAATCGGCTTCCCGT CAGAAGAGGATCACTGGCGCCTCAATTTTGG
TTTTTATAGTACCGGTGCAGCACGGCTAAACGTTCTCTTTCTACGGCCC
GCATCTCATAAGCAGCCAGGTACAGAAAAGCAAGAATAGAAAATT CAGGA
AAAACCATCCCAGCATCCAACCTGGTGCCAGAAATGGCGGAAACGTCGGA
TATAAGGAGCAATGGCTATCATTACCGACTGAACTTTTGCAGGAGATAC
TCCTATTTCGCTGACTTCCAGTCGTTCTTTTCGGCGAGTTGGACGTGCAA
GATTGGCGGAAACGCGGCGTTAAGCTCTTATGTACTTCGGCACCCAGCTCAA
CACTGTTCCCACTGTTCCCACTCGCCGAGGCAGACATTGAACAGGCGA
CACCACGAGAACTGAGAATACTATTCCACCGTGTCTGCCGGCAGAACTC
ATGGGGGATACGGAGCAACGTTTCCCTCAGCAATACGGAGGAGAAAACAGT
AAGACCAATGTCGGCTATTGCGGTTCAATCTCGGCATGGGTGCCAATACG
CGCAGTTGCGTGGGATGACATTCATACTCAAGACGTCGATAGGAATTCTG
CACAGCGGCCGCAATTCCTTGTATCTCTACACACAGGCTCAAATCAATA
AGAAGAACGGTTCGTCTTTTTCGTTTATATCTTGCATCGTCCCAAAGCTA
TTGGCGGGATATTCTGTTTGCAGTTGGCTGACTTGAAGTAATCTCTGCAG
ATCTTTTCGACACTGAAATACGTTCGAGCCTGCTCCGCTTGGAAAGCGGCGAG
GAGCCTCGTCCTGTCACA ACTACCAACATGGAGTACGATAAGGGCCAGTT
CCGCCAGCTCATTAAAGAGCCAGTTTCATGGGCGTTGGCATGATGGCCGTCA
TGCATCTGTACTTCAAGTACACCAACCCTCTTCTGATCCAGTCGATCATC
CCGCTGAAGGGCGCTTTTCGAATCGAATCTGTTAAGATCCACGTCTTCGG

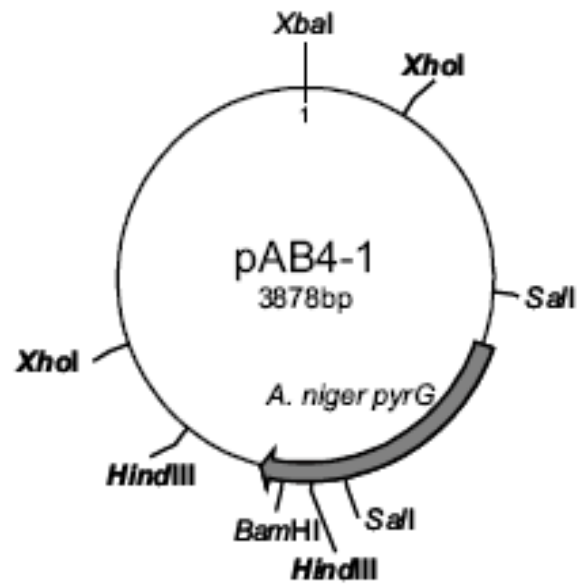
GAAGCCAGCGACTGGTGACCTCCAGCGTCCCTTTAAGGCTGCCAACAGCT
TTCTCAGCCAGGGGCCAGCCCAAGACCGACAAGGCCTCCCTCCAGAACGCC
GAGAAGAAGCTGGAGGGGTGGTGTCAAGGAGGAGTAAGCTCCTTATTGAAG
TCGGAGGACGGAGCGGTGTCAAGAGGATATTCTTCGCTCTGTATTATAGA
TAAGATGATGAGGAATTGGAGGTAGCATAGCTTCATTTGGATTTGCTTTC
CAGGCTGAGACTCTAGCTTGGAGCATAGAGGGTCCCTTTGGCTTTCAATA
TTCTCAAGTATCTCGAGTTTGAACCTTATTCCCGTGAACCTTTTATTACC
AATGAGCATTGGAATGAACATGAATCTGAGGACTGCAATCGCCATGAGGT
TTTCGAAATACATCCGGATGTGGAAGGCTTGGGGCACCTGCGTTGGTTGA
ATTTAGAACGTGGCACTATTGATCATCCGATAGCTCTGCAAAGGGCGTTG
CACAATGCAAGTCAAACGTTGCTAGCAGTTCAGGTGGAATGTTATGATG
AGCATTGTATTAATCAGGAGATATAGCATGATCTCTAGTTAGCTCACCA
CAAAGTCAGACGGCGTAACCAAAGTACACACAACAAGCTGTAAGGAT
TTCGGCACGGCTACGGAAGACGGAGAAGCCCACCTTCAGTGGACTCGAGT
ACCATTTAATTCTATTTGTGTTTGTATCGAGACCTAATACAGCCCCTACAA
CGACCATCAAAGTTCGTATAGCTACCAGTGAGGAAGTGGACTCAAATCGAC
TTCAGCAACATCTCCTGGATAAACTTTAAGCCTAAACTATAAGAATAAG
ATGGTGGAGAGCTTATACCGAGCTCCCAAATCTGTCCAGATCATGGTTGA
CCGGTGCCTGGATCTTCTATAGAATCATCCTTATTCGTTGACCTAGCTG
ATTCTGGAGTGACCCAGAGGGTCATGACTTGAGCCTAAAATCCGCCGCCT
CCACCATTTGTAGAAAAATGTGACGAACTCGTGAGCTCTGTACAGTGACC
GGTGACTCTTCTGGCATGCGGAGAGACGGACGGACGCAGAGAGAAGGGC
TGAGTAATAAGCGCCACTGCGCCAGACAGCTCTGGCGGCTCTGAGGTGCA
GTGGATGATTATTAATCCGGGACCGGCCGCCCTCCGCCCCGAAGTGGAA
AGGCTGGTGTGCCCTCGTTGACCAAGAATCTATTGCATCATCGGAGAAT
ATGGAGCTTCATCGAATCACCGGCAGTAAGCGAAGGAGAATGTGAAGCCA
GGGGTGTATAGCCGTCGGCGAAATAGCATGCCATTAACCTAGGTACAGAA
GTCCAATTGCTTCCGATCTGGTAAAAGATTACAGAGATAGTACCTTCTCC
GAAGTAGGTAGAGCGAGTACCCGGCGCGTAAGCTCCCTAATTGGCCCATC
CGGCATCTGTAGGGCGTCCAAATATCGTGCCTCTCCTGCTTTGCCCGGTG
TATGAAACCGGAAAGGCCGCTCAGGAGCTGGCCAGCGGCGCAGACCGGGA
ACACAAGCTGGCAGTCGACCCATCCGGTGTCTGTCACTCGACCTGCTGAG
GTCCCTCAGTCCCTGGTAGGCAGCTTTGCCCGTCTGTCCGCCCGGTGTG
TCGGCGGGGTTGACAAGGTCGTTGCGTCAGTCCAAATTTGTTGCCATAT
TTTCTGCTCTCCCAACAGCTGCTCTTTTCTTTTCTTTTCTTTTCCCA
TCTTCAGTATATTCATCTTCCCATCCAAGAACCTTTATTTCCCTAAGTA
AGTACTTTGCTACATCCATACTCCATCCTTCCATCCCTTATTCTTTGA
ACCTTTCAGTTCGAGCTTTCCCACTTCATCGCAGCTTGACTAACAGCTAC
CCCGCTTGAGCAGACATCACCATGTTCTCCAAGGTCTTCCCTTCGTGGG
AGCGGTTGCCGCCCTCCCTCACTCCGTCCGTGAGGAGCCTGGCTCCGGCA
TTGGCTACCCATACGACAACAACACCCTGCCATATGTGCCCCAGGTCCT
ACCGACTCTCGTGCTCCTTGCCCAGCTCTGAACGCTCTTGCCAAACCACGG
TTACATTCCTCACGATGGCCGTGCCATCAGCAGGGAGACCCTCCAGAACG
CTTTCCTCAACCAATGGGTATTGCCAACTCCGTCAATTGAGCTTGTCTG
ACCAACGCCTTCGTGCTCTGCGAGTACGTTACTGGCTCCGACTGTGGTGA
CAGCCTTGTCAACCTGACTCTGCTCGCCGAGCCCCACGCTTTCGAGCACG
ACCACTCCTTCTCCCGCAAGGATTACAAGCAGGGTGTGCGCAACTCCAAC
GACTTCATCGACAACAGGAACCTTCGATGCCGAGACCTTCCAGACCTCTCT
GGATGTCGTTGCAGGCAAGACCCACTTCGACTATGCCGACATGAACGAGA
TCCGCCTTCAGCGCGAGTCCCTCTCCAACGAGCTTGACTTCCCCGGTTGG
TTCACCGAGTCCAAGCCAATCCAGAACGTCGAGTCTGGCTTCATCTTCGC

CCTTGTCTCTGACTTCAACCTGCCCGACAACGATGAGAACCCTCTGGTTC
GCATTGACTGGTGGAAAGTACTGGTTACCAACGAGTCCTTCCCATAACCAC
CTCGGCTGGCACCCCCCGTCTCCAGCCAGGGAGATCGAGTTCGTCACCTC
CGCCTCCTCCGCTGTCCTGGCTGCCTCTGTACCTCTACTCCATCTTCCC
TTCCATCCGGTGCCATCGGCCAGGTGCCGAGGCTGTCCCTCTCTCCTTC
GCCTCCACCATGACCCCATTCCTCCTCGCCACCAATGCTCCTTACTACGC
CCAGGACCCAACTCTCGGCCCAACGACAAGCGTGAGGCTGCCCCAGCTG
CCACCACCTCCATGGCCGTCTTCAAGAACCATACTCGAGGCCATTGGC
ACCCAGGACATCAAGAACCAGCAGGCTTACGTCAGCTCCAAGGCTGCTGC
CATGGCCTCTGCCATGGCCGCCAACAAGGCCCGCAACCTTTAAGCTTGAG
ATCCACTTAACGTTACTGAAATCATCAAACAGCTTGACGAATCTGGATAT
AAGATCGTTGGTGTGATGTCAGCTCCGGAGTTGAGACAAATGGTGTTC
GGATCTCGATAAGATACGTTCAATTTGTCCAAGCAGCAAAGAGTGCCTTCT
AGTGATTTAATAGCTCCATGTCAACAAGAATAAAACGCGTTTTCGGGTTTA
CCTCTTCCAGATACAGCTCATCTGCAATGCATTAATGCATTGGACCTCGC
AACCTAGTACGCCCTTCAGGCTCCGGCGAAGCAGAAGAATAGCTTAGCA
GAGTCTATTTTCATTTTCGGGAGACGAGATCAAGCAGATCAACGGTCGTC
AAGAGACCTACGAGACTGAGGAATCCGCTCTTGGCTCCACGCGACTATAT
ATTTGTCTCTAATTGTACTTTGACATGCTCCTCTTCTTTACTCTGATAGC
TTGACTATGAAAATTCCGTCACCAGCCCCTGGGTTTCGCAAAGATAATTGC
ACTGTTTCTTCTTGA ACTCTCAAGCCTACAGGACACACATTTCATCGTAG
GTATAAACCTCGAAAATCATTCTACTAAGATGGGTATAACAATAGTAACC
ATGCATGGTTGCCCTAGTGAATGCTCCGTAACACCCCAATACGCCGGCCGAA
ACTTTTTTACA ACTCTCCTATGAGTCGTTTACCCAGAATGCACAGGTACA
CTTGTTTAGAGGTAATCCTTCTTTCTAGAGCTTGGCACTGGCCGTCGTTT
TACAACGTCGTGACTGGGAAAACCCTGGCGTTACCCAACTTAATCGCCTT
GCAGCACATCCCCCTTTCGCCAGCTGGCGTAATAGCGAAGAGGCCCGCAC
CGATCGCCCTTCCCAACAGTTGCGCAGCCTGAATGGCGAATGGCGCCTGA
TGCGGTATTTTCTCCTTACGCATCTGTGCGGTATTTACACCCGCATATGG
TGCACTCTCAGTACAATCTGCTCTGATGCCGCATAGTTAAGCCAGCCCCG
ACACCCGCCAACACCCGCTGACGCGCCCTGACGGGCTTGTCTGCTCCC GG
CATCCGCTTACAGACAAGCTGTGACCGTCTCCGGGAGCTGCATGTGTGAG
AGGTTTTACCGTCATCACCGAAACGCGCGAGACGAAAGGGCCTCGTGAT
ACGCCTATTTTTATAGGTTAATGTCATGATAATAATGGTTTCTTAGACGT
CAGGTGGCACTTTTCGGGGAAATGTGCGCGGAACCCCTATTTGTTTATTT
TTCTAAATACATTCAAATATGTATCCGCTCATGAGACAATAACCCTGATA
AATGCTTCAATAATATTGAAAAAGGAAGAGTATGAGTATTCAACATTTCC
GTGTCGCCCTTATTCCTTTTTTTCGGGCATTTTGCCTTCTGTTTTTGTCT
CACCCAGAAACGCTGGTGAAAGTAAAAGATGCTGAAGATCAGTTGGGTGC
ACGAGTGGGTTACATCGAACTGGATCTCAACAGCGGTAAGATCCTTGAGA
GTTTTTCGCCCGAAGAACGTTTTTCCAATGATGAGCACTTTTAAAGTTCTG
CTATGTGGCGCGGTATTATCCCGTATTGACGCCGGGCAAGAGCAACTCGG
TCGCCGCATACACTATTCTCAGAATGACTTGGTTGAGTACTACCCAGTCA
CAGAAAAGCATCTTACGGATGGCATGACAGTAAGAGAATTATGCAGTGTCT
GCCATAACCATGAGTGATAACACTGCGGCCAACTTACTTCTGACAACGAT
CGGAGGACCGAAGGAGCTAACCGCTTTTTTGCACAACATGGGGGATCATG
TAACTCGCCTTGATCGTTGGGAACCGGAGCTGAATGAAGCCATACCAAAC
GACGAGCGTGACACCACGATGCCTGTAGCAATGGCAACAACGTTGCGCAA
ACTATTA ACTGGCGAACTACTTACTCTAGCTTCCCGGCAACAATTAATAG
ACTGGATGGAGGCGGATAAAGTTGCAGGACCACTTCTGCGCTCGGCCCTT
CCGGCTGGCTGGTTTATTGCTGATAAATCTGGAGCCGGTGAGCGTGGGTC

TCGCGGTATCATTGCAGCACTGGGGCCAGATGGTAAGCCCTCCCGTATCG
TAGTTATCTACACGACGGGGAGTCAGGCAACTATGGATGAACGAAATAGA
CAGATCGCTGAGATAGGTGCCTCACTGATTAAGCATTGGTAAGTGTGAGA
CCAAGTTTACTCATATATACTTTAGATTGATTTAAAACCTTCATTTTTAAT
TTAAAAGGATCTAGGTGAAGATCCTTTTTTGATAATCTCATGACCAAATC
CCTTAACGTGAGTTTTTCGTTCCACTGAGCGTCAGACCCCGTAGAAAAGAT
CAAAGGATCTTCTTGAGATCCTTTTTTTCTGCGCGTAATCTGCTGCTTGC
AAACAAAAAAACCACCGCTACCAGCGGTGGTTTTGTTTGCCGGATCAAGAG
CTACCAACTCTTTTTCCGAAGGTAAGTGGCTTCAGCAGAGCGCAGATACC
AAATACTGTTCTTCTAGTGTAGCCGTAGTTAGGCCACCACCTTCAAGAACT
CTGTAGCACCGCCTACATACCTCGCTCTGCTAATCCTGTTACCAGTGGCT
GCTGCCAGTGGCGATAAGTCGTGTCTTACCGGGTTGGACTCAAGACGATA
GTTACCGGATAAAGGCGCAGCGGTGCGGGCTGAACGGGGGGTTTCGTGCACAC
AGCCCAGCTTGGAGCGAACGACCTACACCGAACTGAGATACCTACAGCGT
GAGCTATGAGAAAGCGCCACGCTTCCCGAAGGGAGAAAGGCGGACAGGTA
TCCGGTAAGCGGCAGGGTCGGAACAGGAGAGCGCACGAGGGAGCTTCCAG
GGGGAAACGCCTGGTATCTTTATAGTCCTGTGCGGTTTTCGCCACCTCTGA
CTTGAGCGTTCGATTTTTGTGATGCTCGTCAGGGGGGCGGAGCCTATGGAA
AAACGCCAGCAACGCGGCCTTTTTACGGTTCCTGGCCTTTTTGCTGGCCTT
TTGCTCACATGTTCTTTCCTGCGTTATCCCCTGATTCTGTGGATAACCGT
ATTACCGCCTTTGAGTGAGCTGATACCGCTCGCCGCAGCCGAACGACCGA
GCGCAGCGAGTCAGTGAGCGAGGAAGCGGAAGAGCGCCCAATACGCAAC
CGCCTCTCCCCGCGCGTTGGCCGATTCATTAATGCAGCTGGCACGACAGG
TTTCCCGACTGGAAAGCGGGCAGTGAGCGCAACGCAATTAATGTGAGTTA
GCTCACTCATTAGGCACCCCAAGGCTTTACACTTTATGCTTCCGGCTCGTA
TGTTGTGTGGAATTGTGAGCGGATAACAATTTACACACAGGAAACAGCTAT
GACATGATTACGAATTGCGGCCGCTGTGTCAGAATTCCGATACGGGGGAATC
GAACCCCGAGCTGCTGTGCACATGCAATGAGAGACAGCGATGTTAACCAT
TACACCATATCGGATGTTATATTTTTATTCTCCTCAAATAAATGTATATA
ACTATAGGAATGGATTCAATAGAATCTCCCAGGTCAAGTGTACTTACTCCG
GACCTCTTAAATATGTCGCCAGAGTGCTTCACTTGAACCGTAATTAGAG
CAGGTATCGCGCAAATTTTACAGGCATTTGAGACACTTTTTTTGTCTGGT
GAGAGTTTATATATCGCATAACAAGCCCTTGTGCTGGACATCTGCTAATG
TGAGGGAAAGCACGAGACCGCCGTCAGACTGAACGCTACGTTTGACCATAA
TCTAAATATACGCTACCTATATTTGTGCTATGGCTACTATTTCCGATGT
TACCGAAGAAGAGATTTTATAAAACCTGGTGAAGTCGAGGAATCGATGAG
CTCGCGAAATAGGTGGGGTATCTTGACACATACTTCTACTTGGGTATATCC
CCATGGCTATTCTCACTACTAAGTCTCTGGTGAGAGGGGATTGAAGCAGG
AACTGCCAGAGCTACGTCCGGTGCTTCCAGTCTTGTGTTGCATCATGAACTC
CACCGCGTCCAGTTGCCACTACTCAGGAATGTACTTCAGAGACTTTTTTCG
AGAATTTTGTGGATTTACGCTTTTCTTGGGCCGACCTGACTCCCACCTGA
CTATCTTGGATTATCTTGCAAAGCCAGCTGCCAACCGAGGTTTCCACTGT
AAAATATGACCCTAACTCAGCACACGTGACCTCCAGGTTGTGCTTTCAGTA
GCTGTACTTAATCGTCTGTATTTTCGTTAACTATGCTTAGCACATACATAT
ATATCATGGCACTCGGTTGATTAGTCTCCGAGAGGTTCTACTTTTTCTTTA
TTGATGCCGTGGCACCGCAGGACAGTCTGCACGTTACTGCTTCTGTGTGT
ATCTACAGCGACAAAGTAGTCCTGATAACAGGAGCTTCAGATGCCAAGGT
GGTAGGAGCGCTCCACTAGGATGGAAAATGTCCTCCTAGGACAACAATAT
AAAAGCGGTACTCTTACTGATGTCTATTGGAAGAAAACCTGGGGACTCGA
CACAGTAATAAGGACAATAGACAGACGCGGAATCACCTGCAAGGCTGAG
CTATCGTTATTACTCTACCGCAAGGCAACAACCAGCTCACCCCTGAGGCA

CGGGTACCATGGGTTGAGTGGTATGGGGCCATCCAGAGTACCTGTGGCA
GCATGAGACTGCACTCGAAGCAGCCATCAACCCAGCCAATATTCTGGGCT
TTCCATCCTTAGATCACATTTGAGATATAACCCATTTGGTGAGAGACT
TGTGCCGTTATACGTGTCTAGACTGGAAACGCAACCCTGAAGGGATTCTT
CCTTTGAGAGATGGAAGCGTGTTCATATCTCTTCGGTTCTACGGCAGGTTT
TTTTCTGCTCTTTTCGTAGCATGGCATGGTCACTTCAGCGCTTATTTACAG
TTGCTGGTATTGATTTCTTGTGCAAATTGCTATCTGACACTTATTAGCTA
TGGAGTCACCACATTTCCCAGCAACTTCCCCACTTCCTCTGCAATCGCCA
ACGTCCTCTCTTCACTGAGTCTCCGTCCGATAACCTGCACTGCAACCGGT
GCCCCATGGTACGCCTCCGGATCATACTCTTCCTGCACGAGGGGCATCAAG
CTCACTAACCGCCTTGAAACTCTCATTCTTCTTATCGATGTTCTTATCCG
CAAAGGTAACCGGAACAACACGCTCGTGAAATCCAGCAGGTTGATCACA
GAGGCATACCCATAGTACCGGAACTGGTCATGCCGTACCGCAGCGGTAGG
CGTAATCGGCGCGATGATGGCGTCCAGTTCCTTCCCGGCCTTTTCTTCAG
CCTCCCGCCATTTCTCAAGGTACTCCATCTGGTAATTCCAATTCTGGAGA
TGCGTGTCCCAGAGCTCGTTCATGTTAACAGCTTTGATGTTTCGGGTTTCAG
TAGGTCTTTGATATTTGGAATCGCCGGCTCGCCGGATGCACTGATATCGC
GCATTACGTCGGCGCTGCCGTCAGCCGCGTAGATATGGGAGATGAGATCG
TGGCCGAAATCGTGCTTGTATGGCGTCCACGGGGTACGGTGTGACCGGC
TTTGCGGAGTGCGGCGACGGTGGTTTTCCACGCCGCGCAGGATAGGAGGGT
GTGGAAGGACATTGCCGTCGAAGTTGTAGTAGCCGATATTGAGCCCGCCG
TTCTTGATCTTGAGGGCAATAATGTCCGACTCGGACTGGCGCCAGGGCAT
GGGGATGACCTTGGAGTCGTATTTCCATGGCTCCTGACCGAGGACGGATT
TGGTGAAGAGGCGGAGGTCTAACATACTTCATCAGTGACTGCCGGTCTCG
TATATAGTATAAAAAGCAAGAAAGGAGGACAGTGGAGGCCTGGTATAG

Figure B2 Map of assistant plasmid pAB4.1. It contains the *pyrG* selection marker for *A. niger*. The *pyrG* gene will be enable the transformed strain the ability to grow without uridine supplement



VITA

ZHENG WANG

June 12, 1975	Born Beijing China
2005-2008	Teaching Assistant & Ph.D.student Florida International University Miami, Florida
Jan. 2004~ Dec. 2004	Ph.D. student Jackson State University Jackson MS
1993~ 1997	B.S. in Biochemistry Jilin University Changchun China

PUBLICATIONS AND PRESENTATIONS

Zheng Wang, Xiaotang Wang (2009) Presentation on 238th ACS meeting, *Tweaking the substrate specificity and product enantioselectivity of chloroperoxidase*

Shuguang Wang, Lei Wang, Jun-Jie Yin, Zheng Wang, Peter P. Fu and Hongtao Yu
Light-induced toxic effects of tamoxifen: A chemotherapeutic and chemopreventive agent
Journal of Photochemistry and Photobiology A: Chemistry Volume 201, Issue 1, 1
January 2009, Pages 50-56

Xiaotang Wang, Zheng Wang, Jiang Yucheng (2007) Presentation on 234th ACS meeting,
Catalytic roles of Phe103 at the substrate-binding pocket of chloroperoxidase: remote control of heme chemistry in heme-thiolate proteins.

Lei Wang, Zheng Wang and Hongtao Yu (2004) Presentation on RCMI 9th Annual meeting
Phototoxicity study of azulene on a bacterial model.